

STEVIN LABORATORY - STEELSTRUCTURES  
DEPARTMENT OF CIVIL ENGINEERING  
DELFT UNIVERSITY OF TECHNOLOGY

BM-2

REPORT 6-83-6

"MEASUREMENTS AND INTERPRETATION OF  
DYNAMIC LOADS ON BRIDGES"

ECSC-contractnr.7210-KD/606.F4.6/80

FINAL REPORT

PHASE 2

by M.H. Kolstein

J. de Back

May 1983



Commission of the European Communities

ECSC-contractnr. 7210.KD/606  
(F4.6/80)

Measurements and interpretation of dynamic loads on  
bridges - Phase 2.

Final report

Circulation

Commission of the European Communities : 12 copies

ECSC-Executive Committee F4 : Mr. Bragard

Bramat

Brozetti

Bernard

De Back

Girardi

Flossdorf

Hagedorn

Hahnewinkel

Hicter

Hoogendoorn

Lieurade

Maddox

Mascanzoni

Rabbe

Rinaldi

Vogt

Walker

Watson

Beneficiaires

: Mr. Bruls

Haibach

Hoffman

Jacob

Kolstein

Page

Pfeifer

Sanpaolesi



CONTENTS	Page
0. Summary - Resume - Zusammenfassung	
1. Introduction	1-1
2. Bridge descriptions and location of the measuring points	2-1
3. Measurement of traffic loads and stresses in the bridge structures	3-1
4. Analysis of the traffic data and stress data in fatigue terms	4-1
5. General discussion of the results	5-1
6. References	6-1
7. Appendix	7-1



0. Summary  
Resume  
Zusammenfassung





"Measurements and interpretation of dynamic loads on bridges"  
Final report ECSC-contractnr. 7210-KD/606.F4.6/80

### Summary

This report describes the first and second phase results of measurements of traffic loadings on three Dutch steel highway bridges and the induced stresses. The aim of this investigation is to study the relation between traffic, traffic loadings and stresses in bridge components in order to allow a better fatigue analysis of bridges. The research program is part of an European program in which Belgium, France, Germany, Great Britain, Italy and The Netherlands were participating. The project was financially supported by the European Coal and Steel Community.

"Mesures et interpretations des charges dynamiques dans les ponts"

Rapport final 2ème phase, CECA-convention 7210/606.F4.6/80

### Resume

Cet rapport presente les resultats de la 1ère phase et la 2ème phase de mesures des charges de la circulation sur trois ponts d'arcier hollandais et des contraintes causées. La but de cette recherche est l'etude de la relation de la circulation des charges de la circulation et des contraintes dans les elements constitutifs des ponts pour obtenir une analyse meilleure de la fatigue des ponts. Le programme de la recherche est un element d'une programme Européenne dans le quel prendent part la Belgique, la France, l'Allemagne, l'Angleterre, l'Italie et les Pays Bas. Une assistance financière avait obtenu de la Communauté Européenne du Charbon et de l'Arcier.

"Messung und interpretation der Verkehrsbelastungen von  
Stahlbrücken"

Schlussbericht Zweite Phase, EGKS-Konvention 7210/606.F4.6/80

Zusammenfassung

Dieses Bericht präsentiert die erste und zweite phase  
resultaten der Messungen von Verkehrslasten und der Bean-  
spruchungen an drei holländischen Stahlbrücken.

Das Ziel von diese Forschungsarbeiten ist die Untersuchung  
nach die Beziehung zwischen die Verkehrslasten und die  
Beanspruchungen der Brückbauteile um der Widerstandsfähig-  
keit gegen Ermüdung von Stahlbrücken besser zu können  
analysieren. Das Forschungsprogramm ist ein Teil von das  
europäischer Programm wo die in Belgien, Frankreich,  
Deutschland, Grossbritannien, Italien und den Niederlanden  
vorgenommenen Untersuchungen wurden koordiniert.

Das Project wurde durch die Europäische Gemeinschaft für  
Kohle und Stahl finanziell unterstützt.



1. Introduction



## 1. INTRODUCTION

For years bridges have been designed using existing codes derived mainly from the behaviour under static loading. A lot of data available from laboratory tests have improved the knowledge about stability and static strength of connections. The ratio between traffic load and dead load, however, is increasing in modern steel bridges due to lower dead loads and higher design stresses. This leads to the conclusion that a fatigue analysis of bridges becomes more and more important.

The fatigue behaviour of a bridge component is influenced by many parameters such as notches (stress concentrations), steel qualities (including heat affected zones due to welding) and corrosion. A very important factor however, is the variations in stresses which the bridge component will see during life. These irregularly varying stresses (stress time history) have to be known and interpreted before they can be used for fatigue life estimates. The knowledge about stress-time histories is hard to get from calculations. Even when the stress induced by a certain load on a certain place is well-known, the lack of information about the load-time history in combination with the lateral distribution of the loads on the bridges will make it impossible to calculate stress time histories.

On the other hand measurements of only stress-time histories will be a waste of time and money.

Measurements during long times would be necessary and even then future changes in traffic can not be taken into account. Therefore in this investigation traffic, traffic loadings and the induced stress-variations have been measured to be able to study the relations between them.

As stated above stress time histories have to be interpreted before they can be used for fatigue life estimates. There are a number of different methods available to do this on a statistical basis. Most widely used are the counting methods from which stress-spectra can be derived. In this report the rainflow and level crossings methods are used for

analysing stress-time histories.

These stress-spectra cannot be used directly for bridge design. They have to be compared with static stress expectancy and extrapolated and corrected for the traffic, the bridge will see during life, with help of the above mentioned relations.

In 1976 the ECSC-Executive Committee F4 installed a working group called "Dynamic loads on bridges" which overall objective is to derive improved and simplified analysis of the traffic induced stresses in steel bridges for the purpose of design against fatigue. The countries participating<sup>1)</sup> executed a coordinated research program. The final reports of the first phase were presented in 1979 (see Ref. 6-1).

The results of the Dutch contribution to the second phase of the research program are presented in four technical progress reports (1-7-1980 until 1-7-1982) (see Ref. 6-2). This final report deals with the complete Dutch contribution to the first and second phase of the European investigation consisting of:

- measurements of the traffic and classification of the data
- measurements of the stresses in some bridge components; analysis by means of rainflow and level crossings methods;
- recording of the influence planes statically as well as dynamically
- calculation of the influence planes

---

1) Participating institutes:

- Transport and Road Research Laboratory - Crowthorne
- Laboratorium für Betriebsfestigkeit - Darmstadt
- Laboratoire Central des Ponts et Chaussées - Paris
- Université de Liège, Institut du Genie Civil - Liège
- Università di Pisa, Laboratoria Officialle par le experience dei material da Construzione - Pisa
- Technische Hogeschool Delft, Stevin laboratorium - Staalconstructies - Delft



(these subjects will be treated in chapter 3 of this report)

- extrapolation of measured axle loadspectra and stress-spectra
- fatigue loads of vehicle types, axle loads and stress-data
- damaging potential of the population of commercial vehicles, axle loadspectra and stress-spectra
- fatigue life expectance calculations using the regulations for calculations of fatigue loaded welded joints in the Netherlands
- relationship traffic-data to stress-data; the effect of temperature of asphalt surfacing; relative contribution of front and rear wheels to fatigue damage

(these subjects will be treated in chapter 4 of the report).

More detailed information about the measurements (shorter periods, other traffic circumstances and the like) on the three bridges is given in the detailed reports (see Ref. 6-3).



2. Bridge descriptions and location of the measuring points.



## 2. BRIDGE DESCRIPTIONS AND LOCATION OF THE MEASURING POINTS

CONTENTS	Page
2.0 Introduction	2-2
2.1 Haagsche Schouw Bridge	
2.1.1 Description of the bridge	
2.1.2 Location of the measuring points	
2.2 Rheden Bridge	2-3
2.2.1 Description of the bridge	
2.2.2 Location of the measuring points	
2.3 Leiderdorp Bridge	2-4
2.2.1 Description of the bridge	
2.2.2 Location of the measuring points	
2.4 Figures	2-5

## 2. BRIDGE DESCRIPTIONS AND LOCATION OF THE MEASURING POINTS

### 2.0. Introduction

Three bridges have been chosen which satisfy the following criteria:

- a single carriage way bridge
- a bridge with two lanes only
- a bridge with a simple structural system
- a bridge in a road where the traffic pattern is not disturbed by exits or entrances close to the bridge.

The first bridge is situated in highway 44 crossing the river "Oude Rijn" at the "Haagsche Schouw".

The second bridge called the "Rheden Bridge" is crossing the river "IJssel" near Arnhem in highway 12.

The "Leiderdorp Bridge" situated in highway 4, also crossing the river "Oude Rijn" is the third measured bridge.

### 2.1. Haagsche Schouw Bridge

#### 2.1.1. Description of the bridge

This bridge consists of two parallel independent movable bascule bridges. The west bridge was chosen for serving the southbound traffic (Amsterdam to the Hague).

The structure is composed of two main steel girders and a number of cross girders with longitudinal stringers on top. The deck is made of wooden boards with an asphalt top layer. Figure 2.1.1 on page 2-6 shows some dimensions of this bridge.

#### 2.1.2. Location of the measuring points

In a cross-section, various strain gauges were applied in order to determine the distribution of the stresses in that cross-section (see figure 2.1.2. on page 2-7 ). From this it appeared that the stress-pattern in the upper flange is disturbed by secondary effects such as transverse bending of the flanges. Therefore the definite measurements were

made with straingauges only applied on the bottom flanges.

At each measuring point four active straingauges were used and combined in such a way that the resulting measured value is not sensitive to variations in temperature and transverse bending of the girder (complete wheatstone Bridge see fig. 2.1.3. on page 2-8 ).

Figure 2.1.4. on page 2-9 give the location of the measuring points. The numbers 1, 2 and 3 on a cross-girder, the numbers 4 - 21 on various stringers.

It appeared that the analysis of the stresses in points 1 and 4.12 gave a lot of problems due to the dynamic response of this bascule bridge. For that reason only the points 2-3 and 13-21 were measured permanently.

## 2.2. Rheden Bridge

### 2.2.1. Description of the bridge

This bridge consists of two parallel independent bridges. The south bridge was chosen for serving the eastbound traffic (Rotterdam to Oberhausen).

The main structure is composed of two main steel girders with five spans ( $45 + 50 + 105 + 50 + 45 = 295$  meters) and a number of cross girders which are welded to the steel deckplate.

The longitudinal stringers are stiffeners of the deckplate (orthotropic deck) which has an asphalt top layer.

Figure 2.2.1. on page 2-10 gives some dimensions of this bridge.

### 2.2.2. Location of the measuring points

Just as the "Haagsche Schouw Bridge" the straingauges were attached to the bottom side of the longitudinal stiffeners and one cross girder.

Figure 2.2.2. on page 2-11 shows the location of these measuring points. The number 1 and 2 on a cross girder,

the numbers 3-18 on various longitudinal stiffeners. The measuring points 3-10 at a midspan point and 11-18 at the point where the continuous stringer is supported by the cross girder.

### 2.3. Leiderdorp Bridge

#### 2.3.1. Description of the bridge

This bridge consists of two parallel independent movable bascule bridges. The west bridge was chosen for serving the southbound traffic (Amsterdam to the Hague and Rotterdam).

The structure is composed of two main steel girders and a number of cross-girders. On top of this primary construction a secondary orthotropic deckplate construction is bolted (see figure 2.3.1. on page 2-12). This secondary construction is a replacement for the structure as given in figure 2.3.2. on page 2-12, where on top of the cross-girder several longitudinal stringers and a deck made of wooden boards was fixed.

More about the constructive performance of the present structure and some dimensions of this bridge are given in figure 2.3.3. on page 2-13.

#### 2.3.2. Location of the measuring points

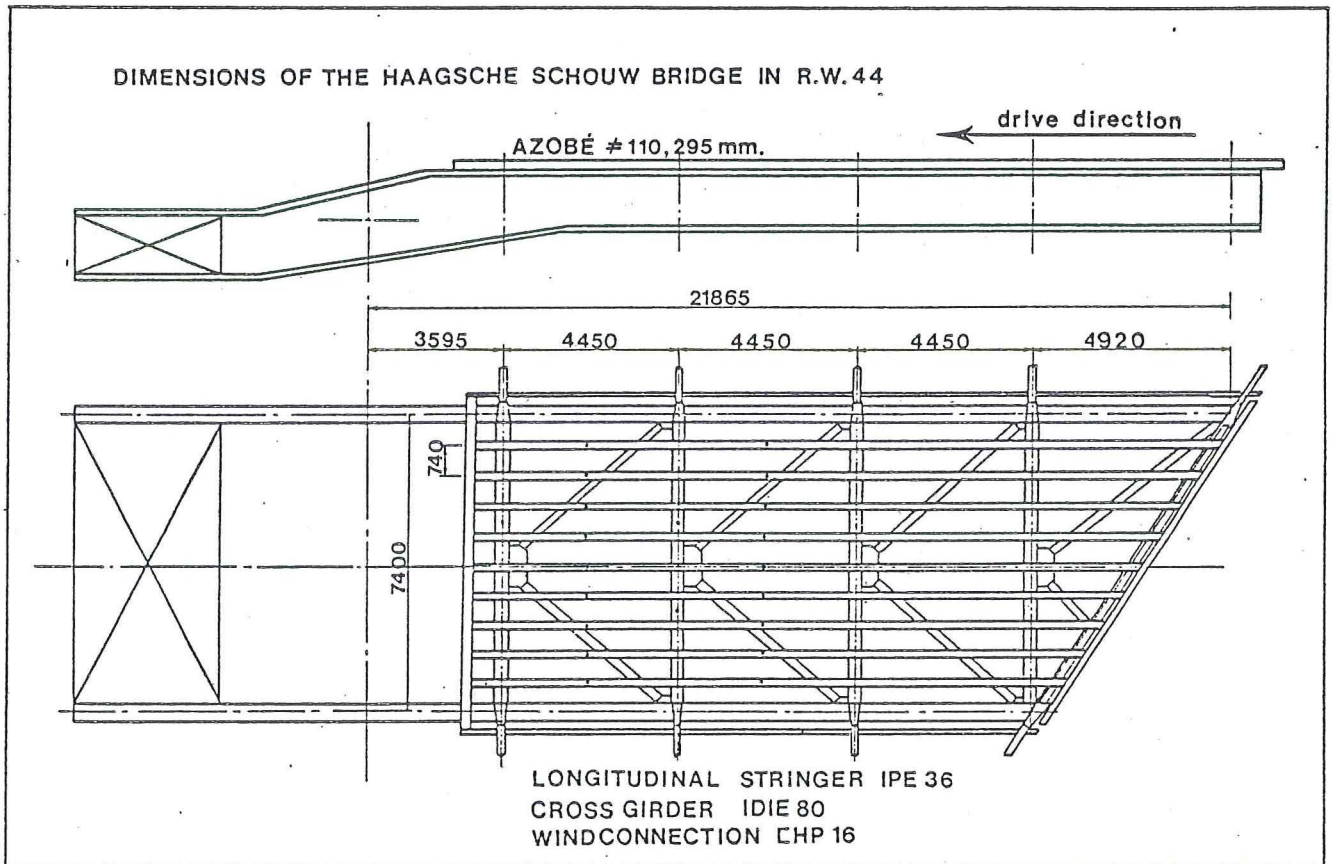
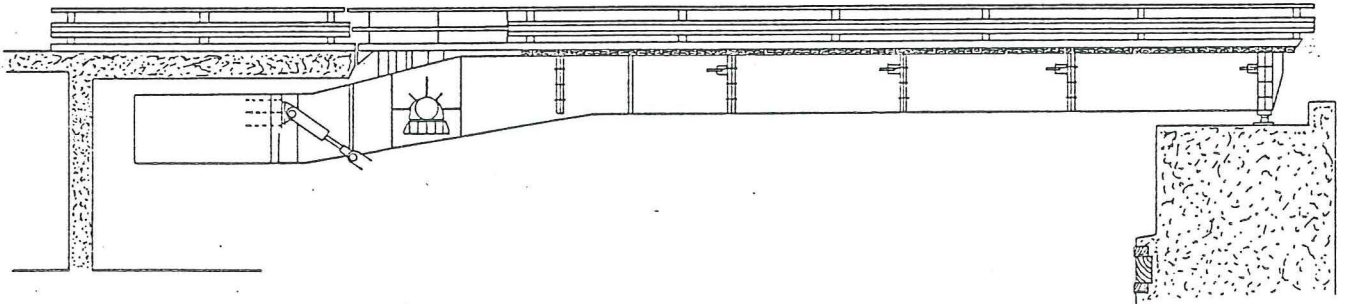
All the straingauges were applied on the orthotropic deckplate construction. At each measuring point four active straingauges were used and combined in such a way that the resulting measured value is not sensitive to variations in temperature and transverse bending of the girder.

Figure 2.3.4. on page 2-14 give the location of the measuring points on various longitudinal stiffeners of the deckplate and on various cross-girders of the deckplate.



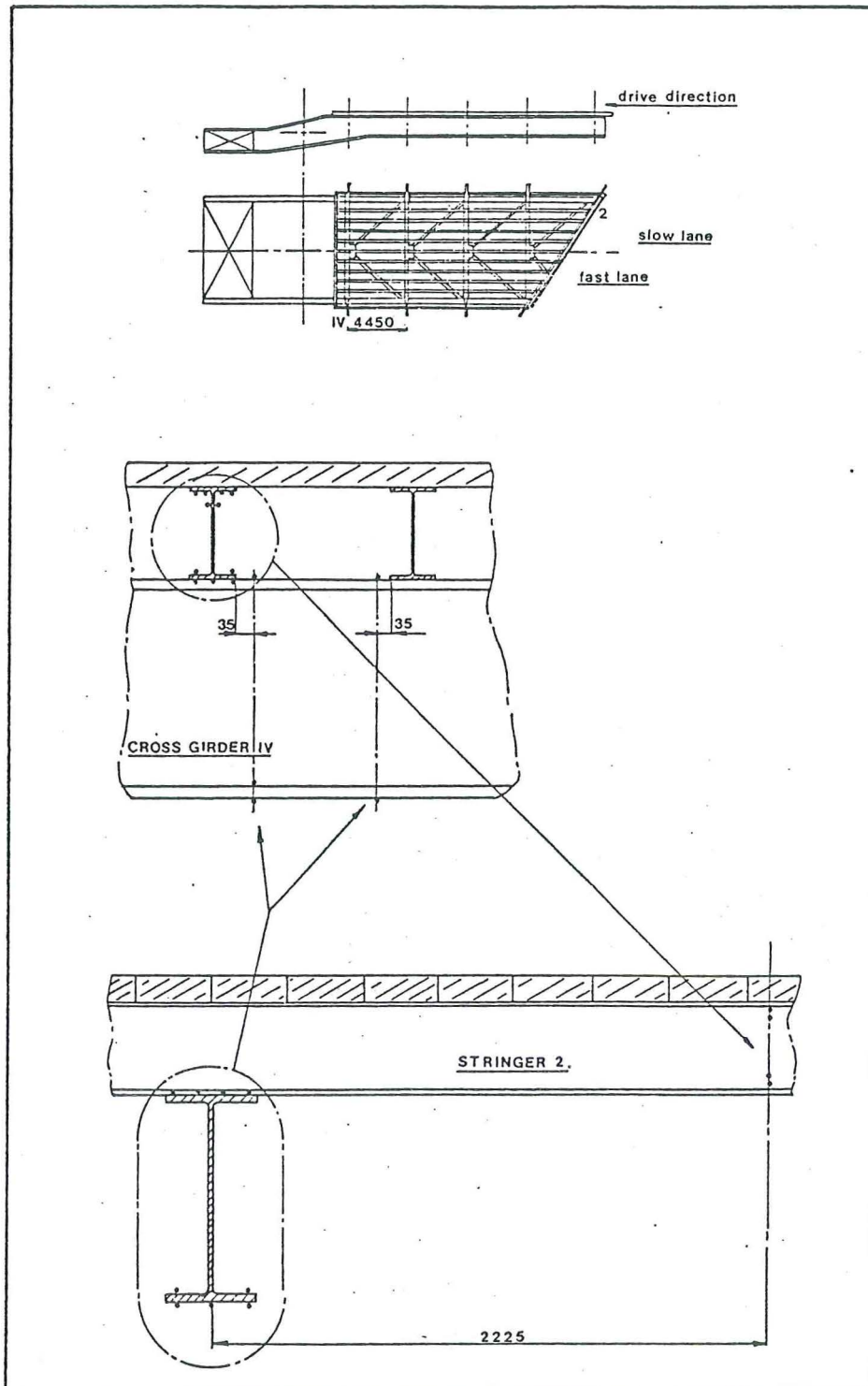
2.4. Figures

List of figures:	Page
<u>Haagsche Schouw Bridge</u>	
2.1.1. Dimensions of the bridge	2-6
2.1.2. First location of several straingauges	2-7
2.1.3. Combination of straingauges per measuring point	2-8
2.1.4. Location of the final measuring points	2-9
<u>Rheden Bridge</u>	
2.2.1. Dimensions of the bridge	2-10
2.2.2. Location of the measuring points	2-11
<u>Leiderdorp Bridge</u>	
2.3.1. Orthotropic deckplate construction	2-12
2.3.2. Replaced construction of the wooden deck	2-12
2.3.3. Dimensions of the bridge	2-13
2.3.4. Location of the measuring points	2-14



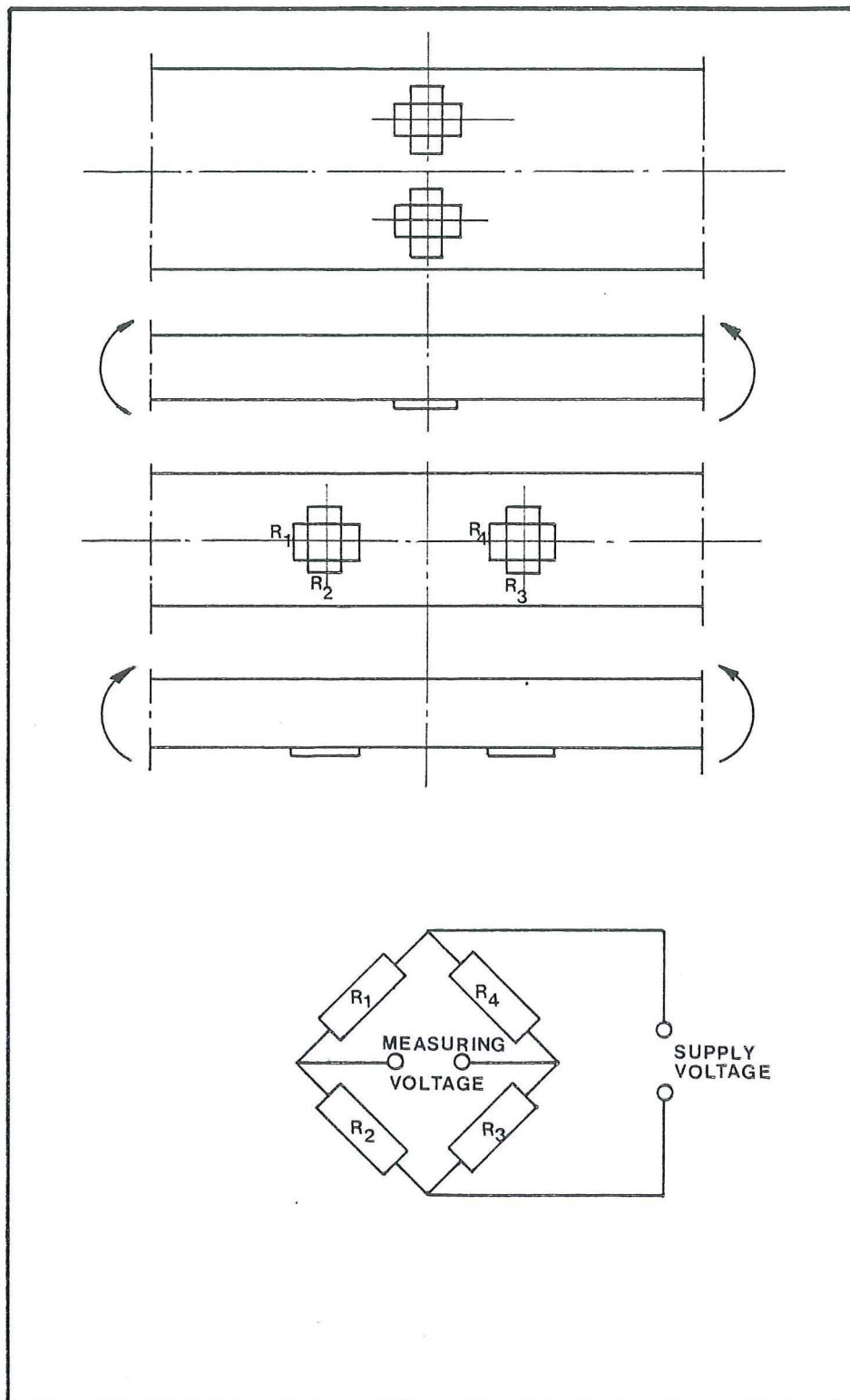
Dimensions of the Haagsche Schouw Bridge

Figure 2.1.1

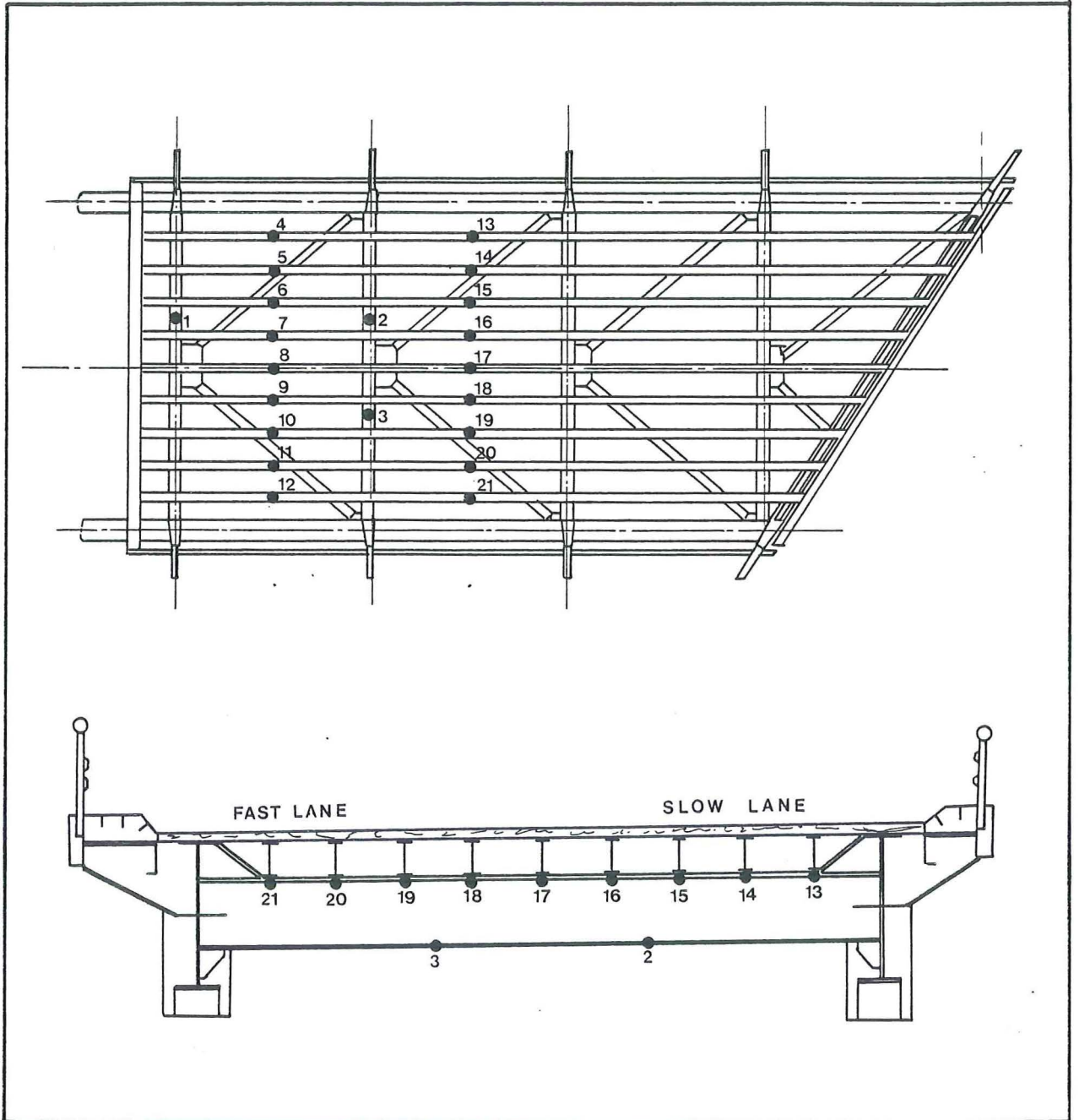


First location of several straingauges on the Haagsche Schouw Bridge

Figure 2.1.2.

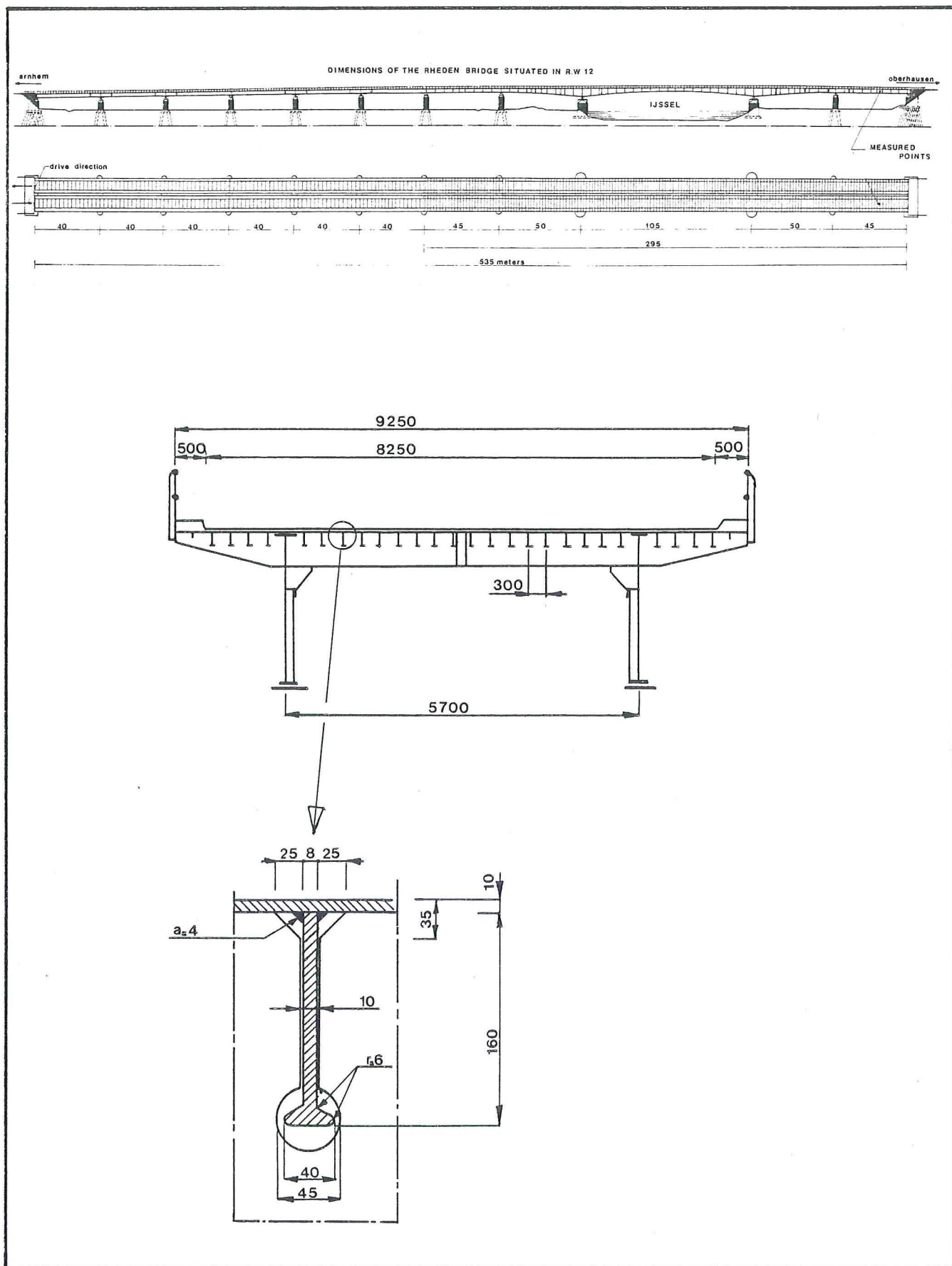


Combination of strain gauges per measuring point  
Figure 2.1.3

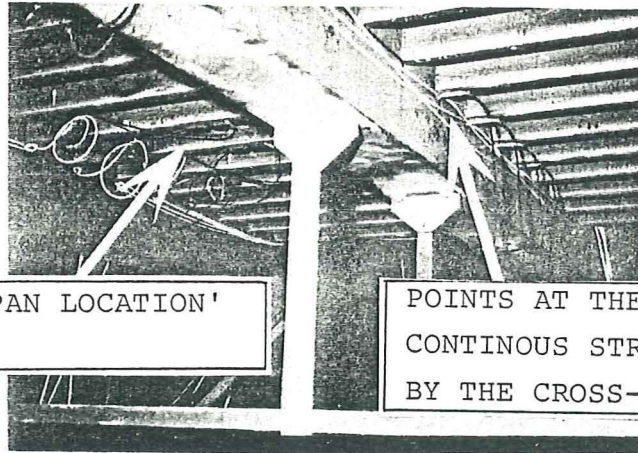


Location of the final measuring points on the Haagsche Schouw Bridge

Figure 2.1.4.

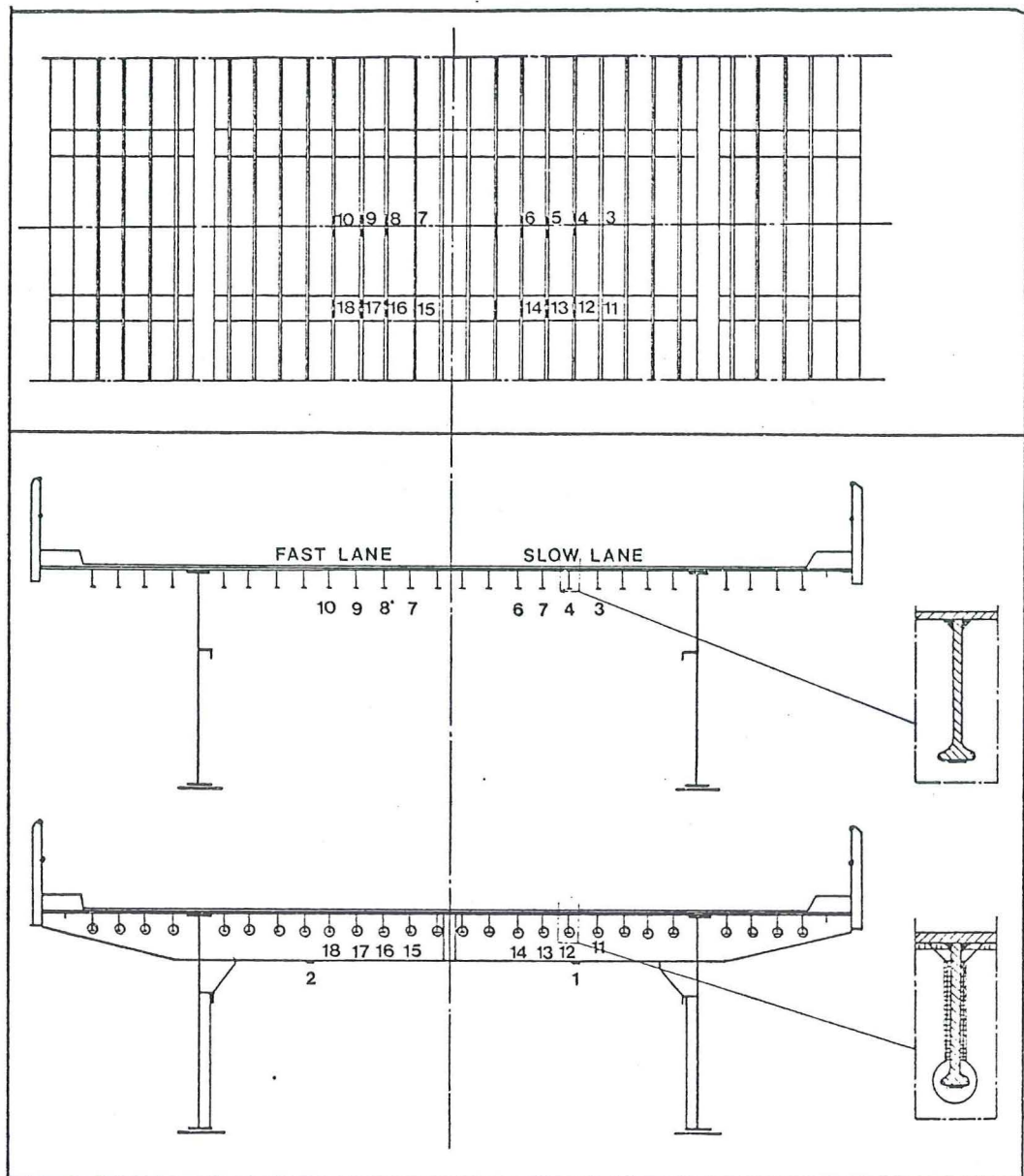


Dimensions of the Rheden Bridge  
Figure 2.2.1.



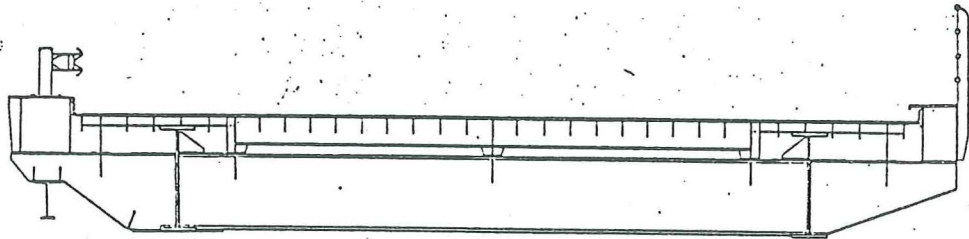
POINTS AT 'MIDSPAN LOCATION'  
(3 - 10)

POINTS AT THE POINT WHERE THE  
CONTINUOUS STRINGER IS SUPPORTED  
BY THE CROSS-GIRDER (11 - 18)



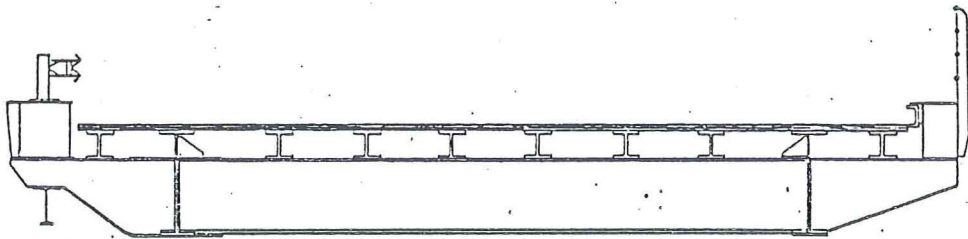
Location of the measuring points  
on the Rheden Bridge

Figure 2.2.2.



Orthotropic deckplate construction of the  
Leiderdorp Bridge

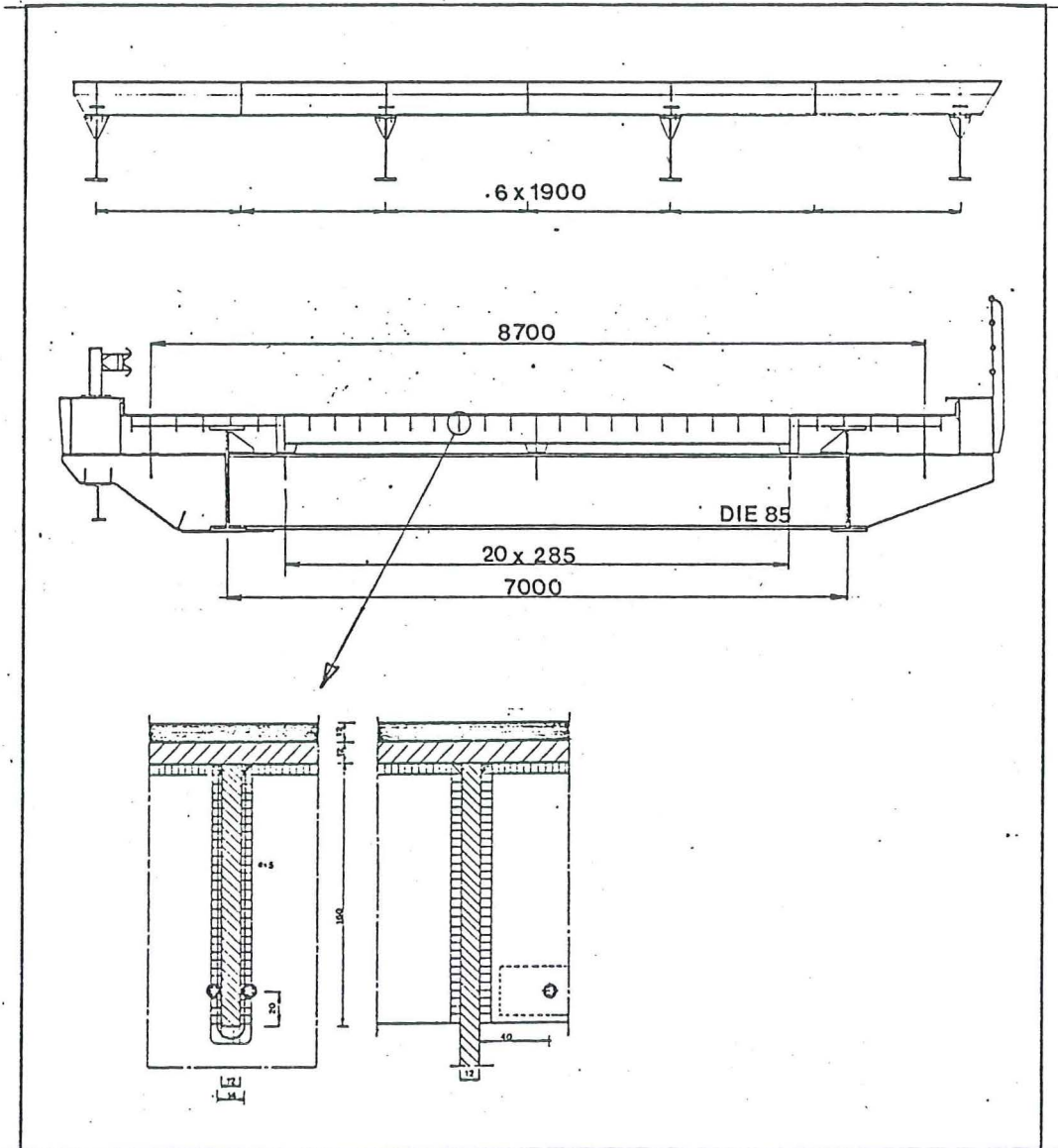
Figure 2.3.1



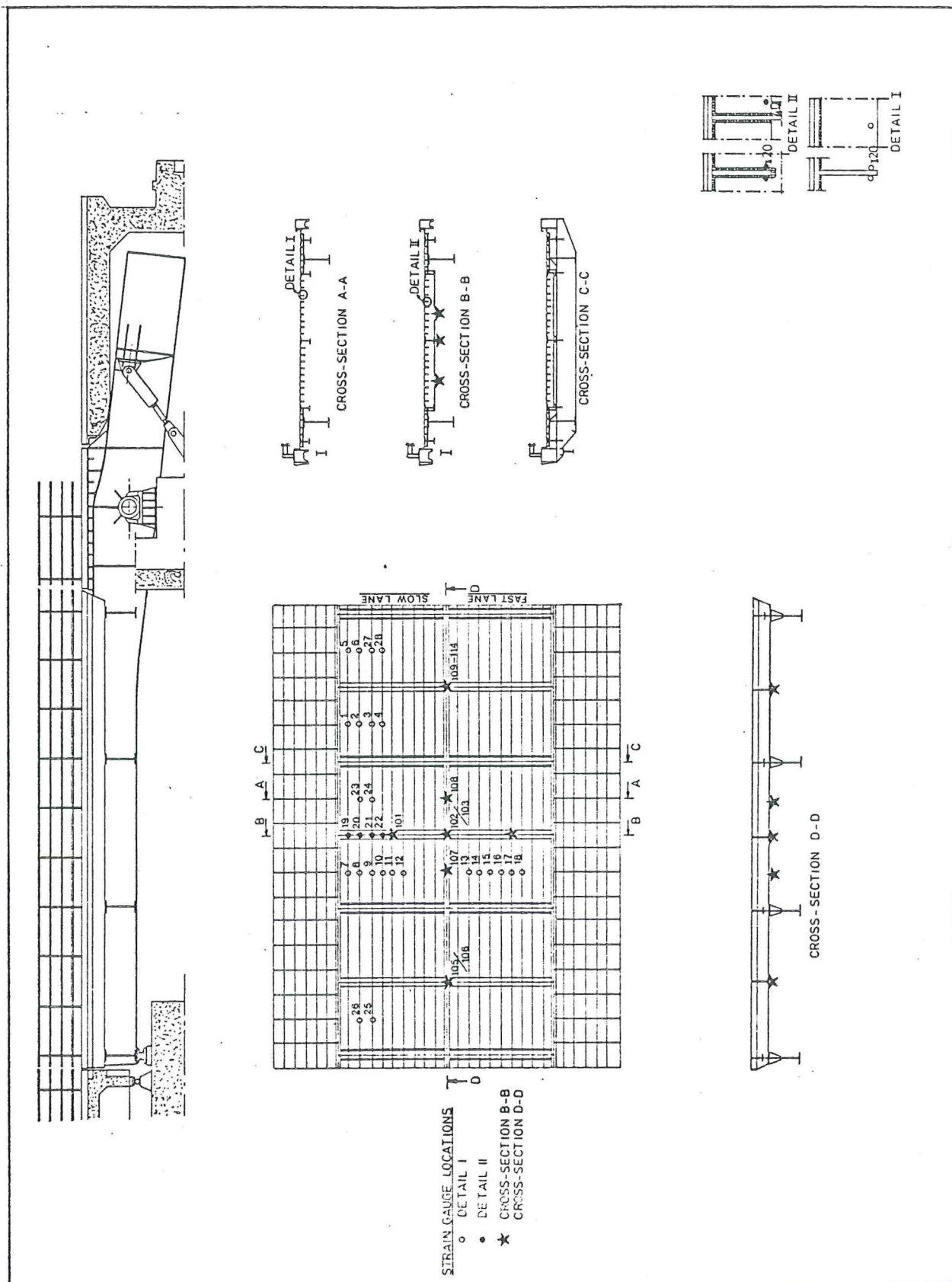
Preliminary construction of the bridge deck  
of the Leiderdorp Bridge

Figure 2.3.2





Dimensions of the Leiderdorp Bridge  
Figure 2.3.3.



Locations of the measuring points on the Leiderdorp Bridge (1)

Figure 2.3.4

3. Measurement of traffic loads and stresses in the bridge structures



### 3. MEASUREMENT OF TRAFFIC LOADS AND STRESSES IN THE BRIDGE STRUCTURES

CONTENTS	Page
3.1. Introduction	3-4
3.2. Instrumentation	3-5
3.2.1. Measurement of vehicle characteristics	3-5
3.2.1.1. Weighbridges	3-5
3.2.1.2. Inductive loops	3-6
3.2.1.3. An alternative method to determine the axle loads	3-6
3.2.2. Measurement of stresses	3-7
3.2.3. Data acquisition system	3-7
3.2.4. Figures	3-8
3.3. The processing of the data	3-14
3.3.1. The processing of the traffic-data	3-14
3.3.1.1. Type classification of vehicles	3-14
3.3.1.2. Preliminary data analysis	3-14
3.3.1.3. Statistical process of the traffic data	3-14
3.3.1.3.1. Axle load code and axle distance code	3-14
3.3.1.3.2. Frequency distributions of axle loads	3-15
3.3.1.3.3. Frequency distributions of axle distances	3-15
3.3.1.3.4. Frequency distributions of vehicle intervals	3-15
3.3.2. The processing of the stress-data	3-15
3.3.2.1. The level crossing counting method	3-16
3.3.2.2. The rainfall counting method	3-16
3.3.2.3. Statistical process of the stress-data	3-16
3.3.2.3.1. Frequency distributions of rainfall counts	3-17

CONTENTS	Page
3.3.2.3.2. Frequency distributions of level crossings	3-17
3.3.3. Figures and tables	3-17
3.4 Results of measured stresses, due to vehicles of which the axle loads, axle distances and vehicle intervals have been measured to	3-20
3.4.1. Introduction	3-20
3.4.2. Data of measurements	3-20
3.4.3. Results of measured traffic-data for three steel bridges	3-21
3.4.3.1. Frequency curves of axle loads	3-21
3.4.3.2. Frequency tables of axle loads and axle distances	3-22
3.4.3.3. Mean value of axle loads and axle distances	3-22
3.4.3.4. Distribution of the vehicle types over the traffic	3-22
3.4.3.5. Frequency distributions of vehicle intervals	3-23
3.4.3.6. Figures and tables	3-24
3.4.4. Comparison with measured traffic on other European bridges	3-33
3.4.4.1. Bridges studied for the ECSC researchprogram	3-33
3.4.4.2. Frequency curves of axle loads	3-33
3.4.4.3. Frequency of occurrence of vehicle types	3-34
3.4.4.4. Frequency distributions of vehicle intervals	3-34
3.4.4.5. Figures and tables	3-34
3.4.5. Measured stresses due to daily traffic loading	3-37
3.4.5.1. Haagsche Schouw Bridge	3-37
3.4.5.1.1. Measured stresses during 66 hours	3-37
3.4.5.2. Rheden Bridge	3-38

CONTENTS	Page
3.4.5.2.1. Influence of the transverse distribution of the traffic on the stress distribution in a cross section of the bridge	3-38
3.4.5.2.2. Comparison of measured stress-spectra in combination of different influence lines	3-39
3.4.5.3. Leiderdorp Bridge	3-40
3.4.5.3.1. Relation between stress distribution in one cross section of the bridge structure and the transverse distribution of wheel positions	3-40
3.4.5.3.2. Stress distribution in a longitudinal stiffener of the bridge deck in several cross sections of the bridge	3-41
3.4.5.3.2.1. The same detail	3-41
3.4.5.3.2.2. Different details	3-41
3.4.5.4. Figures and tables	3-42
3.4.6. Comparison with measured stress-data on other European bridges	3-58
3.4.6.1. Maximum measured stresses	3-58
3.4.6.2. Some remarks	3-58
3.4.6.3. Figures and tables	
3.5. Results of measured stress data in relationship of influence lines	3-60
3.5.1. The processing of statical measured data	3-60
3.5.2. Results of statical measured data	3-60
3.5.3. Dynamical influence factors	3-60
3.5.4. Figures and tables	3-61
3.6. Comparison between computed and measured stress data	3-64
3.6.1. Simulation of stress-spectra	3-64
3.6.2. Computed static influence lines	3-64
3.6.3. Figures and tables	3-65
3.7. Concluding remarks chapter 3	3-70

### 3. MEASUREMENT OF TRAFFIC LOADS AND STRESSES IN THE BRIDGE STRUCTURES

#### 3.1. Introduction

This chapter of the final report contains results of measurements on three Dutch bridges.

Installed weighbridges and magnetic coils recorded the traffic in terms of axle loads, axle distances, vehicle length, vehicle speed and vehicle intervals. The lorries were classified according to their number of axles in 19 types of which 5 types are dual lorries subdivided into different axle distances.

Installed straingauges on several stringers and cross girders recorded the stresses in the bridge structures.

A computerprogramme was made to record the traffic loads and inductive loop output and to detect the peakvalues of the measured stresses. Other computerprogrammes were made to arrange the data in a convenient order (statistical process) with the help of the laboratory computer.

The relation between the load on the bridge deck and the stresses in the measuring points has been recorded by measuring the influence planes statically as well as dynamically.

For one bridge the measured and calculated static influence planes are compared together and an investigation took place to deduce the traffic from the peakvalues of the measured stresses on the bridge. |Ref. 6-4|



## 3.2. Instrumentation

### 3.2.1. Measurement of vehicle characteristics

To determine the features of the traffic weighbridges and inductive loops have been installed in the pavement behind the bridge (see figure 3.2.1. on page 3-9 ).

The weighbridge in the slow lane measures the wheelloads of the righthand wheels of the vehicles in that lane and the weighbridge in the fast lane measures the wheelloads of the lefthand wheels of the vehicles in that lane.

The demands on the flatness of the road in the vicinity of a weighbridge are rather high. Therefore it is doubtful whether one will always succeed in installing a good functioning weighbridge close to the bridge.

Besides, measuring with weighbridges has more disadvantages namely the high costs and the hampering of the traffic involved with the installation and maintenance of the weighbridges as well as the alterations in the traffic flow between the measuring points on the bridge and the weighbridge. Therefore an investigation has been done to deduce the static axle loads, from the measured stresses in the Haagsche Schouw Bridge. |Ref. 6-4|.

#### 3.2.1.1. Weighbridges (loads, lateral distribution)

The weighbridges consists of a steel frame in which two steel measuring plates are fitted. The steelframe is held by resinmortar in a pocket cut-out in the asphalt pavement. The deflection of a weighplate is proportional to the wheel load exerted. It was measured with straingauges.

The traffic distribution in the lateral distribution was determined coarsely by detecting loads in the fast and slow lane while a fine determination was made using the measurings of the stresses in the longitudinal girders or stiffeners of the bridge.

The weighbridges were recommended by the Government Laboratory for highway designs and installed under their supervision. Figure 3.2.2. on page 3-9 shows a weighbridge as installed while figure 3.2.3. on page 3-10 gives the dimensions of it.

3.2.1.2. Inductive loops (speed, vehicle length, axle distance)

An inductive loop consists of a copper wire, placed in a groove in the pavement which is then filled with a resin mortar.

When a vehicle passes over the loop the reactance of the loop changes. The speed and length of a vehicle can be determined from the difference in time of passing two subsequent loops and their distance apart.

The distance between two vehicles can be determined from the difference in time of the loop being passed over and the vehicle speed. The axle distance can be determined from the vehicle speed and the difference in time of touching the weighbridges by the wheels.

The "Dienst Verkeerkunde" of "Rijkswaterstaat" installed two inductive loops in each lane. Figure 3.2.4. on page 3-10 shows four inductive loops as installed.

3.2.1.3. An alternative method to determine the axle loads

From figure 3.2.5. on page 3-11 appear, that every passing of an axle causes a maximum in the measured stresses. Such a maximum is mainly determined by the magnitude of the static axle loads.

Deviations will occur due to:

- a. dynamic effects of the bridge
- b. dynamic effects of the vehicle
- c. presence of other vehicles
- d. lateral position of the vehicle
- e. width of the track of the vehicle.

From mentioned research appears that the relation between the axle loads and axle distances of a passing vehicle, an influence plane of the bridge structure and a signal generated by a transducer can be presented by a convolution. The axle loads and axle distances can be solved from this by means of inverse filtering. This method is rather laborious, because the detection has to take place on line, a simplified solution has been searched for.

It appeared that the influence of the lateral position of the passing vehicle on the measured results can be minimized by weighing and summing the signals of several transducers. For this method of detection it is necessary to know several influence planes. The determination of these planes appear to be very difficult as a cause of practical and theoretical limitations.

Reasonable useful results were obtained by approximating a solution of an overdetermined system by the least square method.

Finally can be concluded that the method to detect the traffic depends on the measuring situation and the construction of the bridge.

### 3.2.2. Measurement of stresses

At each measuring point on the bridge structure, four active strain gauges were positioned and connected in such a way that the resulting measured quantity is not sensitive to variations in temperature and transverse bending of the girder (complete wheatstone bridge see chapter 2).

### 3.2.3. Data acquisition system

The data acquisition system was based in the Raytheon 704 mini computer. The addition of a highspeed reader and high speed punch increased the possibilities e.g. greater data storage.

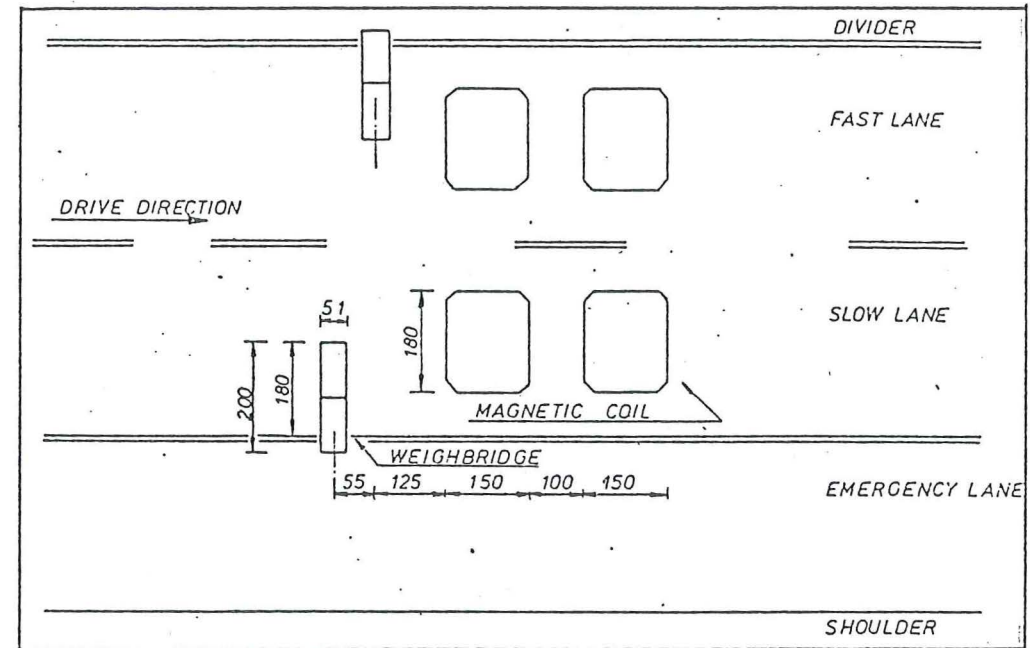
A computer programme was made to record the traffic loads and inductive loop output and to detect the peak values of the measured stresses. All these quantities were recorded on punch tape.

Other computerprogrammes were made to analyse the signals and to arrange them in a convenient order (statistical process, see chapter 3.3) with help of the laboratory computer.

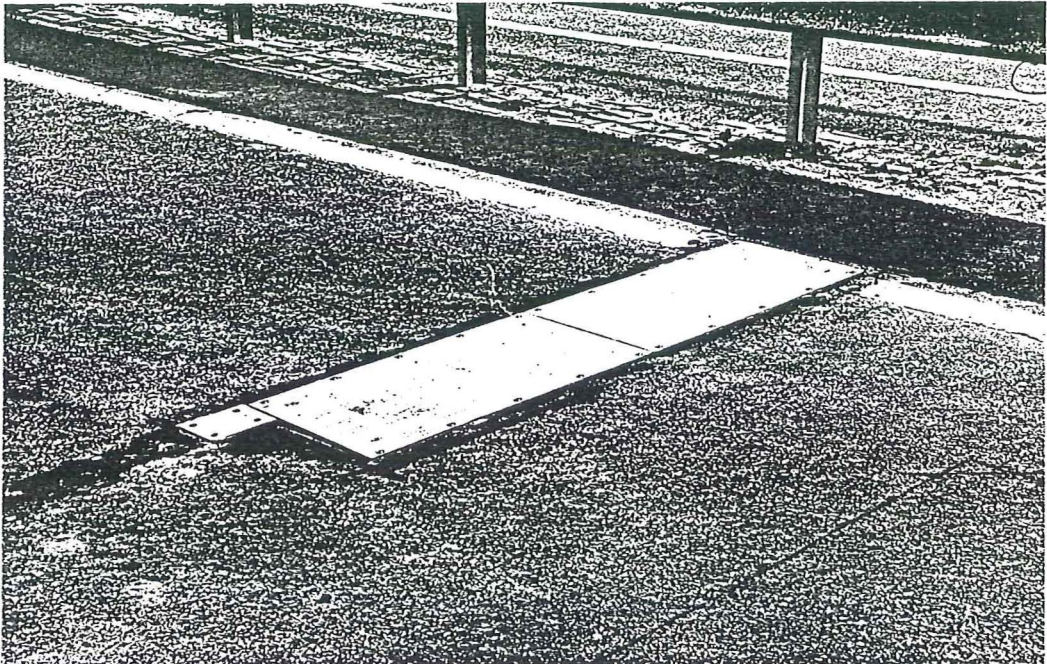
Figure 3.2.6 on page 3-12 shows the block outline of the measuring system and figure 3.2.7 on page 3-13 shows the measuring lorry including the measuring system and his own current supply.

#### 3.2.4. Figures

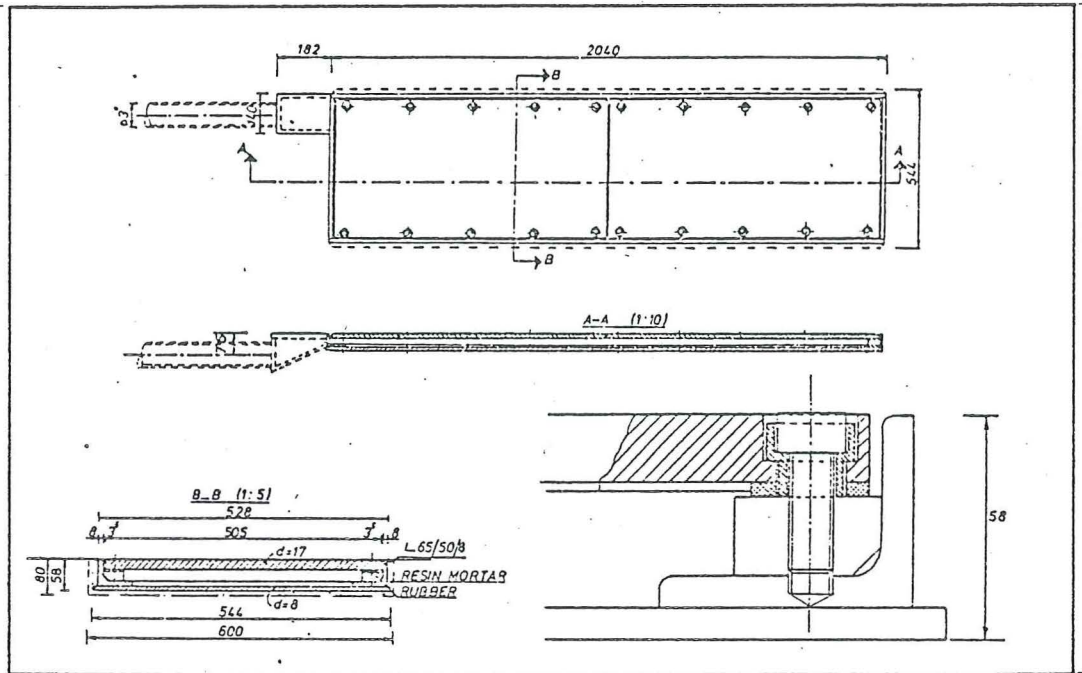
List of figures	Page
3.2.1. Weighbridges and inductive loops configuration	3-9
3.2.2. Photograph of an installed weighbridge	3-9
3.2.3. Dimensions of a weighbridge	3-10
3.2.4. Photograph of installed inductive loops	3-10
3.2.5. Digitalised recording of measuring point 14 of the Haagsche Schouw Bridge	3-11
3.2.6. Blockoutline of the measuring system	3-12
3.2.7. Photograph of measuring equipment	3-13



Weighbridges and inductive loops configuration  
Figure 3.2.1



Photograph of an installed weighbridge  
Figure 3.2.2



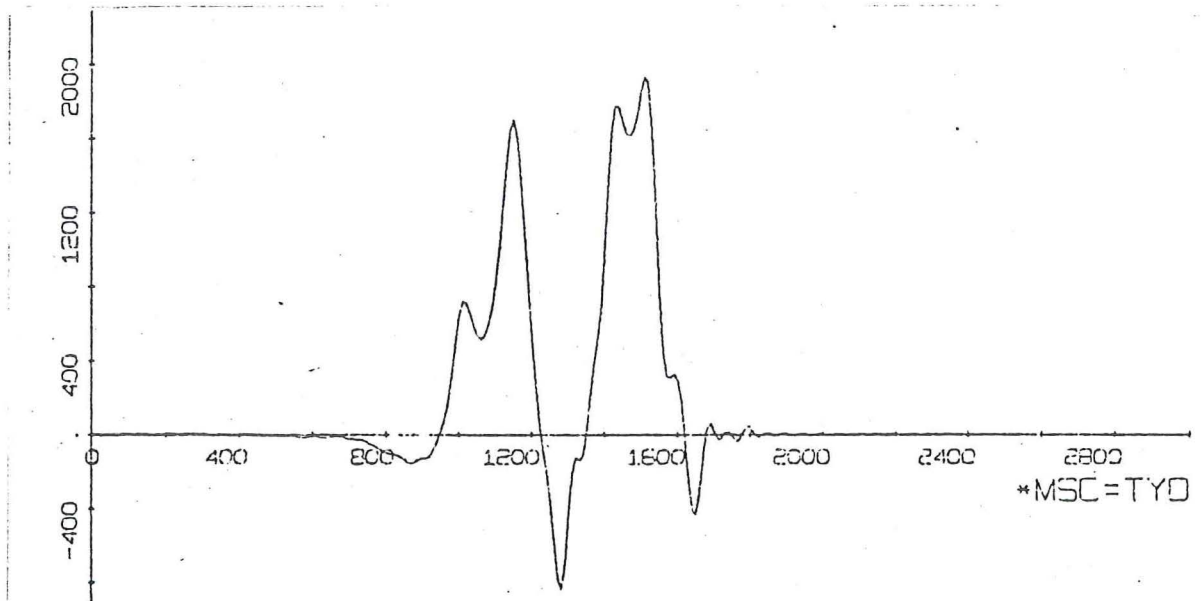
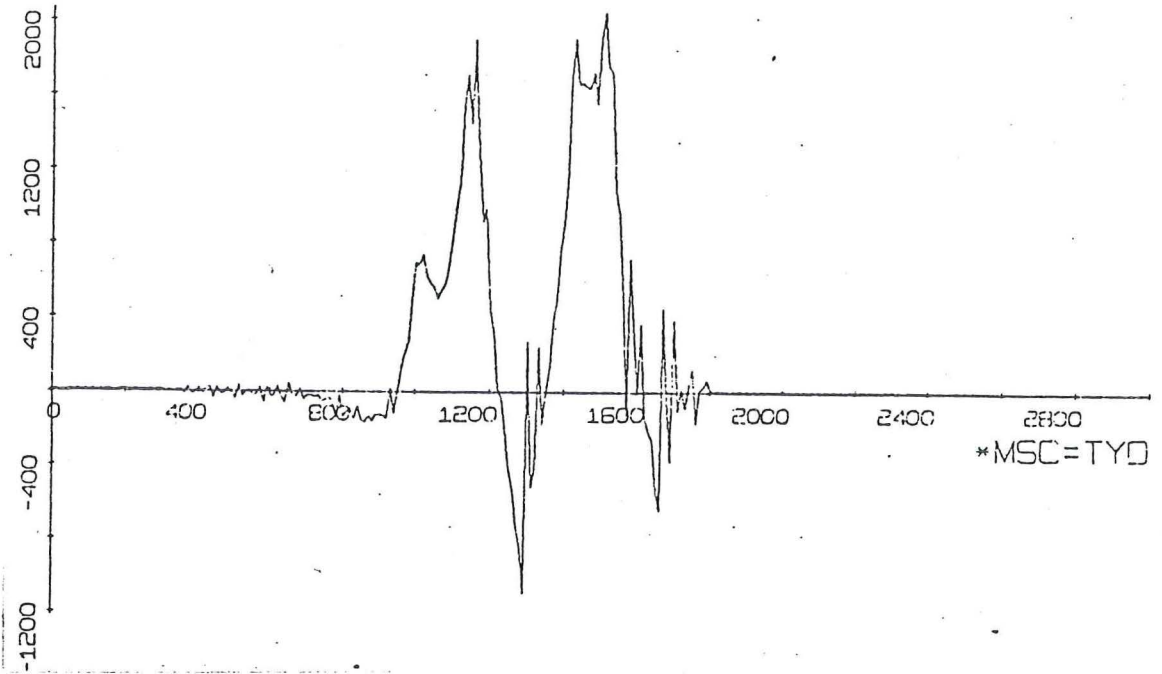
Dimensions of a weighbridge

Figure 3.2.3



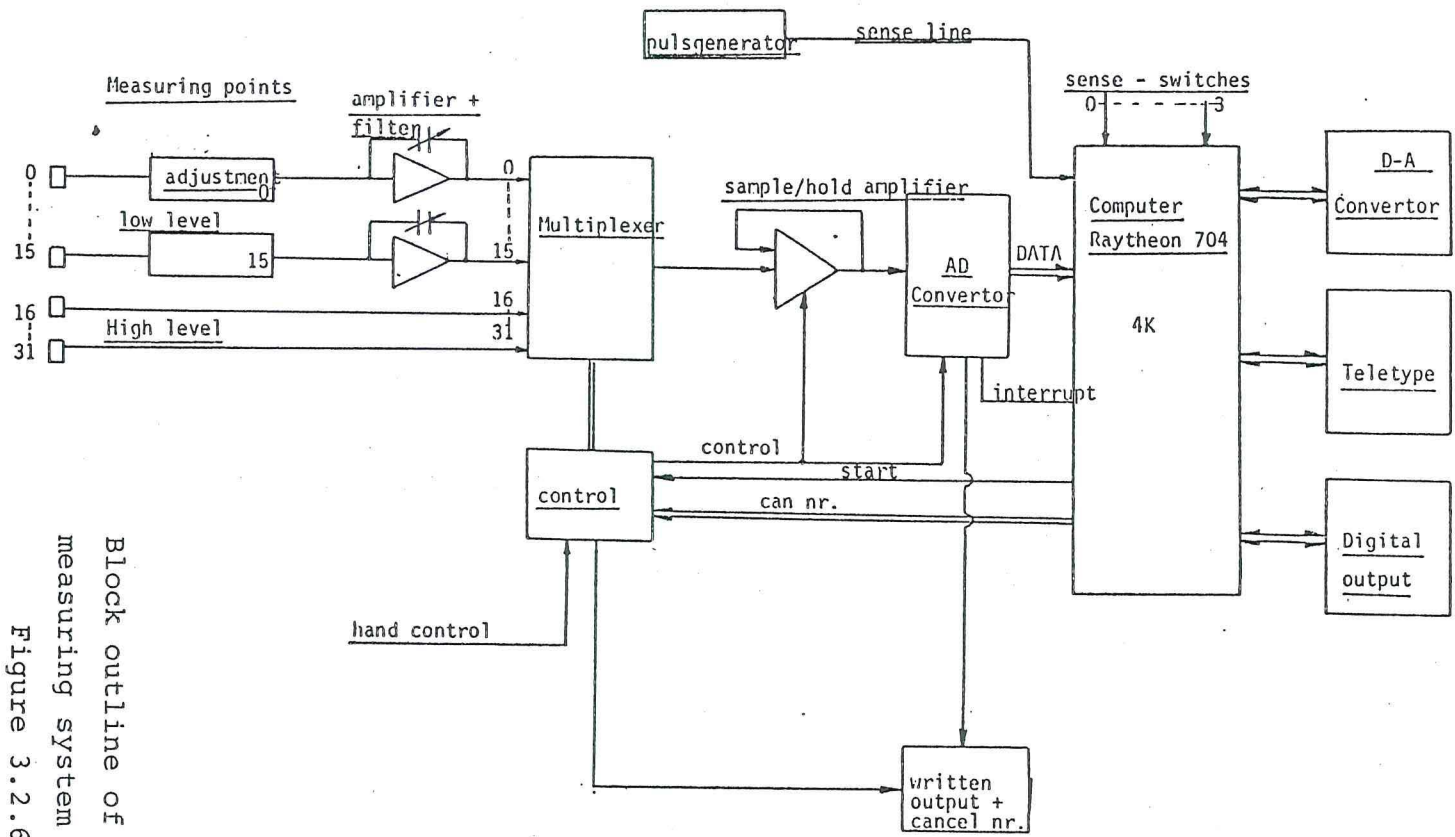
Photograph of installed inductive loops

Figure 3.2.4.



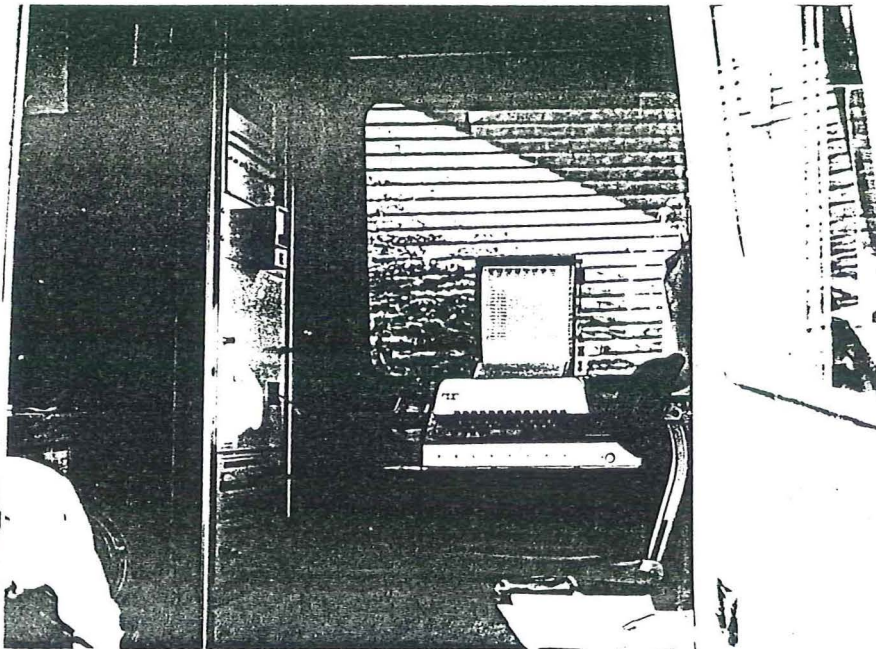
Digitalised recording of measuring point 14  
on the Haagsche Schouw Bridge

Figure 3.2.5



Block outline of the  
measuring system  
Figure 3.2.6





Photograph of the measuring equipment  
Figure 3.2.7

### 3.3. The processing of the data

#### 3.3.1. The processing of the traffic data

##### 3.3.1.1. Type classification of vehicles

To arrange the traffic data in a convenient order, the vehicles are grouped into types according to their number of axles as given in figure 3.3.1. on page 3-18.

In group 1 all vehicles are placed, which do not belong to other groups. All vehicles with two axles but with different axle distances are classified in groups 16 up to and including 20.

In group 21, all two axle vehicles are placed which have only one axle greater than 8 kN.

##### 3.3.1.2. Preliminary data analysis

Each punch tape containing the measured quantities has been analysed according to the mentioned system of vehicle identification in periods spanning a train of vehicles which are less than 300 m apart.

Figure 3.3.2. on page 3-18 shows a part of the preliminary analysis of the traffic data.

##### 3.3.1.3. Statistical process of the traffic data

###### 3.3.1.3.1. Axle load code and axle distance code

All axle loads are denoted by two numbers. The first one of which represents the class the vehicle belongs to.

The second indicates the number of the wheel counting from the front of the vehicle to its rear.

When the later is a zero obviously it is not a wheelnumber but the figure to which this number pertains is the average of axle loads of the specified type.

Just as the axle loads, the axle distances are grouped both into classes according to their magnitude and to their location between axles.

Both, axle load codes and axle distance codes are indicated in figure 3.3.3. on page 3-18.

#### 3.3.1.3.2. Frequency distributions of axle loads

The frequency distributions of axle loads are divided over eight frequency distribution tables and two cumulative relative frequency curves (see table III.3.1. on page 3-19).

The numbers of axle loads of a specific type and magnitude are tabulated over 80 axle load classes with a maximum of 160 kN. At the bottomlines of the columns the sum of the vehicles of a specific type and the mean and standard deviation of the columns are given. A sum of all measured axles per lane with a specific class of magnitude are given in the column headed "sum" of table 4 and 8 (see table III.3.1.).

Cumulative relative frequency curves are plotted for axle loads greater than or equal to 8 kN for both lanes. The loads are accumulated from the largest class to the class of 10 - 12 kN and divided by the total value.

#### 3.3.1.3.3. Frequency distributions of axle distances

With a method analogous to the one used for the axle load data, the axle distances are divided over four frequency distribution tables (see table III.3.2. on page 3-19 ).

The axle distances determined as stated in section 3.3.1.3.1. are grouped both into 80 classes according to their magnitude and to their location between the axles with a maximum of 8.1 meter.

#### 3.3.1.3.4. Frequency distributions of vehicle intervals

The numbers of commercial vehicle intervals per lane are tabulated over 30 classes with a maximum of 145 meter.

#### 3.3.2. The processing of the stress data

After analysing the traffic in periods spanning a train of vehicles which are less than 300 m apart, the measured stresses in these periods are analysed by rainfall counting and level crossings counting.

All stresses are counted including the values caused by the cars of which axle loads were not counted ( $< 8$  kN).

Both are worked out in frequency tables and in modified relative frequency curves.

### 3.3.2.1. The level crossings counting method

Only the levels in upward direction were counted

### 3.3.2.2. The rainflow counting method

Applying the rainflow counting method, the load time course is looked after a time axle directed down. It is considered as a collection roofs via the rain flows down.

Following rules must be applied:

The minimum and maximum value of the load time must be fixed. The whole course is divided in three periods namely:

1st start till first extreme

2nd first extreme till second extreme

3rd second extreme till end

The load interval always starts at the innerside of a peak-value. When the starting point of an interval is a minimum, a half fluctuation is counted between this minimum and the most positive maximum that occur before the load becomes more negative than the starting point of the interval.

When the starting point of an interval is a maximum, a half fluctuation is counted between this maximum and the most negative minimum that occurs, before the load becomes more positive than the starting point of the interval.

Figure 3.3.4. on page 3-19 shows an example of the rain flow counting method.

### 3.3.2.3. Statistical process of the stress data

Rainflow counts as well as level crossing counts are worked out in modified relative frequency curves. Usually, of course, a relative frequency is defined as the frequency of the individual divided by the sum of all frequencies. Since this definition was not used here, the word modified is inserted. This may lead to function values greater or lower than 1.

### 3.3.2.3.1. Frequency distribution of rainflow counts

The rainflow counts are gathered in frequency tables and modified cumulative relative frequency curves.

In the frequency tables the rainflow counts of a specific measuring point are tabulated over 40 stress range classes with a maximum of  $80 \text{ N/mm}^2$ .

Modified cumulative relative frequency curves of rainflow counts are plotted. The rainflow counts are accumulated from the largest class to the lowest class. The results are divided by the number of axle loads larger or equal to 10 kN which passed over the bridge.

### 3.3.2.3.2. Frequency distributions of levelcrossings

The levelcrossings counts are gathered in frequency tables and modified relative frequency curves.

In the frequency tables the levelcrossings of a specific measuring point are tabulated over 80 level classes with a minimum of  $-59.9 \text{ N/mm}^2$  and a maximum of  $+78.8 \text{ N/mm}^2$ .

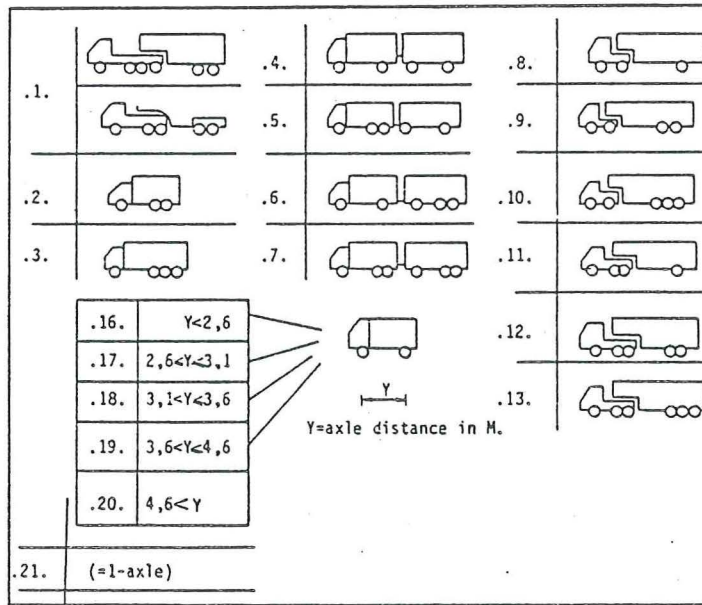
Modified relative frequency curves of levelcrossings counts are plotted. The levelcrossings counts are divided by the number of axle loads larger or equal to 10 kN which passed over the bridge.

### 3.3.3. Figures and tables

List of figures	Page
3.3.1. Vehicle type classification	3-18
3.3.2. Preliminary analysis of traffic data	3-18
3.3.3. Axle load code and axle distance code	3-18
3.3.4. The rainflow counting method	3-19

#### List of tables

III.3.1. View of the frequency distribution of axle loads	3-19
III.3.2. View of the frequency distribution of axle distances	3-19



Vehicle type classification

Figure 3.3.1.

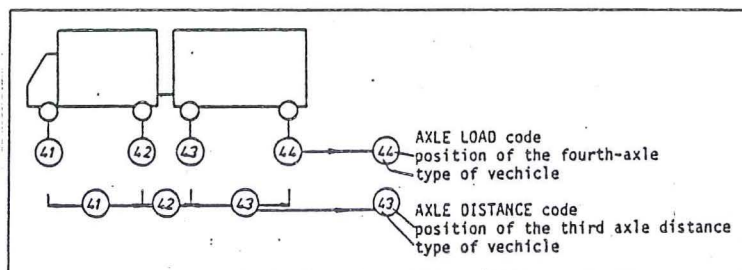
KARAKTERISERING VRACHTAUTO'S 3243 E METING DD32767 VAN DIE HAAGSCHE SCHOUW BRUG

CODENR. KARVD : 2319  
 PROEFNUMMER : 3243  
 DATUM METING : 32767  
 PROJECT NR. : 2131  
 GROEPSNR. : 24270

NR	L/R	TYPE	CAR.	L.	SNEELH.	AFSTAND	TIJD							
								M.	M/SEC	M	SEC	1	2	3
								LAST AFST	LAST AFST	LAST AFST	LAST AFST	LAST AFST		
8	RE	8		10.21	20.33	1952.7	96.04	20	2.70	22	4.82	30	.00	
11	RE	21		4.95	20.96		110.76	5	.02					
13	RE	21		4.87	19.20		114.37	5	.57					
								96.409						
ER IS RECHTS EEN TYPE ZONDER CODENR. MET 2 ASSEN EN CLG:								12.56	M. OP TIJDSTIP:	116.28 SEC				
14	RE	1		12.56	18.52	362.2	115.97	26	5.85	46	.00			
18	LI	21		4.67	25.18		122.14	5	.69					
19	RE	21		4.66	21.69		121.66	5	2.92					
20	RE	21		4.75	20.52		125.72	5	.64					
28	LI	21		4.44	30.44		159.38	5	.51					
33	RE	21		4.94	21.23		176.67	6	.17					
								116.281						
49	RE	19		7.84	19.38	2058.5	222.47	22	4.54	26	.00			
54	RE	20		10.34	21.66	153.6	279.80	5	7.18	5	.00			
55	LI	21		4.11	25.93		231.03	5	2.45					
59	LI	21		4.39	31.25		238.63	5	2.87					
								230.131						
62	RE	20		8.18	20.35	418.6	250.71	28	5.87	56	.00			
67	RE	21		4.77	23.98		271.24	8	.82					

Preliminary analysis of traffic data

Figure 3.3.2.



Axle load code and axle distance code

Figure 3.3.3.

Axle load histograms		
Nr.1.		Types 1-4
2.	Fast lane	„ 5-8
3.		„ 9-12
4.		„ 13,16-21
5.		„ 1-4
6.	Slow lane	„ 5-8
7.		„ 9-12
8.		„ 13,16-21
Axle load curves		
Fast lane: all axle loads $\geq 8kN$ .		
Slow lane: all axle loads $\geq 8kN$ .		

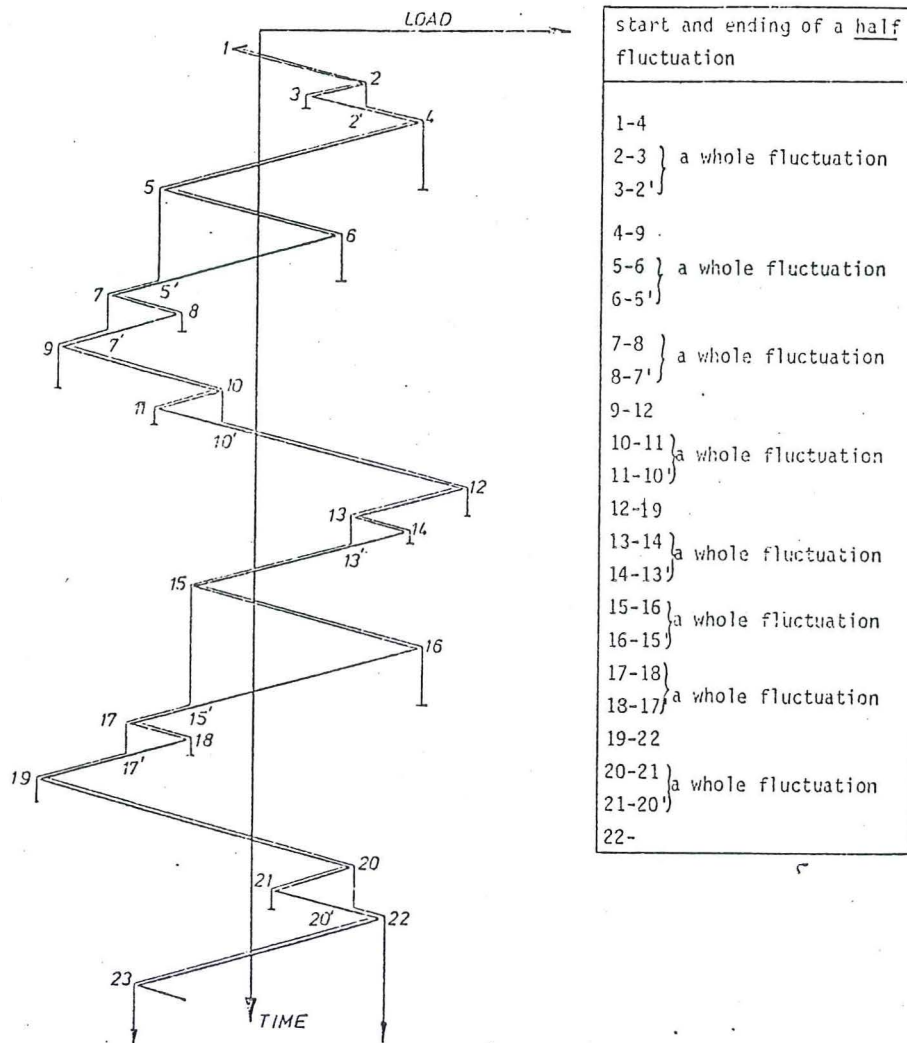
View of the frequency distributions of axle loads

Table III.3.1.

Axle distance histograms		
Nr.1.	Fast lane	Types 1-8
2.	Slow lane	„ 9-13,16-20
3.		„ 1-8
4.		9-13,16-20

View of the frequency distributions of axle distances

Table III.3.2.



The rain flow counting method

Figure 3.3.4

3.4. Results of measured stresses, due to vehicles of which the axle loads, axle distances and vehicle intervals have been measured to

3.4.1. Introduction

For the three bridges about 250 hours of measurements have been analysed. These measurements contains results of measured stresses, due to vehicles of which the axle loads, axle distances and vehicle intervals have been measured to. Due to the measuring system, ten measuring points could be measured per measuring period at the same time.

In this chapter for each of the bridges one period of measurements, mostly the largest, is given.

Results of other periods are summarised in the detailed appendix-reports (see Ref. 6-3) and available at the laboratory.

3.4.2. Date of measurements

Table A-III.4.1. and A-III.4.2. on page A-1 up to A-3 of appendix A shows the analysed hours and the date of measurements of the Haagsche Schouw Bridge.

Due to roadworks the results of the Rheden Bridge had to be split up into three main periods:

- Group A : Traffic in both, fast and slow, lanes (during 61,71 hrs)
- Group B : Traffic in the slow lane only (during 22.81 hrs)
- Group C : Traffic in the fast lane only (during 13.27 hrs)

The subdivision of these periods and the date of measurements are given in Table A-III.4.3. up to A-III.4.6. on page A-4 up to A-8 of appendix A

A view of the analysed hours and the date of measurements of the Leiderdorp Bridge are given in Table A-III.4.7. and A-III.4.8. on page A-9 up to A-11 of appendix A.



### 3.4.3. Results of measured traffic data for three steel bridges

#### 3.4.3.1. Frequency curves of axle loads

The cumulative relative frequency curves of the measured axle loads  $\geq 8$  kN and the number of axle loads  $\geq 10$  kN per hour for the three bridges are given in figure 3.4.3.1. on page 3-25. From this figure it appears that there is a difference between the traffic distribution in the slow lane and fast lane of each bridge. Besides that, it is remarkable that concerning the axle load curves of the slow lanes, there is a lot of difference between them.

So it can be concluded that:

- 1. The heavy weighing commercial vehicles are concentrated in the slow lane
- 2. The traffic distribution on the three bridges differs much.

Concerning the number of axle loads  $\geq 10$  kN per hour it appears the slow lane of the Leiderdorp Bridge gets the highest frequency (1024) against 615 on the Rheden Bridge and 176 on the Haagsche Schouw Bridge.

The period of 82 hours of measurements on the Haagsche Schouw Bridge is subdivided into 13 shorter periods and the period of 62 hours of measurements on the Rheden Bridge is subdivided into 18 shorter periods to investigate the difference between the results of the slow lane and the fast lane.

Results of this investigation are available in the detailed reports [Ref. 6-3], only a view graphs are given in figure 3.4.3.2. - 3.4.3.5 on page 3-26 up to 3-27.

For the Haagsche Schouw Bridge it appears that 6036 axle loads  $\geq 10$  kN are enough to record the cumulative relative frequency curves of the axle loads in the slow lane.

To obtain this curve with sufficient accuracy for the fast lane on the other hand, it appears that this curve -calculated after measuring 1476 axle loads  $\geq 10$  kN in 82 hours - is hardly enough to extend this graph for a longer period.

For the Rheden Bridge 3500 axle loads  $\geq 10$  kN appeared to be sufficient to recorded the cumulative relative frequency curves of the axle loads in the slow lane and 7964 axle loads  $\geq 10$  kN measured in the fast lane during 62 hours appeared to be not sufficient.

Although in principle one would expect the fast lane curve to coincide with the slow lane curve, such a result is impossible to obtain in a finite measuring time.

#### 3.4.3.2. Frequency tables of axle loads and axle distances

Appendix B of this report gives for each of the three bridges the frequency tables of measured axle loads and axle distances for one period of measurements.

A view of these frequency tables is given in Table III.4.3.1. on page 3-28.

#### 3.4.3.3. Mean values of axle loads and axle distances

Mean values of the measured axle loads and axle distances as they are presented in the frequency tables of chapter 3.4.3.2., are gathered for each of the three bridges in table III.4.3.2. to III.4.3.4. on page 3-29.

From these tables it appears that the differences between the values for a specific type on the three bridges differs much. So it is not possible to give for each vehicle type unanimous values of axle loads and axle distances which are operative for the three bridges.

#### 3.4.3.4. Distribution of the vehicle types over the traffic

Results of different distributions concerning the measured vehicles on the three bridges are given in table III.4.3.5. on page 3-30.

One reads:

- 1. 16 - 30% of the total traffic has axle loads  $\geq 8$  kN
- 2. 10 - 24% of the traffic consists of commercial vehicles
- 3. the number of commercial vehicles per bridge, amounts  
93 - 305 vehicles per hour.

The distribution of the vehicle types 1-20 over the two lanes of each bridge are given in table III.4.3.6 on page 3-30. In this figure one reads for example:

- 1. 49.1 - 92% are dual-axle lorries
- 2. other frequent types are type 9, an artic, 2-axle tractor with a 2-axle semi-trailer and type 4, an rigid 2-axle commercial vehicle with a 2-axle drawbar trailer.
- 3. 44.1% on the fast lane of the Haagsche Schouw Bridge is presented by type 17, a dual-axle lorry with axle distances between 2.6 and 3.1 meter.

The frequencies of occurrence of commercial vehicles in the slow lane of the three bridges are listed in table III.4.3.7. on page 3-31.

Results shows that:

- 1. 49 - 80% are dual-axle lorries (type 16-20)
- 2. 10 - 25% are artic tractors with a semi-trailer (type 8-13)
- 3. 5 - 14% are rigid commercial vehicles with a drawbar trailer (type 4-7).

Splitting up the results into the total number of axles per vehicle a distribution for the slow lane of the three bridges can be given as tabulated in table III.4.3.8. on page 3-31.

It appears that:

- |                                       |          |   |
|---------------------------------------|----------|---|
| -1. 2-axle commercial vehicle amounts | 49 - 80% | of the total<br>number of<br>commercial<br>vehicles |
| -2. 3-axle commercial vehicle amounts | 7 - 11%  |   |
| -3. 4-axle commercial vehicle amounts | 9 - 20%  |   |
| -4. 5-axle commercial vehicle amounts | 2 - 13%  |   |
| -5. 6-axle commercial vehicle amounts | .1 - 5%  |   |

#### 3.4.3.5. Frequency distributions of vehicle intervals

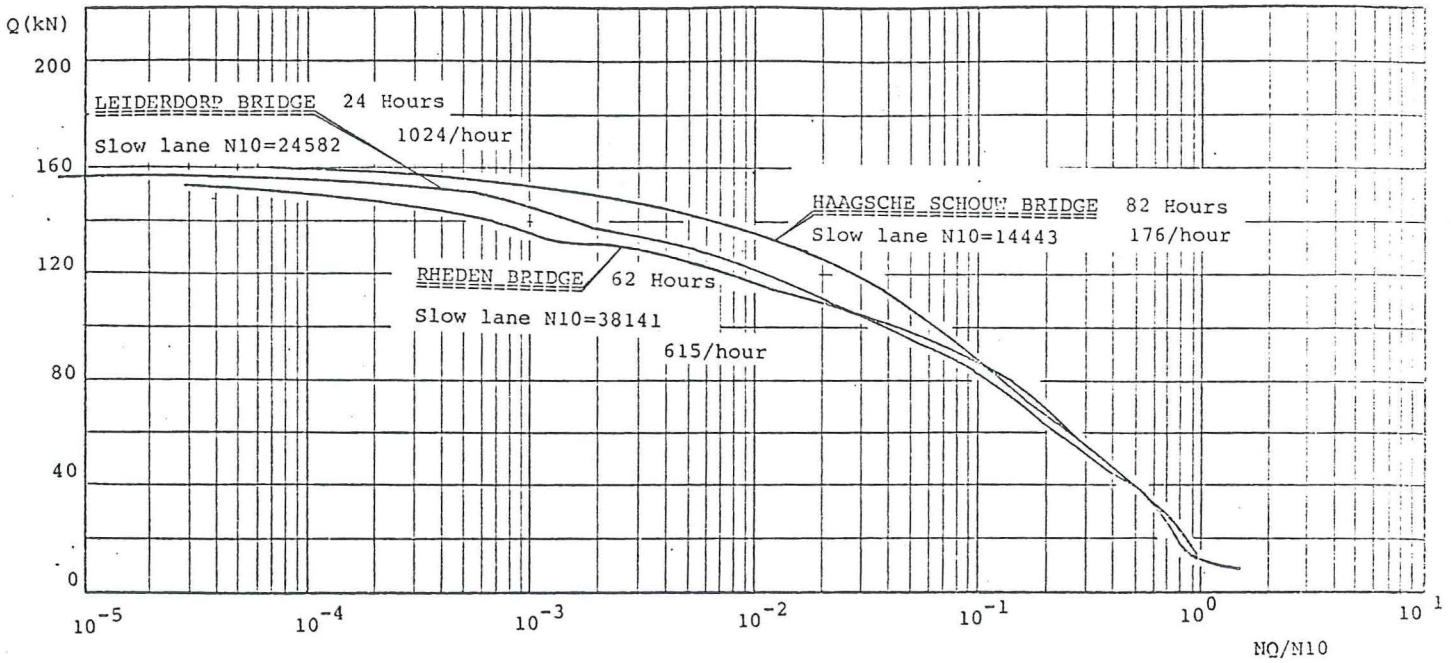
The frequency distribution of commercial vehicle intervals for both lanes of the three bridges is given in table III.4.3.9. on page 3-32. The cumulative distributions of these frequency distributions are given in figure 3.4.3.6. on page 3-32. Information about intervals greater than 145 m is not available.

It appears, concerning the percentage of intervals, that:

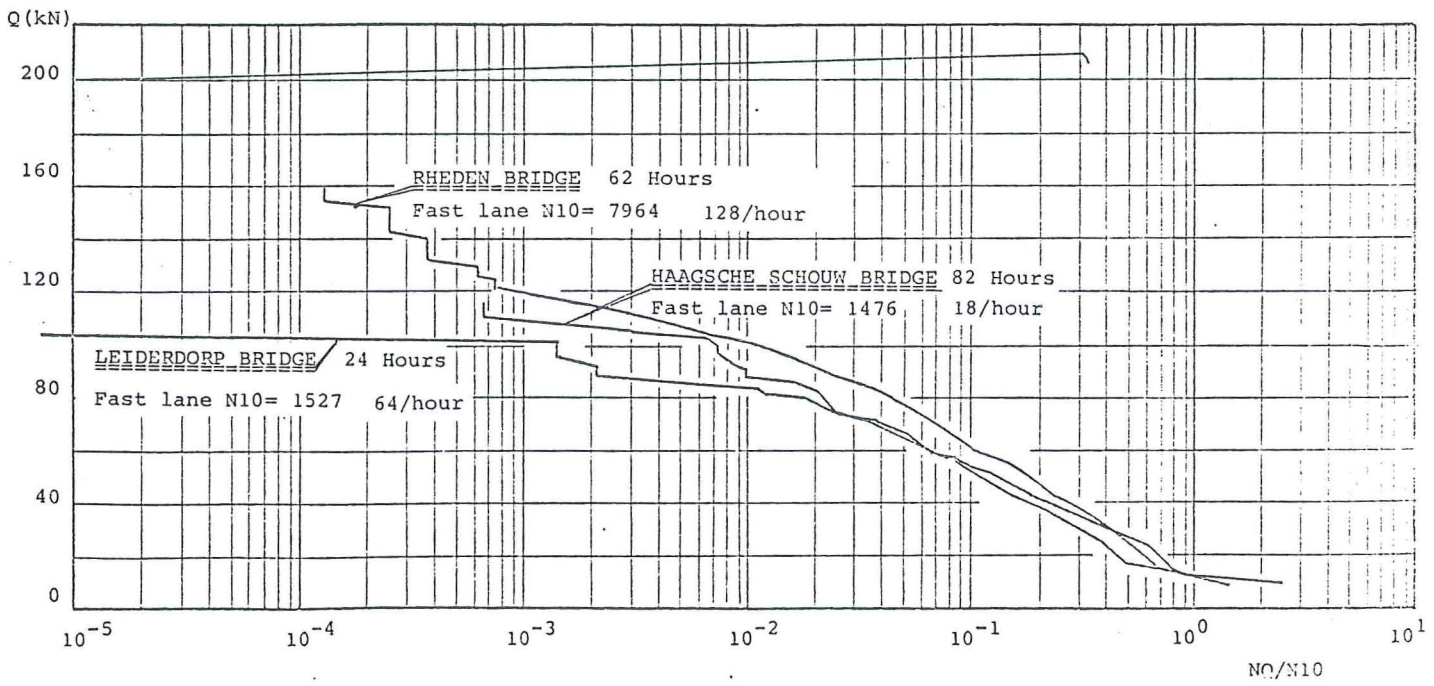
- 1. 82 - 96% in the slow lane and  
84 - 98% in the fast lane > 50 m
- 2. 67 - 91% in the slow lane and  
83 - 93% in the fast lane > 100 m
- 3. 58 - 87% in the slow lane and  
68 - 93% in the fast lane > 145 m

### 3.4.3.6. Figures and tables

List of figures	Page
3.4.3.1. Cumulative relative frequency curves of measured axle loads $\geq$ 8 kN on three Dutch highway bridges	3-25
3.4.3.2. Frequency curves slow lane Haagsche S.B.	3-26
3.4.3.3. Frequency curves fast lane Haagsche S.B.	3-26
3.4.3.4. Frequency curves slow lane Rheden Bridge	3-27
3.4.3.5. Frequency curves fast lane Rheden Bridge	3-27
3.4.3.6. Cumulative frequency curves of vehicle intervals	3-32
 List of tables	
III.4.3.1. View of the in appendix B given fre- quency tables of measured axle loads and axle distances	3-28
III.4.3.2. Mean values of axle loads and axle distances on the Haagsche Schouw Bridge	3-29
III.4.3.3. Idem Rheden Bridge	3-29
III.4.3.4. Idem Leiderdorp Bridge	3-29
III.4.3.5. Distribution of all vehicle types over the traffic	3-30
III.4.3.6. Vehicle type distribution 1-20	3-30
III.4.3.7. Frequency of occurrence of commercial vehicles in the slow lane of the three Dutch bridges	3-31
III.4.3.8. Frequency of occurrence of the total number of axles per vehicle in the slow lane of the bridges	3-31
III.4.3.9. Frequency distributions of vehicle intervals	3-32

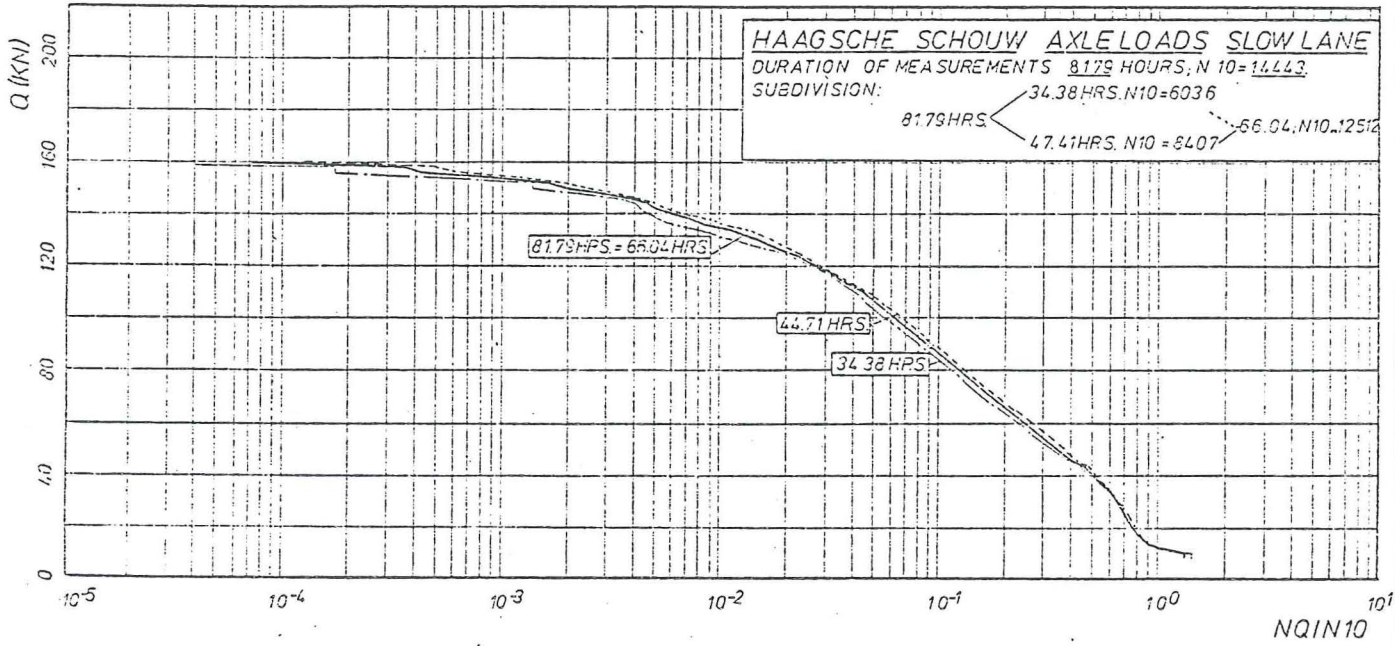


FL + SL	
Haagsche Schouw	194/hour
Rheden	743/hour
Leiderdorp	1088/hour

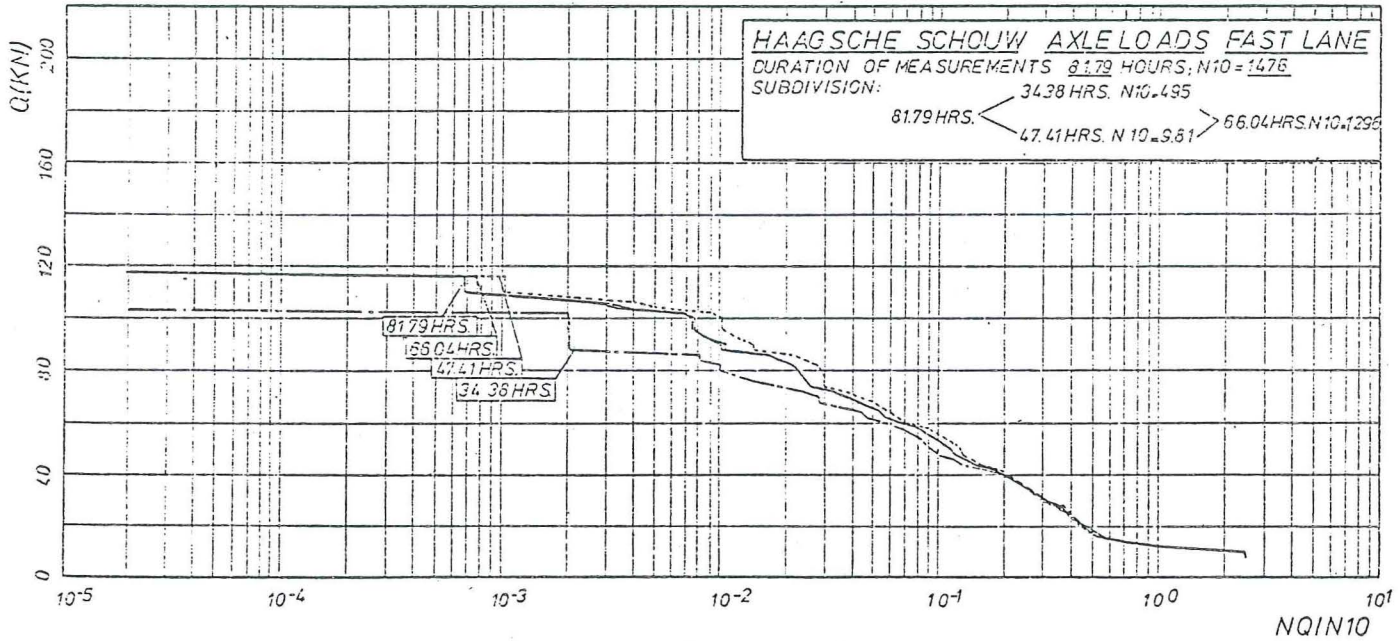


$$\frac{NQ}{N10} = \frac{\text{NUMBER OF AXLE LOADS } \geq Q}{\text{TOTAL NUMBER OF AXLE LOADS } \geq 10 \text{ kN}}$$

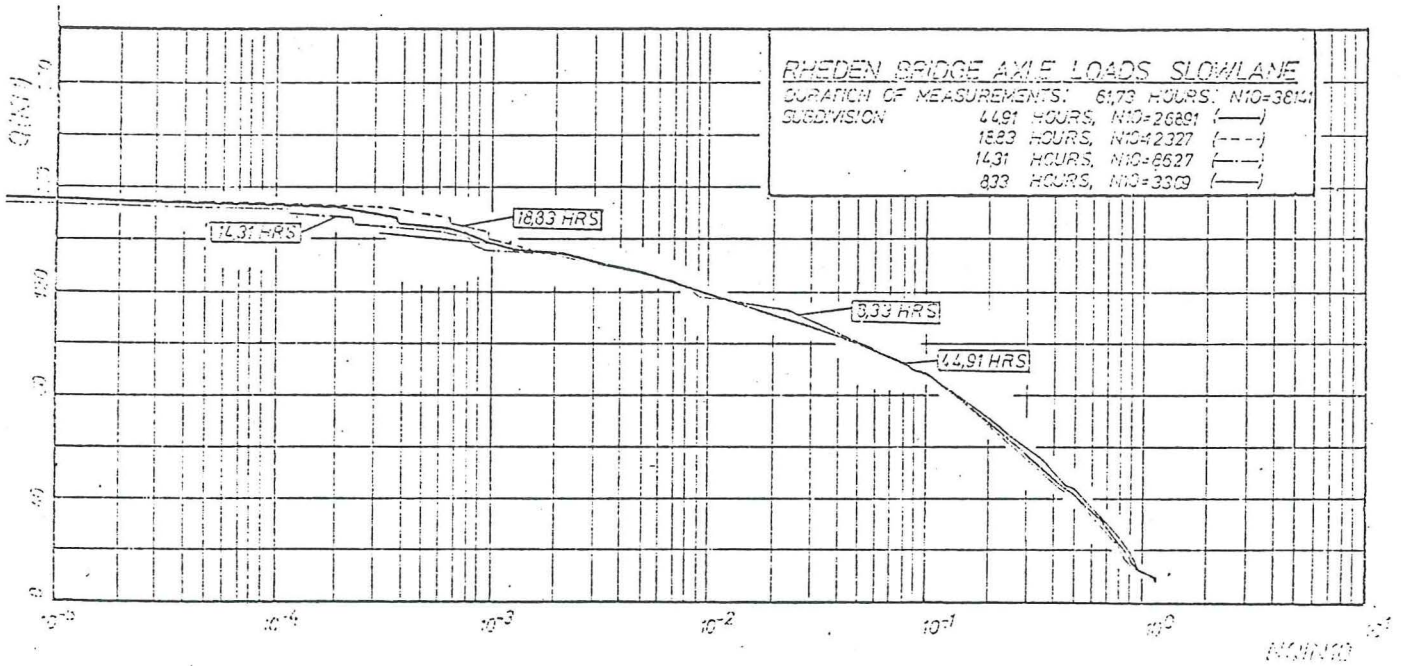
Cumulative relative frequency curves of measured axle loads  $\geq 8$  kN on three Dutch bridges  
Figure 3.4.3.1.



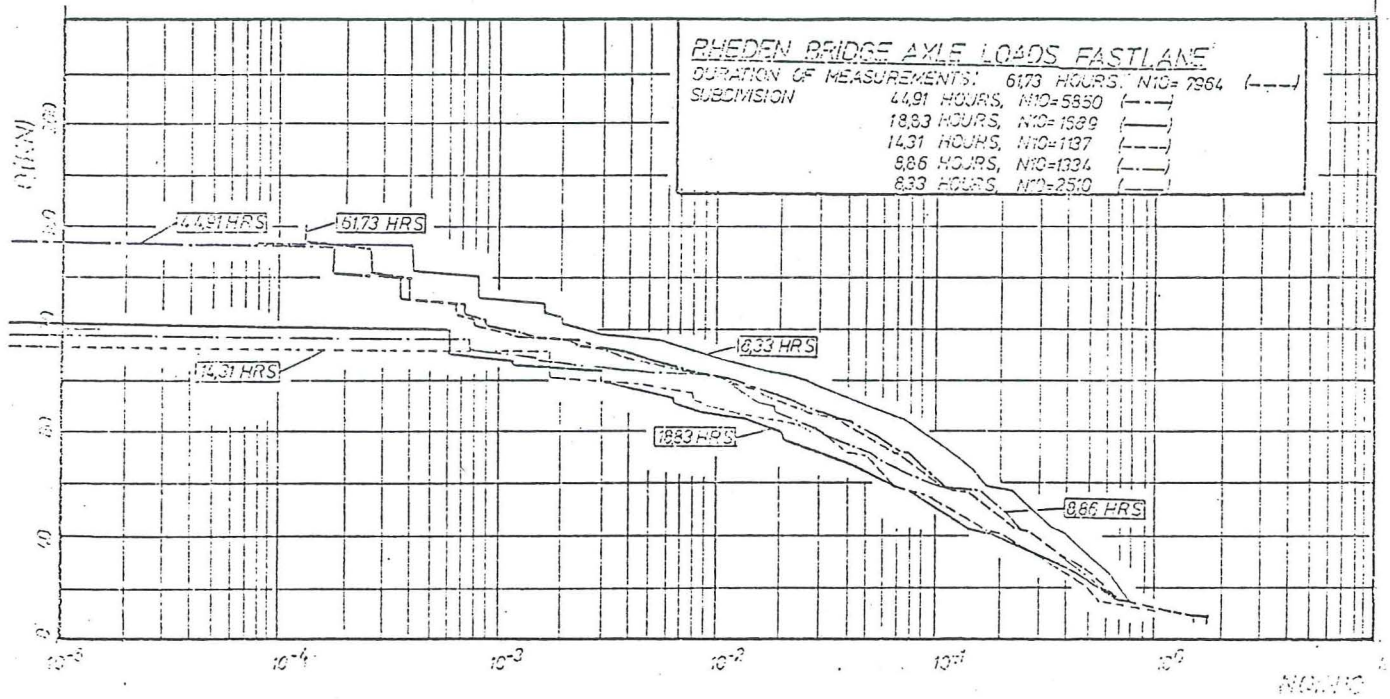
Frequency curves slow lane - Haagsche Schouw Bridge  
Figure 3.4.3.2.



Frequency curves fast lane - Haagsche Schouw Bridge  
Figure 3.4.3.3.



Frequency curves slow lane Rheden Bridge  
Figure 3.4.3.4.



Frequency curves fast lane Rheden Bridge  
Figure 3.4.3.5.

View of the axle load histograms and axle distance histograms in fast and slow lane during one period of measurements on three Dutch bridges.				
APPENDIX -B- OF STEVINREPORT 6-83-6				
Page	Bridge	Fast lane(FL) or Slow lane(SL)	Axle loads(AL) or Axle distance(AD)	Vehicle types
8-1	HAAGSCHE SCHOONW BRIDGE 82 HRS.	FL	AL	1-4
2				5-8
3				9-12
4				13,16-21
5		SL	AL	1-4
6				5-8
7				9-12
8				13,16-21
9	HAAGSCHE SCHOONW BRIDGE 82 HRS.	FL	AD	1-8
10				9-13,16-20
11		SL	AD	1-8
12				9-13,16-20
13	RHEDEN BRIDGE 62 HRS.	FL	AL	1-4
14				5-8
15				9-12
16				13,16-21
17		SL	AL	1-4
18				5-8
19				9-12
20				13,16-21
21	RHEDEN BRIDGE 62 HRS.	FL	AD	1-8
22				9-13,16-20
23		SL	AD	1-8
24				9-13,16-20
25	LEIDERDORP BRIDGE 24 HRS.	FL	AL	1-4
26				5-8
27				9-12
28				13,16-21
29		SL	AL	1-4
30				5-8
31				9-12
32				13,16-21
33	LEIDERDORP BRIDGE 24 HRS.	FL	AD	1-8
34				9-13,16-20
35		SL	AD	1-8
36				9-13,16-20

Contents Appendix -B- of Stevinreport 6-83-6  
Table III-4-3-1



HAASCHE SCHOUW BRIDGE

3-29

AXLE LOADS AND AXLE DISTANCES PER TYPE DURING MEASUREMENTS OF 82 HOURS

Types	slow lane											fast lane												
	Counted vehicles	Mean axle load per axle kN						Mean axle distance per axle M					Counted vehicles	Mean axle load per axle kN						Mean axle distance per axle M				
		A1	A2	A3	A4	A5	A6	A1	A2	A3	A4	A5		A1	A2	A3	A4	A5	A6	A1	A2	A3	A4	A5
	295	60	78	67			2.8	1.3				10	41	42	27			3.8	1.1					
	9	55	53	32	40		3.9	1.3	1.2			1	30	20	36	26		4.2	1.2	1.2				
	245	51	69	43	42		4.7	5.4	4.4			16	32	42	20	21		4.7	5.6	4.5				
	24	64	82	57	68	64	4.4	1.7	4.5	5.3														
	47	57	78	47	43	43	4.9	4.2	4.4	1.4		5	50	64	42	38	40	4.6	4.6	4.2	1.4			
	3	57	124	72	89	59	66	4.4	1.4	4.6	4.3	1.7												
	211	49	55	57			3.1	6.0				7	28	29	33			3.5	6.7					
	514	57	86	64	67		3.3	5.9	1.7			22	44	61	45	47		3.2	6.2	1.8				
	73	61	101	52	64	64	3.3	5.4	1.2	1.4		7	51	59	26	32	33	3.3	5.3	1.3	1.3			
	4	48	29	30	34		2.8	1.4	5.7															
	23	63	90	64	73	90	2.9	1.3	5.2	1.9		1	58	68	58	46	46	2.9	1.3	4.4	1.2			
	35	64	89	77	80	76	99	3.1	1.3	4.8	1.3	1.8	2	52	87	64	51	59	109	3.2	1.3	4.5	1.2	1.6
	5429	12				54	3.8					822	11			48	3.4							

Sum type 1 : 50

Sum type 21 : 4767

Table III-4-3-2

Total numbers of lorries : 7655

RHEDEN BRIDGE																								
AXLE LOADS AND AXLE DISTANCES PER TYPE DURING MEASUREMENTS OF 62 HOURS																								
Types	slow lane											fast lane												
	Counted vehicles	Mean axle load per axle kN						Mean axle distance per axle M					Counted vehicles	Mean axle load per axle kN						Mean axle distance per axle M				
		A1	A2	A3	A4	A5	A6	A1	A2	A3	A4	A5		A1	A2	A3	A4	A5	A6	A1	A2	A3	A4	A5
	790	43	48	49			3.7	1.3				116	36	46	34			3.4	1.1					
	19	48	56	57	58		4.0	1.0	0.8			4	51	41	54	46		3.9	0.8	1.2				
	984	43	57	40	33		4.8	5.3	4.7			135	37	50	30	28		4.8	5.1	4.7				
	187	54	66	52	61	60	4.5	1.3	4.8	4.9		24	49	63	47	53	47	4.4	1.3	4.7	4.7			
	494	51	71	50	43	44	4.9	4.7	4.4	1.3		63	40	50	31	27	26	4.6	4.6	4.3	1.3			
	141	59	80	51	69	55	49	4.3	1.2	4.2	4.1	1.4	16	49	69	50	57	53	42	4.2	1.2	4.2	3.9	1.3
	526	38	50	51			3.2	6.0				71	35	48	45			3.2	6.1					
	1528	48	60	53	59		3.4	6.0	1.8			249	40	53	38	41		3.3	5.8	1.8				
	892	51	76	50	50	53	3.5	5.3	1.3	1.4		150	43	60	34	36	36	3.4	5.1	1.3	1.3			
	27	48	43	41	52		2.9	1.2	6.1															
	152	50	55	55	65	71	3.0	1.3	5.4	1.9		18	42	37	39	42	47	2.8	1.2	5.3	1.9			
	155	51	51	53	48	50	56	2.9	1.3	4.0	1.3	1.4	16	44	37	40	32	32	44	2.8	1.5	4.0	1.1	1.5
	6749	13				43	3.9					2654	12			45	3.3							

Sum type 1 : 375

Sum type 21 : 6613

Table III-4-3-3

Total numbers of lorries : 16.544

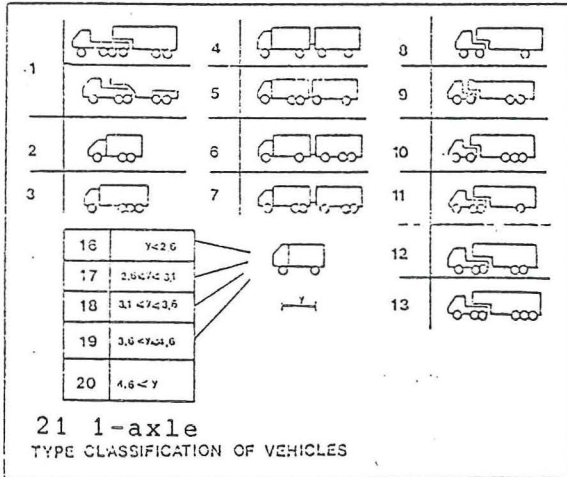
LEIDERSLOEP BRIDGE																								
AXLE LOAD AND AXLE DISTANCES PER TYPE DURING MEASUREMENTS OF 24 HOURS																								
Types	Slow lane											Fast lane												
	Counted vehicles	Mean axle load per axle kN						Mean axle distance per axle M					Counted vehicles	Mean axle load per axle kN						Mean axle distance per axle M				
		A1	A2	A3	A4	A5	A6	A1	A2	A3	A4	A5		A1	A2	A3	A4	A5	A6	A1	A2	A3	A4	A5
2	621	39	40	39			5.7	6.2				32	26	27	27			5.3	5.7					
3	57	47	43	67	75		4.4	1.3	3.7									4.8	5.2	5.1				
4	309	51	53	45	48		4.8	5.3	4.9			35	33	41	29	27		4.8	5.2	5.1				
5	33	62	73	64	69	73	5.0	1.8	4.7	5.2		7	47	44	33	39	30	5.6	1.8	4.5	5.2			
6	158	54	65	45	38	49	5.2	5.0	4.5	1.5		23	34	44	25	16	23	4.8	4.8	4.1	1.6			
7	74	60	83	69	72	60	66	4.9	3.4	3.9	4.6	1.4	4	39	45	39	46	35	33	5.1	3.3	4.4	4.6	2.9
8	136	41	46	50			3.1	6.3				14	26	28	26			3.4	6.0					
9	752	51	62	51	53		3.3	5.7	1.3			85	34	42	29	30		3.3	5.8	1.8				
10	313	52	65	44	42	58	3.4	5.6	1.4	1.2		28	34	40	25	31	44	3.4	5.5	1.4	1.3			
11	5	40	26	42	24		2.6	3.9	5.1															
12	40	49	47	41	50	57	3.2	1.0	5.4	1.8														
13	60	50	55	43	57	58	66	2.7	1.4	4.2	1.7	1.3	4	37	37	36	39	42	45	2.8	1.3	4.7		1.2
15 - 20	3590	15				57	3.2					242	11			38	4.2							

Sum type 1 : 899

Sum type 21 : 2125

Total number of lorries: 7313

Table III-4-3-4



Number %	Total number of vehicles	Number of vehicle types 1-21	Number of vehicle types 1-20	Number of commercial vehicles	
				hour SL	hour SL+FL
Rheden	89.126	23.157	16.544	209	267
62 hours	100	26	17		
Haagsche Schouw	79.210	12.442	7.655	83	93
82 hours	100	16	10		
Leiderdorp	30.578	9.267	7.313	284	305
24 hours	100	30	24		

Distribution of all vehicles over the traffic

Tabl III-4-3-5

VEHICLE TYPE	RHEDEN BRIDGE 62 hours			HAAGSCHE-SCHOUW BRIDGE 82 hrs			LEIDERDORP BRIDGE 24 hours		
	Fast lane %	Slow lane %	F1 + S1 %	Fast lane %	Slow lane %	F1 + S1 %	Fast lane %	Slow lane %	S1 + F1 %
1	1.6	2.5	2.3	0.1	0.7	0.7	3.3	12.7	12.1
2	3.2	6.1	5.5	1.1	4.4	4.0	6.5	9.1	8.9
3	0.1	0.2	0.1	0.1	0.1	0.1	-	0.8	0.8
4	3.8	7.6	6.8	1.8	3.6	3.4	7.1	4.5	4.7
5	0.7	1.4	1.3	-	0.4	0.3	1.4	1.2	1.2
6	1.8	3.8	3.4	0.6	0.7	0.7	4.7	2.3	2.5
7	0.5	1.1	1.0	-	0.04	0.04	0.8	1.1	1.1
8	2.0	4.1	3.6	0.8	3.1	2.9	2.9	2.0	2.1
9	7.0	11.8	10.7	2.5	4.6	4.4	17.4	11.0	11.5
10	4.4	5.9	6.4	0.8	1.1	1.1	5.7	4.6	4.7
11	0.0	0.2	0.2	-	0.06	0.05	-	0.07	0.07
12	0.5	1.2	1.0	0.1	0.3	0.3	-	0.6	0.6
13	0.5	1.2	1.0	0.2	0.5	0.5	0.8	0.9	0.9
16	19.9	6.2	9.2	9.4	7.7	7.9	2.9	6.0	5.8
17	23.8	9.4	12.5	44.1	19.4	22.3	6.5	12.2	11.8
18	3.0	6.9	7.1	15.0	13.1	13.3	6.1	8.2	8.1
19	10.8	14.5	13.7	8.2	17.2	16.2	11.8	11.8	11.8
20	11.6	15.1	14.4	15.3	22.9	22.1	22.0	10.9	11.6
Type: t/m 20	3582	12962	16544	894	6761	7655	490	6823	7313

Vehicle type distributions 1 -20 on three Dutch bridges

Table III-4-3-6

Vehicle types		Haagsche Schouw 82 hours	Rheden 62 hours	Leiderdorp 24 hours
	1	0.7	2.6	12.7
	2	4.4	6.1	9.1
	3	0.1	0.2	0.8
rigid commercial vehicles with a draw bar trailer	4	3.6	7.6	4.5
	5	0.4	1.4	1.2
	6	0.7	3.8	2.3
	7	0.04	1.1	1.1
artic tractors with a semi-trailer	8	3.1	4.1	2.0
	9	4.6	11.8	11.0
	10	1.1	6.9	4.6
	11	0.06	0.2	0.07
	12	0.3	1.2	0.6
	13	0.5	1.2	0.9
dual-axle lorries	16	7.7	6.2	6.0
	17	19.4	9.4	12.2
	18	13.1	6.9	8.2
	19	17.2	14.5	11.8
	20	22.9	15.1	10.9

Frequency of occurrence of commercial vehicles in the slow lane of the three Dutch bridges

Table III-4-3-7

Commercial vehicles with :	Haagsche Schouw 82 hrs.	Rheden 62 hours	Leiderdorp 24 hours
2 axles	80.0	52.0	49.0
3 "	7.5	10.0	11.0
4 "	8.9	20.0	16.0
5 "	2.5	13.0	9.0
6 "	1.24	5.0	2.0
> 6 "			13.0

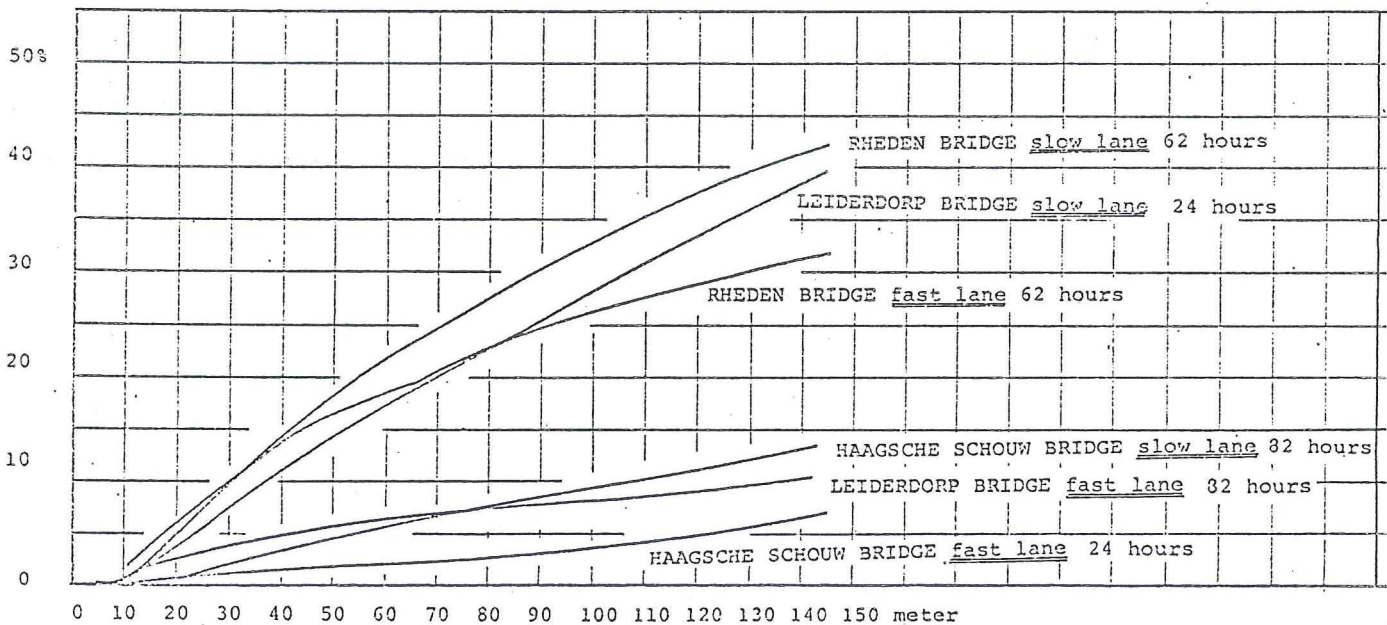
Frequency of occurrence of the total number of axles per vehicle in the slow lane of the bridges

Table III-4-3-8

Vehicle intervals	Haagsche Schouw 82 Hours		Rheden 62 Hours		Leiderdorp 24 Hours	
	F1	S1	F1	S1	F1	S1
0 - 5	0	3	12	19	3	17
5 - 10	3	10	48	98	2	51
10 - 15	4	36	70	195	4	73
15 - 20	2	22	62	245	2	114
20 - 25	2	32	65	250	5	120
25 - 30	2	44	81	282	3	127
30 - 35	2	36	49	255	2	138
35 - 40	1	26	65	274	0	123
40 - 45	2	43	46	228	3	115
45 - 50	0	40	33	199	2	113
50 - 55	2	38	30	205	2	98
55 - 60	1	38	32	199	2	102
60 - 65	1	30	37	181	0	83
65 - 70	0	43	36	164	1	101
70 - 75	1	28	43	148	2	98
75 - 80	1	28	23	165	2	79
80 - 85	3	29	33	137	1	97
85 - 90	2	43	26	140	1	95
90 - 95	1	35	23	154	0	99
95 - 100	2	42	31	148	2	68
100 - 105	26	8	17	136	1	100
105 - 110	0	29	29	116	0	86
110 - 115	0	31	17	128	2	106
115 - 120	0	25	16	133	4	106
120 - 125	2	35	19	110	0	92
125 - 130	1	36	20	114	0	83
130 - 135	0	28	22	111	0	87
135 - 140	1	38	21	98	3	78
140 - 145	2	24	14	93	1	60
145	855	5822	2200	6417	441	4127

Frequency distributions of vehicle intervals on the three bridges

Table III-4-3-9



Cumulative frequency curves of vehicle intervals

Figure 3.4.3.6.

### 3.4.4. Comparison with measured traffic on other European bridges

#### 3.4.4.1. Bridges studied for the ECSC research program

Fifteen roadbridges and three railbridges were surveyed during the first and second phase of the research.

Table III.4.4.1. on page 3-35. shows for each bridge, the locality, the type of deck, type of structures, span and number of traffic lanes. The bridges were selected to provide a variety of different structural types. The most frequent was the type with an orthotropic deck.

#### 3.4.4.2. Frequency curves of axle loads

Figure 3.4.4.1. on page 3-35 shows the axle load distribution recorded for the slow lane for the roadbridges i.e. the number of axles  $n_Q$  heavier than  $Q$  divided by the number of axles  $n_{10}$  heavier than 10 kN.

The maximum loads measured on axles varied between 125 and 205 kN; these were highly variable values and always exceeded the authorised loads.

One might nevertheless be tempted to establish three traffic groups according to loads, i.e.:

- traffic of heavy axles occurring often in the vicinity of ports on the continent: Rio Verde, Caronte, Saint Nazaire and Haagsche Schouw
- medium traffic: Monthéry, Autreville, Rheden, Limburger bahn, Leiderdorp and Forth
- light traffic: Manchester Road and Wye.

In conclusion, the composition of road traffic exhibits significant variations with the country and local circumstances. The maximum axle loads observed also vary from region to region, and always exceed the authorised values. In appreciating these loads, one must realise however, that the measurements include the dynamic effects of the vehicle itself, but not the dynamic response of the bridge.

#### 3.4.4.3. Frequency of occurrence of vehicle types

The table III.4.4.2. on page 3-36 shows for the roadbridges the frequency of principal vehicle types, the duration of measurement and traffic intensity.

The composition of road traffic indicates differences between the traffic observed in the various countries. Thus, in France, Netherlands and Great Britain the most common vehicle is the 2-axled lorry (32 - 84%) followed by the articulated lorries (13 - 48%); rigid lorries with trailers are less frequent.

In contrast, in Germany rigid lorries with trailers are the most frequent (60%), whilst articulated lorries are less frequent. In Italy 32% of the heavy lorries comprised vehicles with seven and eight axles.

The diversity in the composition of the traffic will affect the choice of the "convoy" to be defined for calculating fatigue in bridges.

#### 3.4.4.4. Frequency distributions of vehicle intervals

Figure 3.4.4.2. on page 3-36 shows the cumulative frequency distributions of vehicle intervals for the slow lane of the roadbridges.

It appears that the frequency of vehicle intervals greater than 100 meter varies between 8% in Caronte against 52% in the Limburger Bahn.

#### 3.4.4.5. Figures and tables

List of figures	Page
-----------------	------

3.4.4.1. Axle load distributions in the ECSC	3-35
3.4.4.2. Vehicle intervals distributions in the ECSC	3-36

List of tables

III.4.4.1. Measured bridges in the ECSC	3-35
III.4.4.2. Distribution of vehicle types in the ECSC	3-36

BRIDGE TESTED

Traffic	Bridge	Country	Deck*	Structure	Span(max)	Number of lanes
Road	CARONTE	F	O	rigid frame	147	6
	AUTREVILLE	F	"	plate girder	90	6
	MONTHLERY	F	"	"	12,7	2
	SAINT-NAZAIRE	F	"	cable stayed	404	3
	HAAGSCHE SCHOUW	NL	L	plate girder	22	2
	RHEDEN	NL	O	"	105	2
	LIMBURGER BAHN	D	"	"	97	6(3)
	FORTH	GB	"	suspension	1006	4
	MANCHESTER	GB	"	box girder	33	2
	WYE	GB	"	cable stayed	235	4
RIO VERDE	I	"	box girder	95	2	
Rail	BISCHOFHEIM	D	L	plate girder	5,3	1
	FRANKFURT	D	"	truss	53	2
	RHEINGAUWALL	D	O	plate girder	21	1

\* O: ortotropic L: longitudinal girder

Table III.4.4.1.

RESULTS OF RESEARCH EC.S.C.: Measurements and interpretation of dynamic loads on steel bridges

Comparison of road traffic: AXLE LOADS (slow lane)

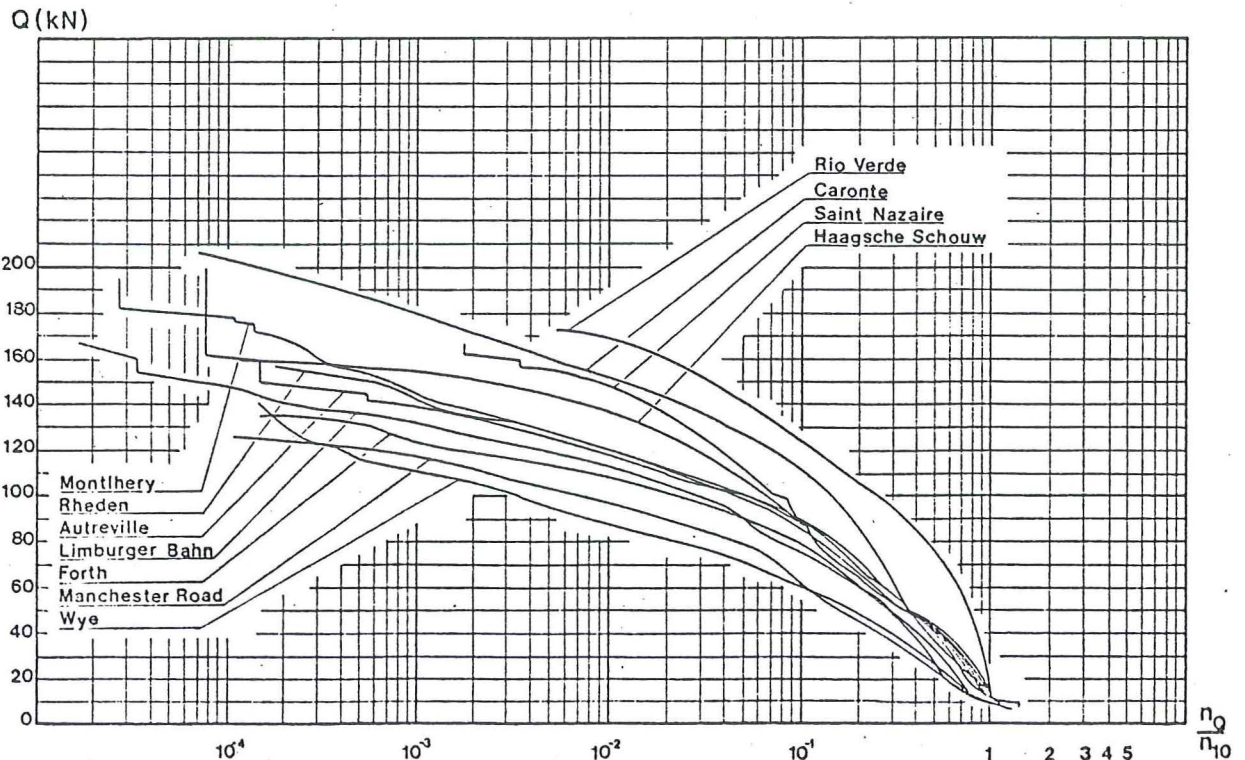

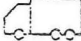
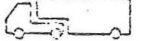
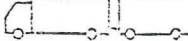
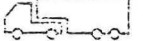
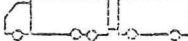
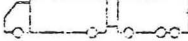
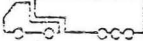
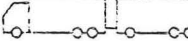


Figure 3.4.4.1.

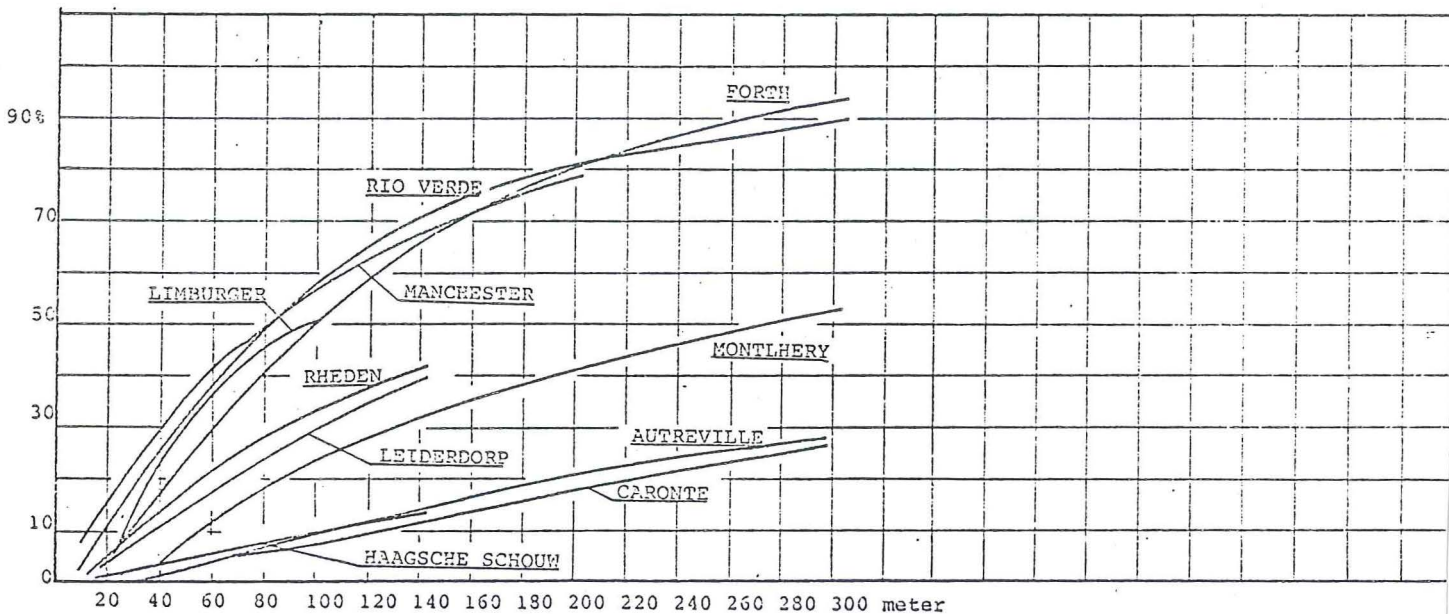
RESULTS OF RESEARCH E.C.S.E.: Measurements and interpretation of dynamic loads on steelbridges

Composition road traffic load: VEHICLE TYPES (slow lane)

Vehicle type	Caronte	Montlhéry	Autreville	St-Nazaire	Haagsche Schouw	Rheden	Limburger	Forth	Manchester	Rio Verde
20 	33,2	48,9	31,7	75,0	81,7	59,6	18,3	67,9	83,6	11,4
31 	5,7	5,1	3,9	4,3	4,0	5,5	1,5	6,1	3,1	2,3
32 	21,4	10,0	14,0	5,8	2,8	6,3	3,7	4,3	1,7	11,7
41 	4,1	6,8	4,2	1,1	3,91	6,1	16,5	0,1	0,1	6,3
42 	27,0	21,6	32,0	12,8	9,39	9,7	4,5	20,2	10,4	4,3
51 	0,2	0,2	0,6	0	0,31	1	11,6	-	-	3,4
52 	1,3	0,7	2,5	0	0,68	3,1	31,5	-	-	2,3
53 	0	6,3	9,2	0	1,05	6,0	8,4	0,2	-	7,4
60 	0,4	0,2	0,2	0	0,1	0,82	0,4	-	-	10,2
70 (A)	-	-	-	-	-	-	-	-	-	32,7
(B)	92	94	65,4	116,7	82	97	6	35,2	34,2	15
(C)	49	123	57	2	94	302	196	136	89	22

(A) More than six axles      (B) Length of measurements      (C) Number of lorries per hour

Distributions of vehicle types in the ECSC  
Table III.4.4.2



Vehicle interval distributions in the ECSC (slow lanes)  
Figure 3.4.4.2.



### 3.4.5. Results of measured stresses due to daily traffic loading on three steelbridges

Rainflow counts as well as levelcrossing counts of measured stresses in the bridge structures are presented in histograms and frequency curves. Results of measured stresses are presented in Appendix C of this report using histograms. A view of the appendix pages containing the results is given in table III.4.5.1. on page 3-44.

In the following paragraphs some results of the stress measurements will be treated using the frequency curves as mentioned before in chapter 3.3.2.3.

#### 3.4.5.1. Haagsche Schouw Bridge

##### 3.4.5.1.1. Measured stresses during 66 hours

Figure 3.4.5.1. on page 3-45 shows the modified relative frequency curves of levelcrossings as well as the modified cumulative relative frequency curves of rainflow counts of the measuring points 2 and 3 on a crossgirder of the Haagsche Schouw Bridge.

These curves of the measuring points situated on several longitudinal girders in one cross-section of this bridge are given in figure 3.4.5.2. on page 3-46. From these figures it appears there is a lot of difference between the stress pattern of mp3 in the fast lane and mp2 in the slow lane. The same phenomena occurs by the measuring points on the longitudinal girders situated in one cross-section of the bridge.

It is clearly seen that the stress distribution in measured cross-section differs markedly. The stresses which are exerted in several points, especially where the traffic is not frequent, are not only smaller but also occur less than in the points where most of the heavy traffic runs. Even in the slow lane there is much deviation.

From table III.4.5.2. on page 3-47, showing precentaly the number of counted maximym peakvalues of measured stresses in various measuring point of this cross section, it appears that about 58% of the traffic runs in the same

track on the bridge. So it is to be expected that a simulation of the stress distributions can give a realistic result if the lateral distribution of the traffic will be taken into account.

Another important effect associated with the lateral distribution is the number of axle loads it takes to reach the final stress distribution.

Figure 3.4.5.4. on page 3-48 shows that about 9000 axle loads  $\geq 10$  kN are enough to construct the stress distribution of the measuring point where 58% of the traffic runs. In general a slightly longer time is taken than in the case of the axle loads.

#### 3.4.5.2. Rheden Bridge

##### 3.4.5.2.1. Influence of the lateral distribution of the traffic on the stress distributions in a cross section of the bridge

The modified cumulative relative frequency curves of rainfall counts and the modified relative frequency curves of level crossings of the measuring points 3-10 are given in figure 3.4.5.5. on page 3-49 for a period of 44.91 hours of measurements.

Measuring points 3-10 were situated at the same midspan point on various longitudinal stringers in one cross section of the bridge structure.

Analogues to the results of measured stress distributions on the Haagsche Schouw Bridge it appears that there is a lot of difference between the stress pattern of the measured points due to the lateral distribution of the traffic on the bridge.

Above mentioned frequency curves of the measuring points 11-18 are given in figure 3.4.5.6. on page 3-50 for a period of 8.86 hours of measurements.

The measuring points 11-18 were situated on the same longitudinal stringers as measuring points 3-10 but in this case on the point where the continuous stringer is supported by the cross girder.

Compering figure 3.4.5.5. and 3.4.5.6. it appears that the difference between the stresses on the point where the continuous stringer is supported by the cross girder in the various stringers due to the lateral distribution is not so much as in the case of the midspan points on these longitudinal stringers.

Table III.4.5.3. on page 3-51 gives for the various measuring points precentaly the number of counted maximum peakvalues of measured stresses in a measuring period.

For the midspan points on various longitudinal stringers in one cross section it appears that mp5 gets 60% of the total number of maximum peakvalues. For the points where the continuous stringer is supported by the cross girder in one cross section it appears that two measuring points 13 and 14 gets both about 40% of the total number of maximum peakvalues. So it can be concluded that about 60% of the traffic was driving in the same track and that the division of maximum peakvalues is strongly dependent of the different influence lines on transverse as well as the longitudinal direction. Just as for the Haagsche Schouw Bridge it appears that about 9000 - 10.000 axle loads  $> 10$  kN are enough to construct the stress distribution of the measuring point where 60% of the traffic runs (see figure 3.4.5.11 on page 3-54).

#### 3.4.5.2.2. Comparison of measured stress-spectra in combination of different influence lines

Figure 3.4.5.8 on page 3-52 gives the modified cumulative relative frequency curves of rainflow counts and the modified relative frequency curves of levelcrossings on the stresses in a midspan point of a stringer and a point where the continuous stringer is supported by the cross girder during 7.96 hours of measurements.

Figure 3.4.5.9 and 3.4.5.10. on page 3-53 gives the static influence lines of these points.

Comparison of the frequency curves and influence lines proves that there is a good correlation.

### 3.4.5.3. Leiderdorp Bridge

#### 3.4.5.3.1. Relationship between stress distribution in one cross section of the bridge structure and the transverse distribution of wheel positions

Figure 3.4.5.16 on page 3-55 shows the modified relative frequency curves of levelcrossing of measuring points 101 and 104 on a cross stiffner of the bridgedeck and figure 3.4.5.14 on page 3-55 the same curves of measuring points at a midspan point of several longitudinal stringers in one cross section of the bridge. The modified cumulative relative frequency curves of rainflow counts of measuring points 101 and 104 are given in figure 3.4.5.15 on page 3-55 and the same curves of measuring points on the longitudinal stringers in figure 3.4.5.13 on page 3-55.

Analogues to the results of measured stresses at the Haagsche Schouw Bridge and the Rheden Bridge it appears that the stress distribution in the measured cross section of the bridge structure differs markedly.

Knowing the axle load distribution in fast and slow lane (see chapter 3.4.3.) it is not surprising that the stresses which are exerted in certain measuring points are smaller and occur less than measuring points where most of the heavy weighing vehicles runs. Even in the slow lane there is much deviation.

Calculating the number of maximum peakvalues of measured stresses in the measuring points situated in the slow lane it appears that 95,5% is concentrated in an area of 855 mm of the cross section of the bridge (see table III.4.5.4 on page 3-56).

The transverse distribution of wheelpositions on this bridge is measured by counting the offside rear wheels of commercial vehicles. Results of figure 3.4.5.17. on page 3-56 shows that the transverse distribution of wheelpositions agree with the stress distribution of the bridge structure. About 88% of the counted wheels is concentrated in the ares of 855 mm.

### 3.4.5.3.2. Stress distribution of a longitudinal stiffner of the bridge deck in several cross sections of the bridge

#### 3.4.5.3.2.1. The same detail

Figure 3.4.5.19 on page 3-57' shows the modified relative frequency curves of level crossings of the measuring points 6, 2, 23 and 26, situated on one longitudinal stiffner of the bridgedeck at the midspan location in several cross sections of the bridge.

The modified cumulative relative frequency cruves of rainflow counts of these measuring points are given in figure 3.4.5.18. on page 3-57'. From these figures it appears that there is a difference between the stress distribution of these measuring points and the total number of stress cycles. These differences are caused by the different lengths of the influence lines of these points.

#### 3.4.5.3.2.2. Different details

Figure 3.4.5.21. on page 3-57 shows the modified relative frequency curve of level crossings of measuring points 7 and 19. The modified cumulative relative frequency curves of rainflow counts of these points are given in figure 3.4.5.20. on page 3-57. From these figures it appears that there is a lot of difference between the stress distribution of these measuring points. However, it corresponds with the influence lines of these points.

3.4.5.4. Figures and tables

List of figures	Page
<u>Haagsche Schouw Bridge</u>	
3.4.5.1. Frequency curves of measuring points 2 and 3	3-45
3.4.5.2. Frequency cruves of measuring points 13, 18, 20, 21	3-46
3.4.5.3. Lateral distribution of the traffic	3-47
3.4.5.4. Frequency curves of measuring point 16	3-48
<u>Rheden Bridge</u>	
3.4.5.5. Frequency curves of measuring points 3 - 10	3-49
3.4.5.6. Frequency curves of measuring points 11 - 18	3-50
3.4.5.7. Lateral distribution of the traffic	3-51
3.4.5.8. Frequency curves of mp5 and mp13	3-52
3.4.5.9. Influence line of a "midspan" point	3-53
3.4.5.10. Influence line of a point where the continuous stringers is supported by the cross girder	3-54
3.4.5.11. Frequency curves of measuring point 5	3-54
<u>Leiderdorp Bridge</u>	
3.4.5.13.- Frequency curves of measuring points	3-55
3.4.5.16 7 - 16, 101 and 104	
3.4.5.17. Lateral distribution of the traffic	3-56
3.4.5.18.- Frequency curves of measuring points	3-57
3.4.5.21. 2, 6, 23, 26 and 7 and 19	

List of tables	Page
III.4.5.1. Contents Appendix C of Stevin report 6-83-6	3-44
III.4.5.2. Lateral distribution on the Haagsche S.B.	3-47
III.4.5.3. Lateral distribution on the Rheden Bridge	3-51
III.4.5.4. Lateral distribution on the Leiderdorp B.	3-56

(Text chapter 3.4.6. on page 3-58).

View of the rainflow counts and levelcrossing counts histograms on three Dutch bridges					
APPENDIX -C- STEVINREPORT 6-83-6					
Page	Bridge	Measured points	Duration of measurements in hours	Rainflowcounts (RF) or Levelcrossings (LC)	
C-1	HAAGSCHE SCHOUW BRIDGE	* 2,3,13-16,18-21	4,25	RF	
2				LC	
3		GROUP -A-	14,15,20	11,45	RF
4					LC
5			2,3,13-18,20,21	66,04	RF
6					LC
7	RHEDEN BRIDGE	1-10	44,91	RF	
8				LC	
9		1,2,11-18	8,86	RF	
10				LC	
11		1-6,11-14	7,96	RF	
12				LC	
13		GROUP-B-	1-6,11-14	19,96	RF
14					LC
15		1-10	2,85	RF	
16				LC	
17		GROUP-C-	1-10	10,17	RF
18					LC
19	1,2,7-10,15-18	3,10	RF		
20			LC		
21	LEIDERDORP BRIDGE	1-6,23,24,27,28	4,03	RF	
22				LC	
23		7-16	5,06	RF	
24				LC	
25		7-12,19-22	3,00	RF	
26				LC	
27		6,8,9,22-26	6,41	RF	
28				LC	
29	101-114	5,60	RF		
30			LC		

\* A: Traffic in fast and slow lane

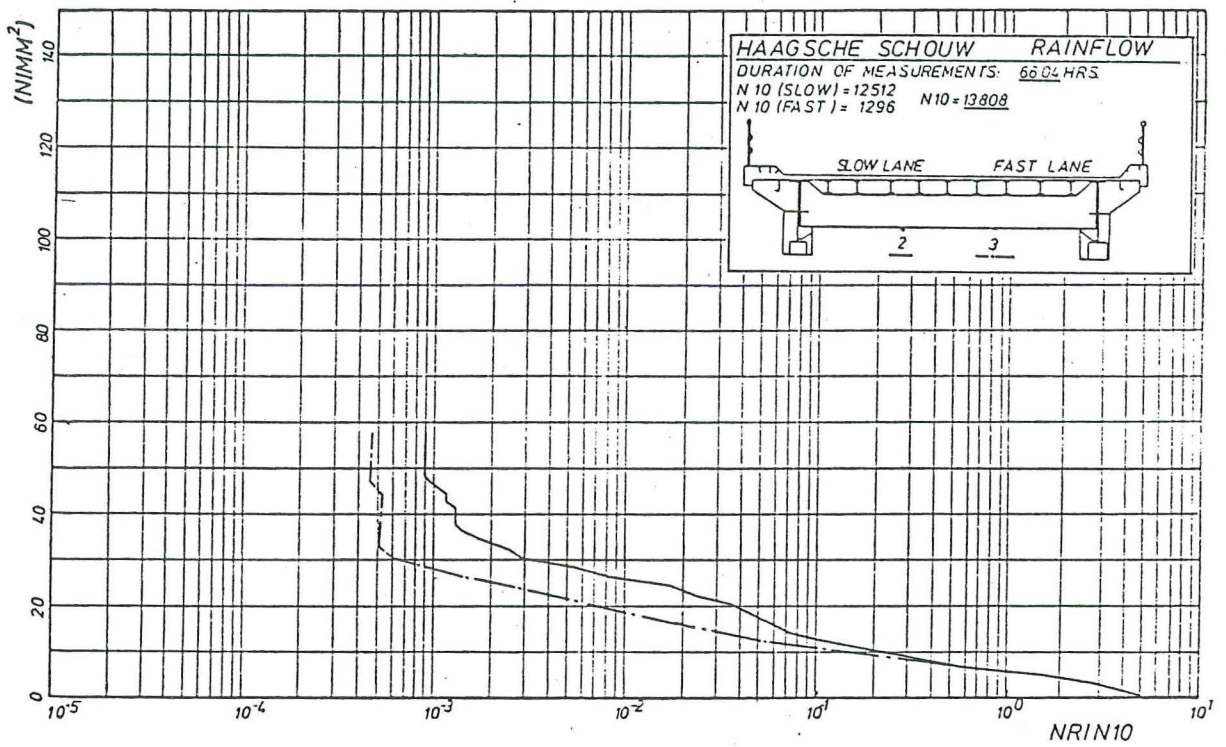
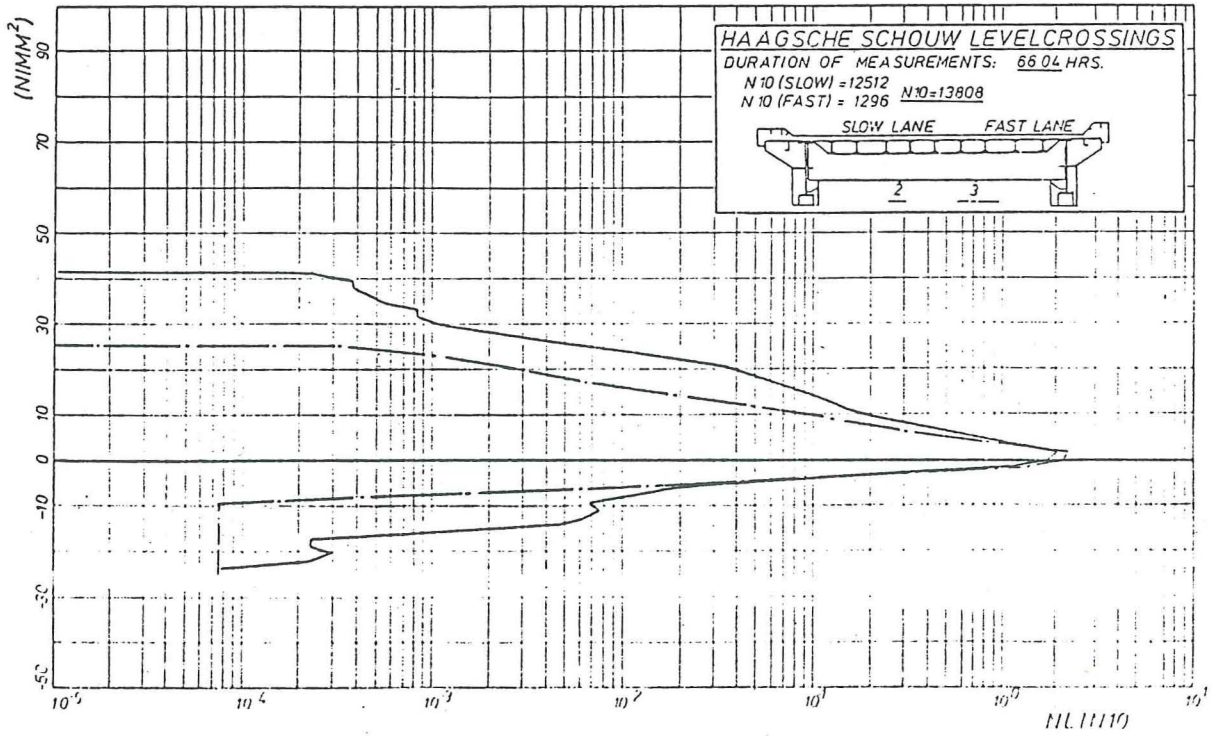
B: Traffic in the slow lane

C: Traffic in the fast lane

Contents Appendix - C- of Stevinreport 6-83-6

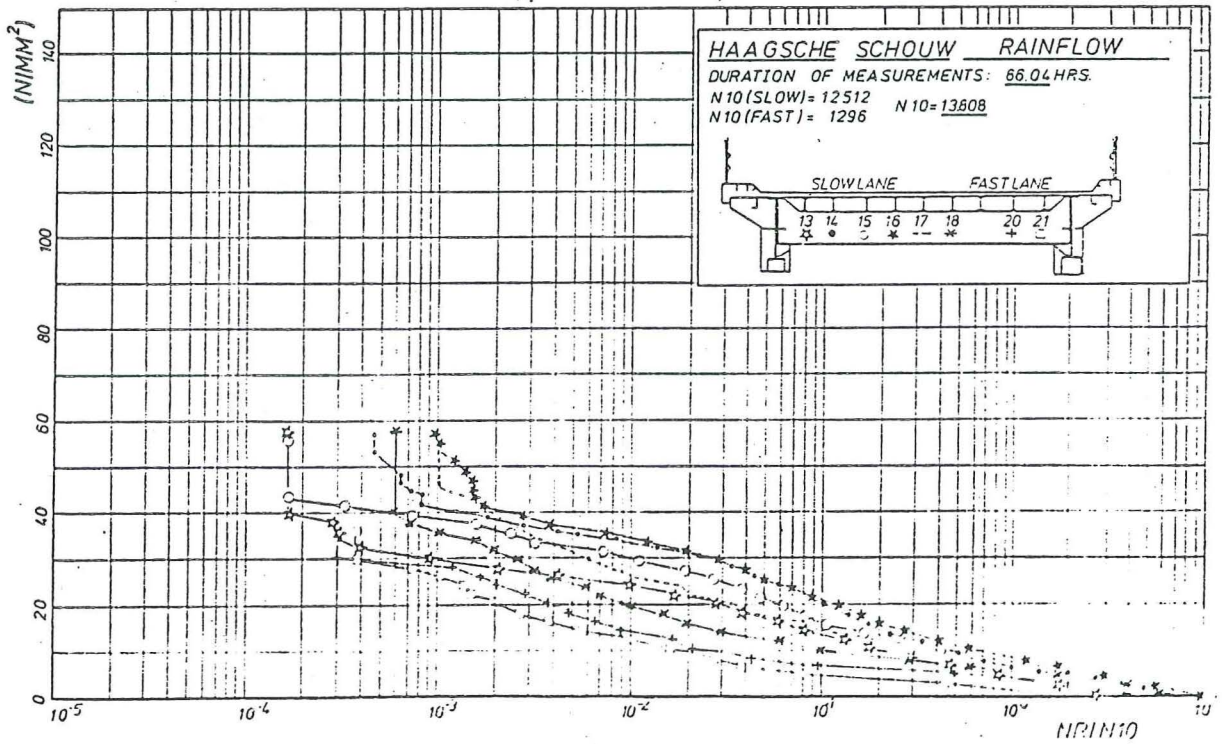
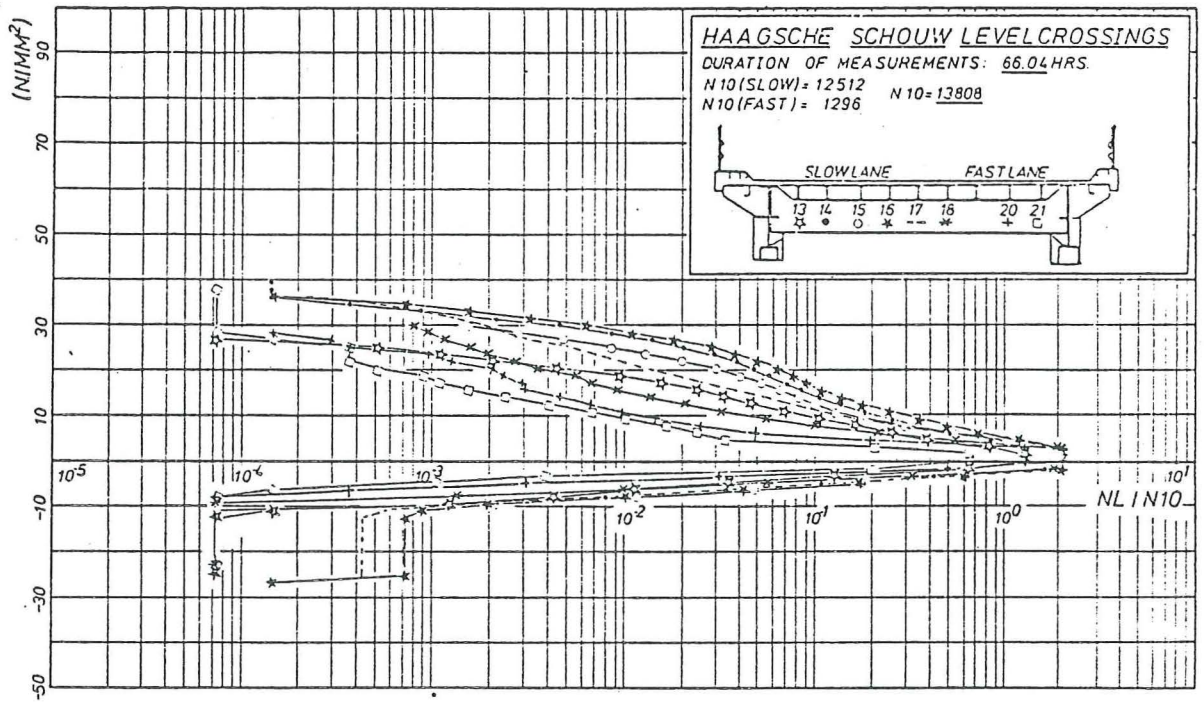
Table III.4.5.1.





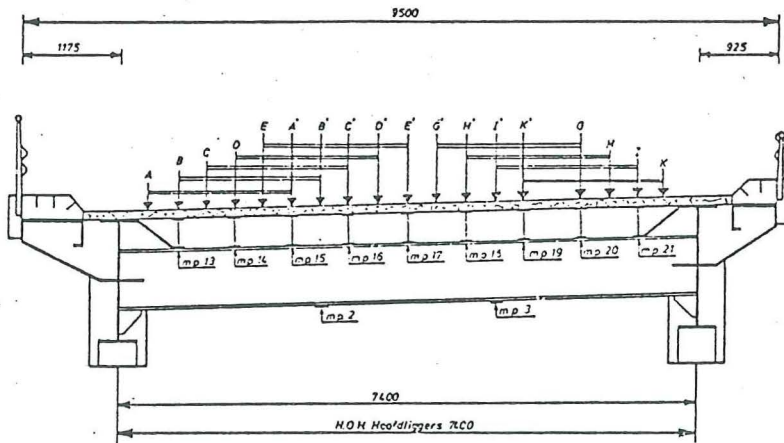
Frequency curves of measuring points 2 and 3 on the Haagsche Schouw Bridge during 66,04 hours

Figure 3.4.5.1.



Frequency curves of measuring points 13 - 18, 20 and 21 on the Haagsche Schouw Bridge during 66,04 hours

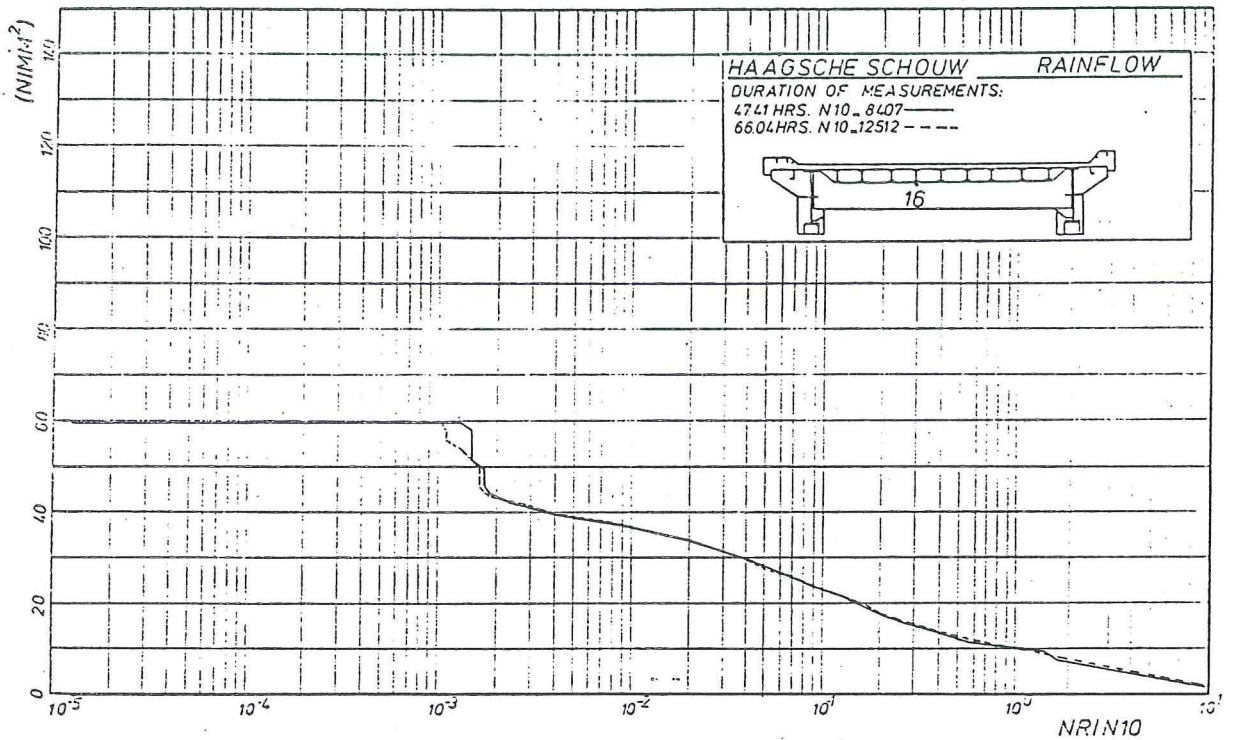
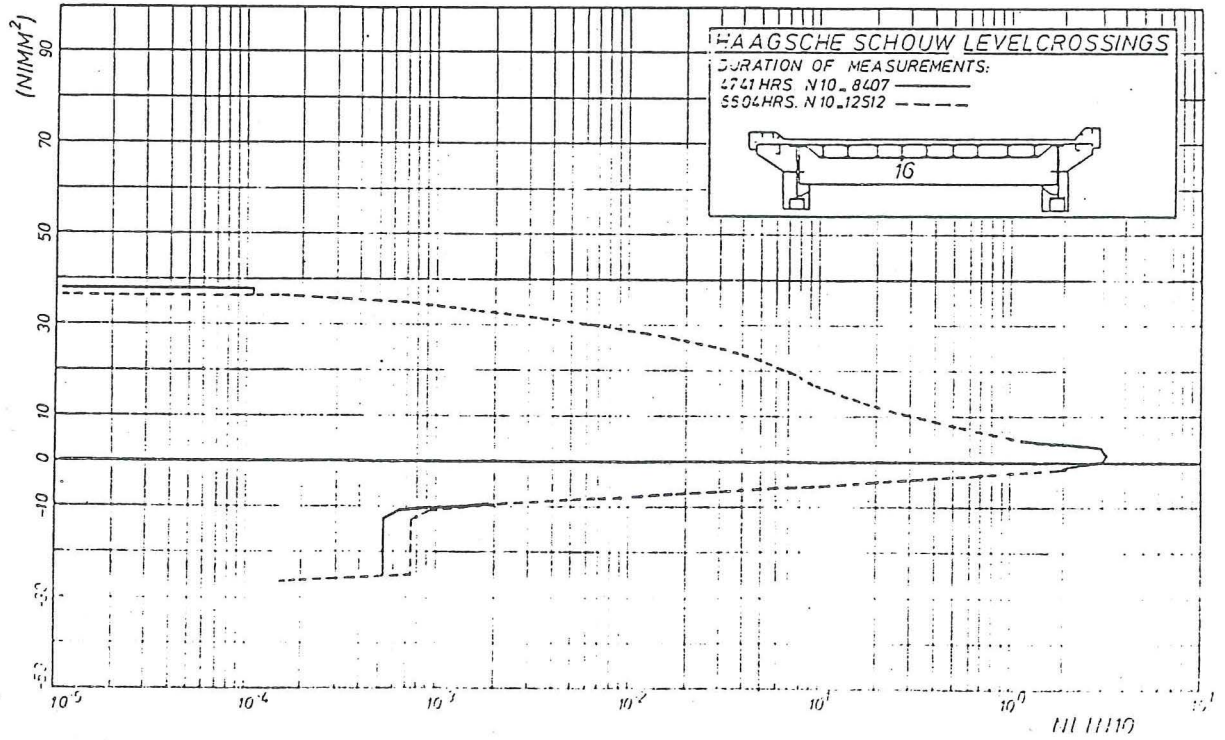
Figure 3.4.5.2.



Lateral distribution of the traffic (1)  
Figure 3.4.5.3.

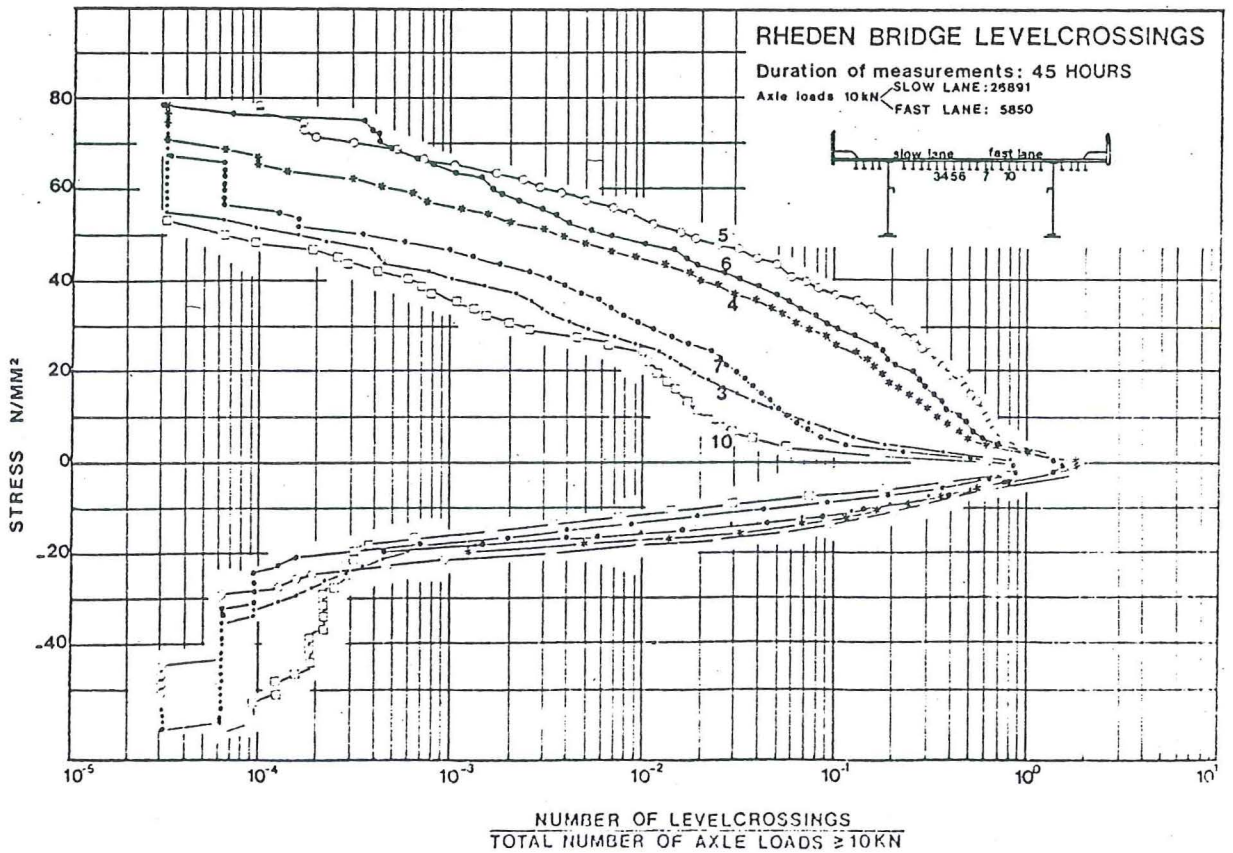
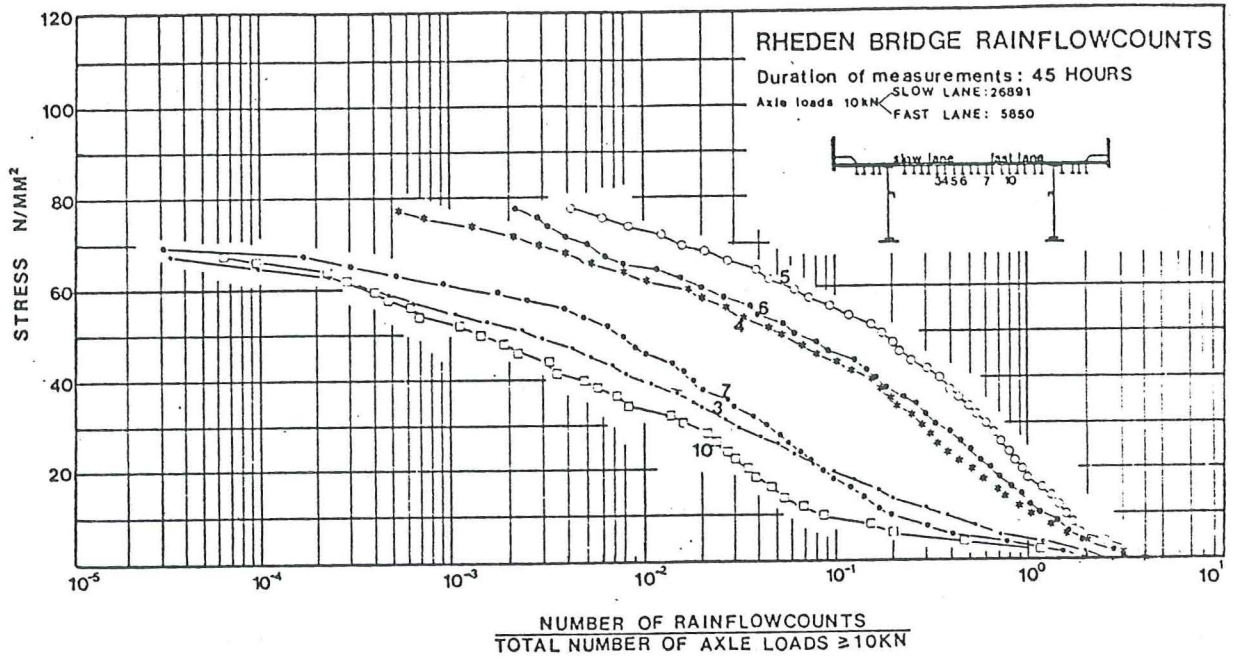
HAAGSCHE SCHOUW BRIDGE		
Duration of measurements 66,04 Hrs		
Measuring point	Track	Percentage division (%)
15	A - A'	4,7
13	B - B'	1,2
16	C - C'	57,7
14	D - D'	12,3
17	E - E'	8,8
20	G - G'	4,2
18	H - H'	7,1
21	I - I'	4,0

Lateral distribution of the traffic (2)  
Table III.4.5.2.



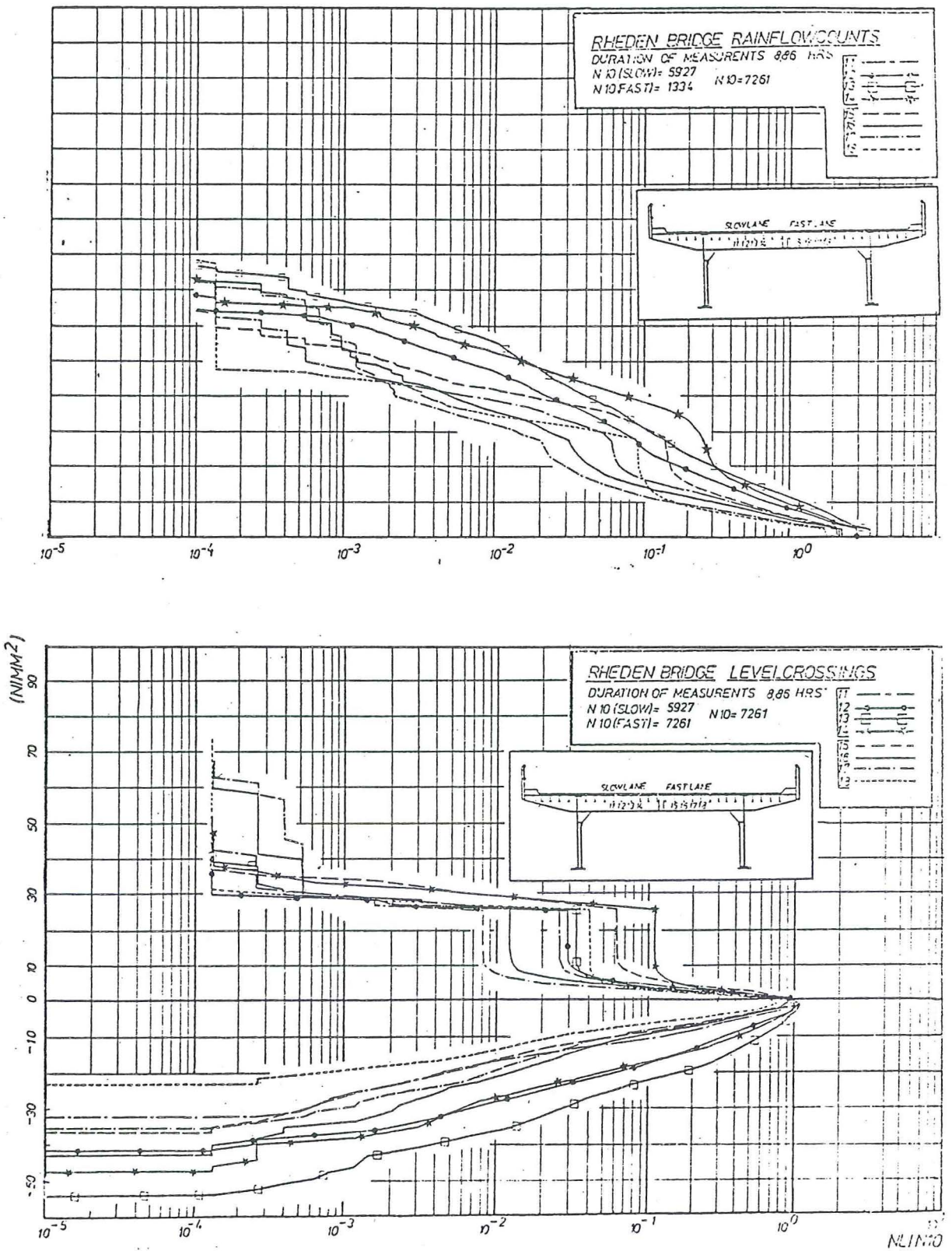
Frequency curves of measuring point 16 on the  
 Haagsche Schouw Bride

Figure 3.4.5.4.

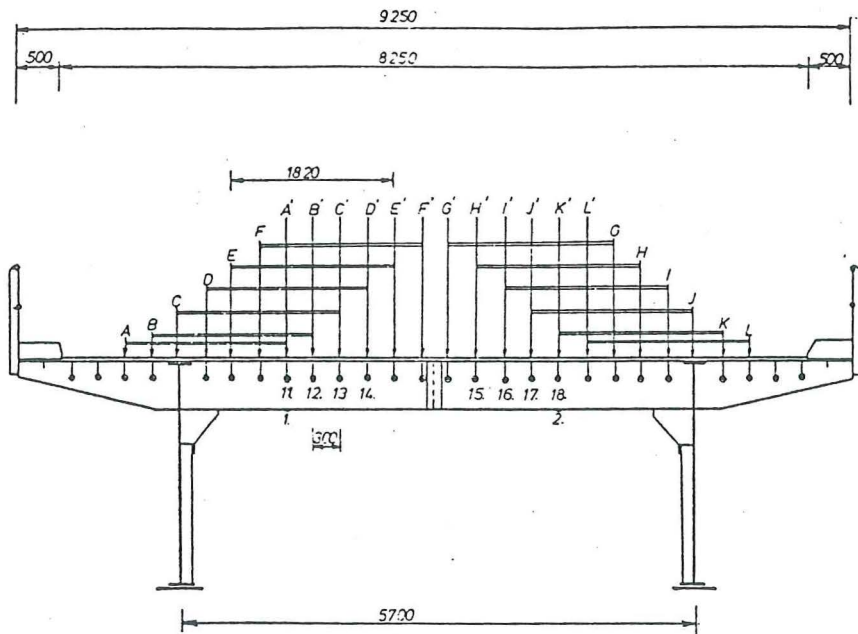


Frequency curves of measuring points 3 - 10 on the Rheden Bridge during 45 hours

Figure 3.4.5.5.



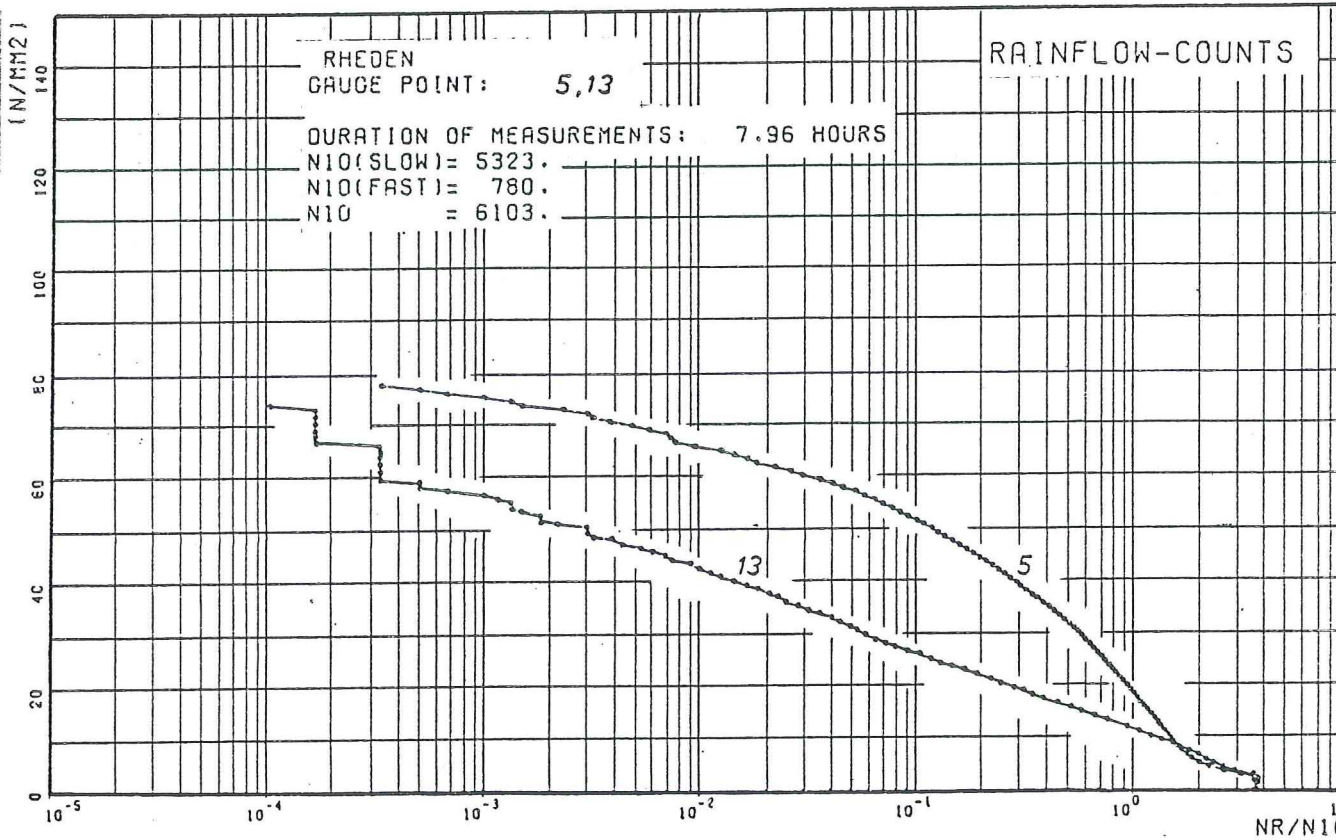
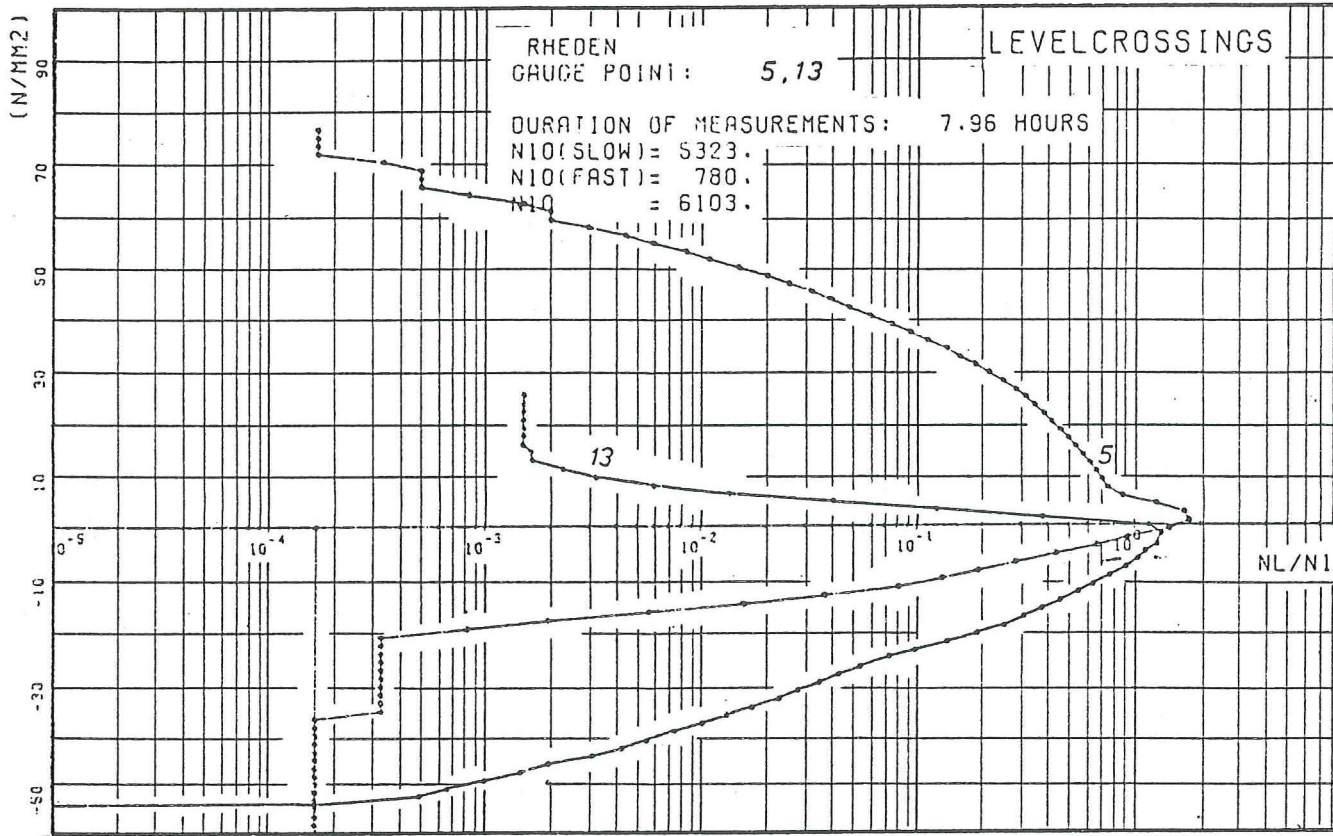
Frequency curves of measuring points 11 - 18 on the Rheden Bridge during 8,86 hours  
 Figure 3.4.5.6.



Lateral distribution of the traffic in the Rheden Bridge (1)  
Figure 3.4.5.7.

RHEDEN BRIDGE					
	Measuring point		Track	Precentaly division (%)	
Midspan points on the continous stiffner	slow lane	3	A - A'	1,3	
		4	B - B'	13,6	
		5	C - C'	55,0	
		6	D - D'	22,0	
	fast lane	7	H - H'	2,7	
		8	I - I'	2,4	
		9	J - J'	1,3	
		10	K - K'	1,9	
		91,9 %			
Points where the continous stiffner is supported by the cross-girder	slow lane	11	A - A'	2,9	
		12	B - B'	11,0	
		13	C - C'	36,9	
		14	D - D'	35,2	
	fast lane	15	H - H'	5,6	
		16	I - I'	2,6	
		17	J - J'	1,0	
		18	K - K'	5,0	
86,0 %					

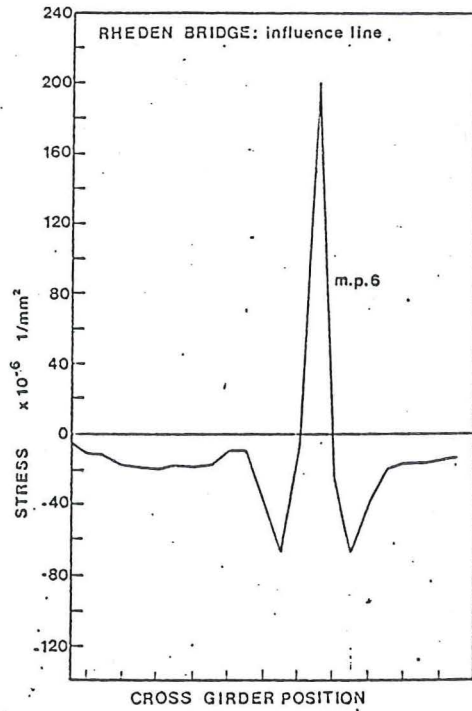
Lateral distribution of the traffic on the Rheden Bridge (2)  
Table III.4.5.3.



Frequency curves of measuring points 5 and 13  
on the Rheden Bridge during 7,96 hours

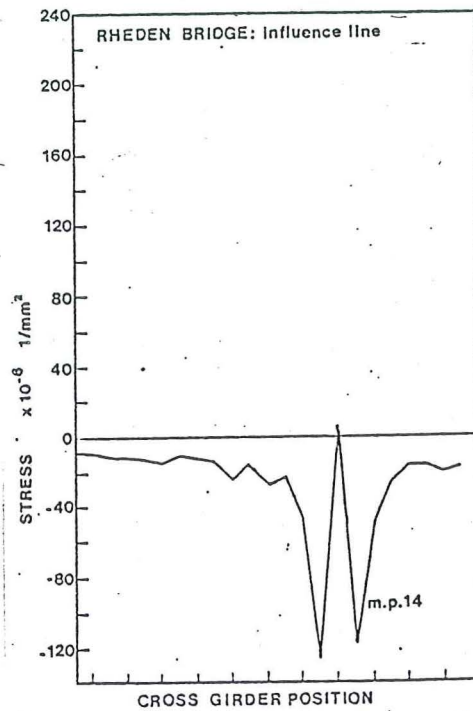
Figure 3.4.5.8.





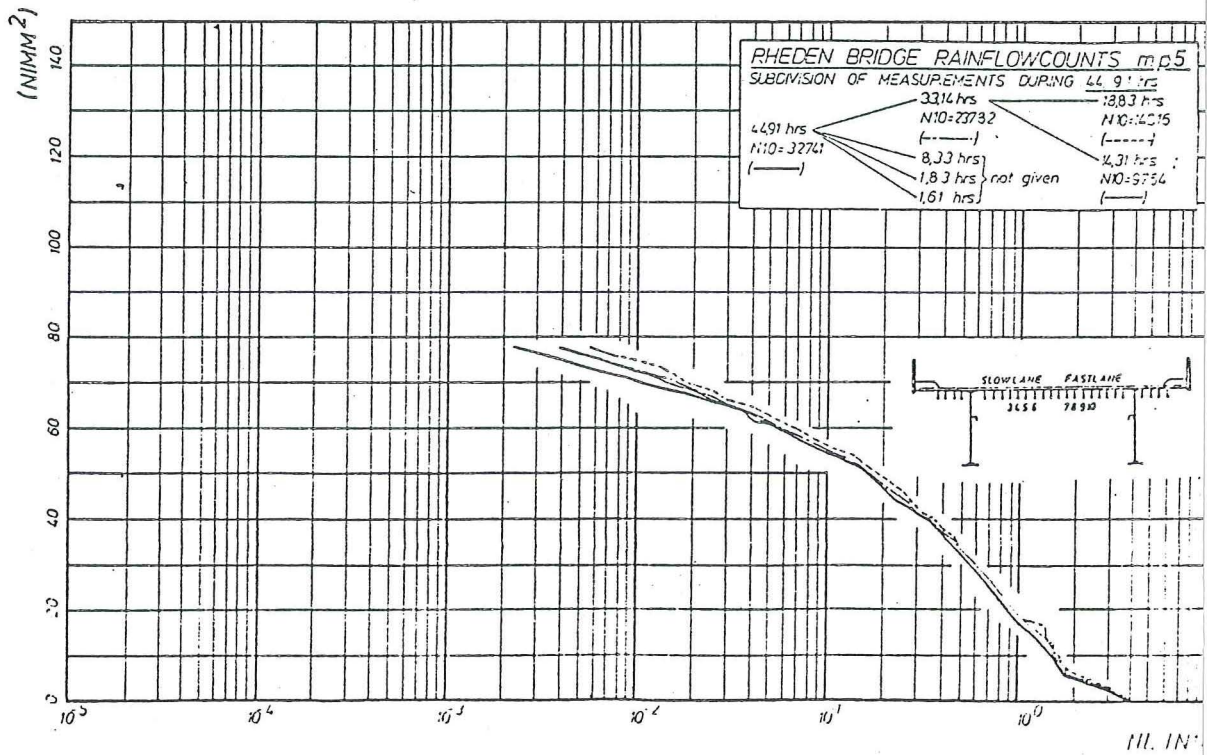
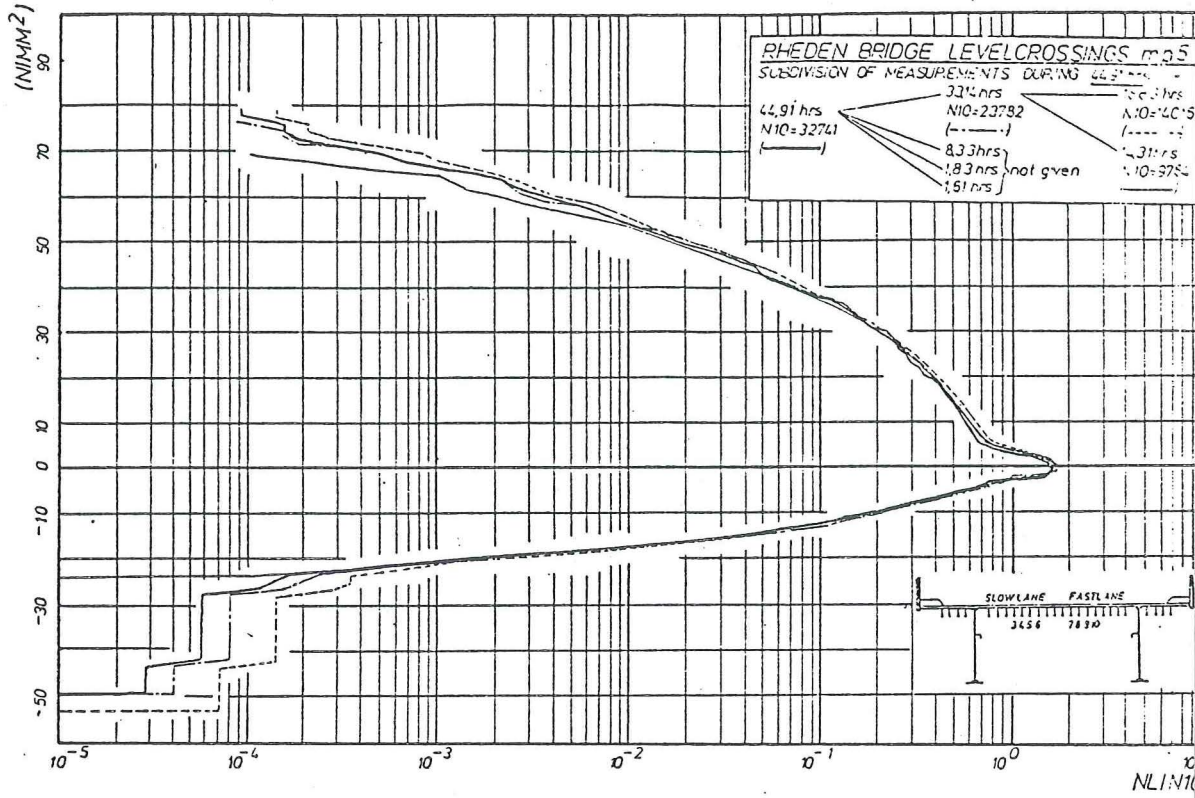
Influence line of a 'midspan point' of a longitudinal stringer of the Rheden Bridge

Figure 3.4.5.9.



Influence line of a 'point where the continuous stringer is supported by the cross girder of the Rheden Bridge

Figure 3.4.5. 10.



Frequency curves of measuring point 5 on the Rheden Bridge  
 Figure 3.4.5.11.

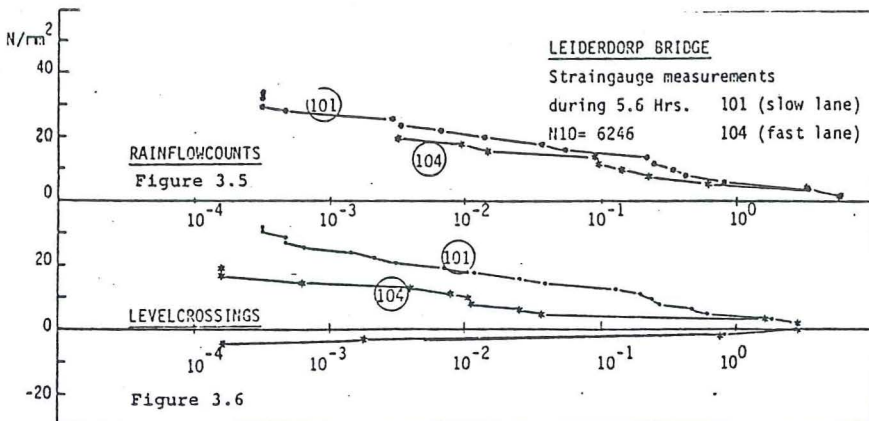
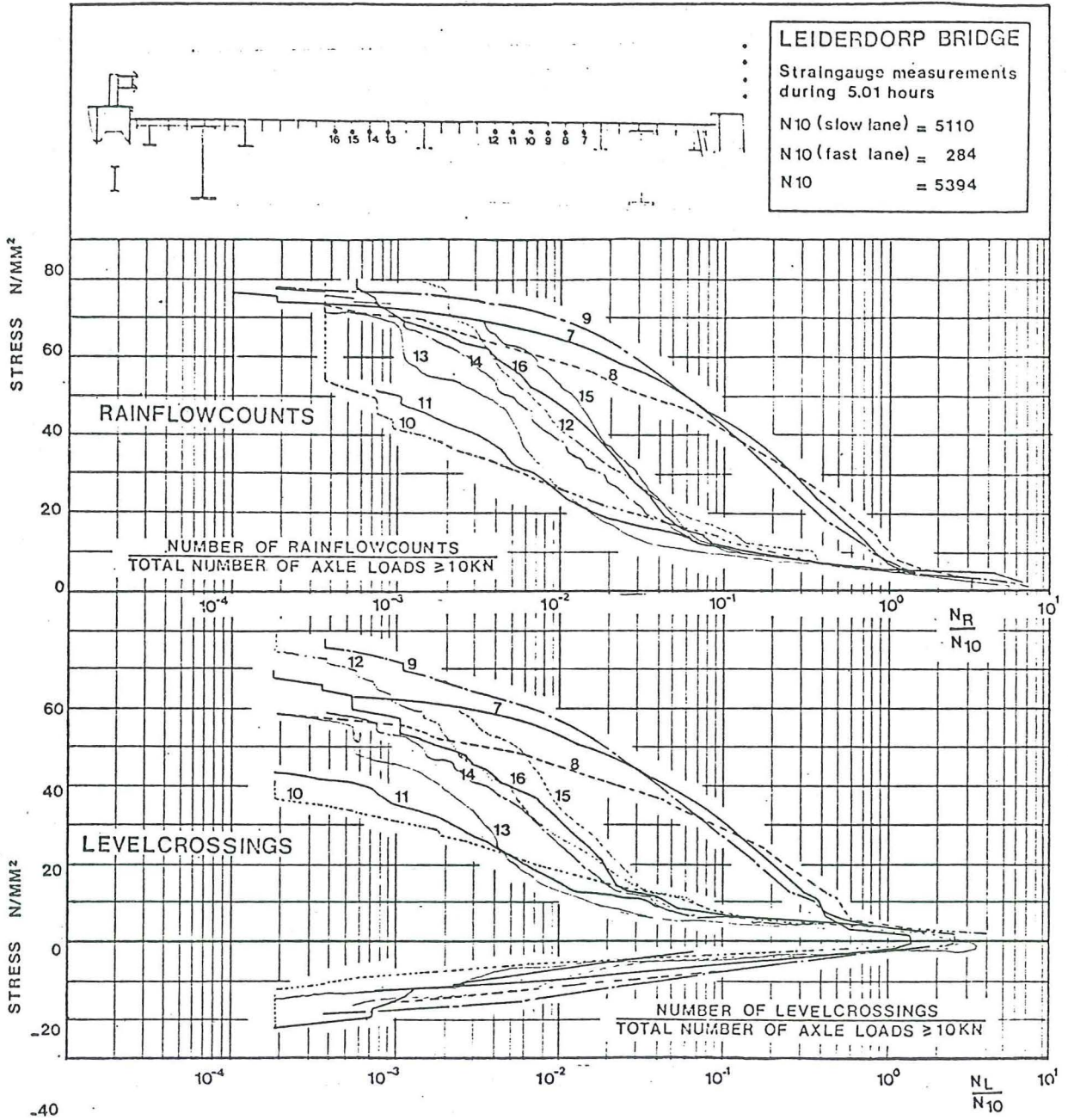


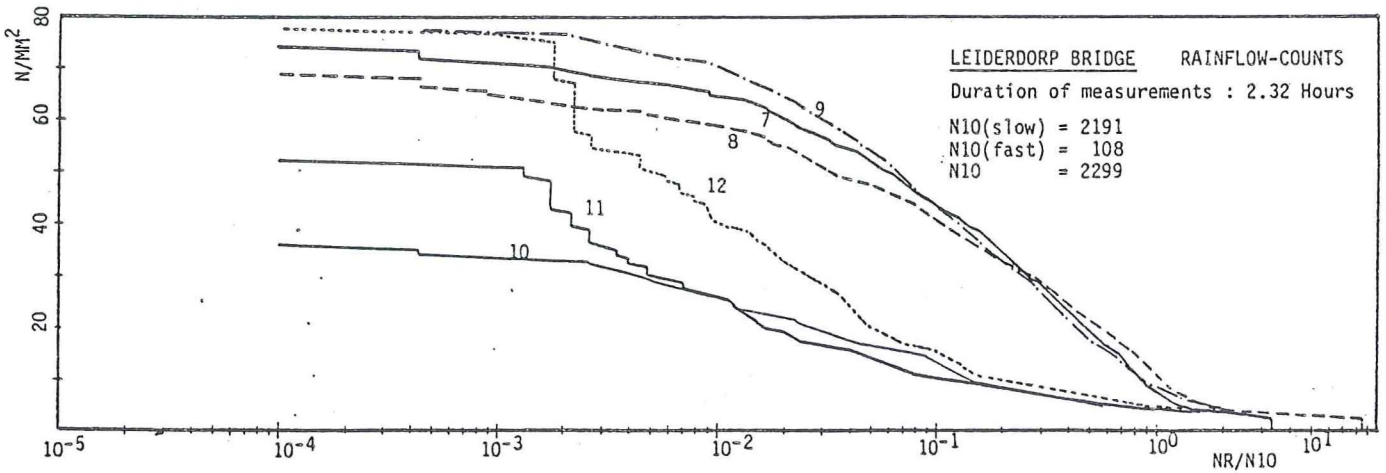
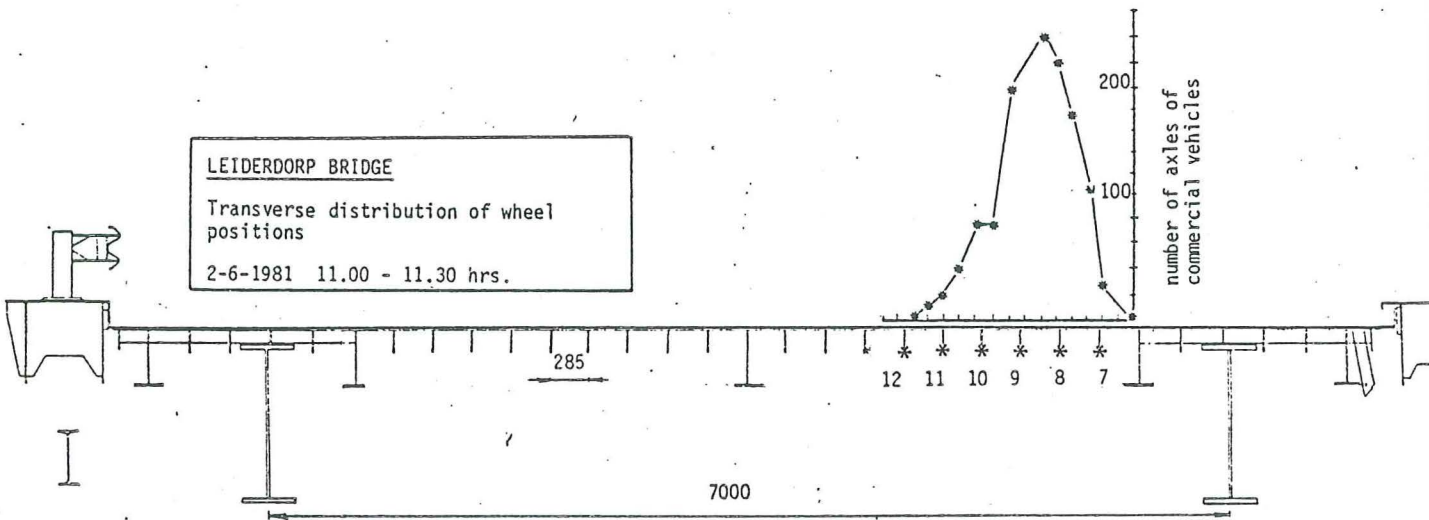
Figure 3.4.5.15.

Figure 3.4.5.16.

Frequency curves of measuring points 7 - 16, 101 and 104 in one cross section of the Leiderdorp Bridge Figures 3.4.5.13.- 16.

LEIDERDORP BRIDGE	
Measuring points	Percentage division (%)
7	34,2
8	20,3
9	41,0
10	0,8
11	0,6
12	3,1

Lateral distribution on the Leiderdorp Bridge (1)  
Table III.4.5.4.



Lateral distribution on the Leiderdorp Bridge (2)  
Figure 3.4.5.17.

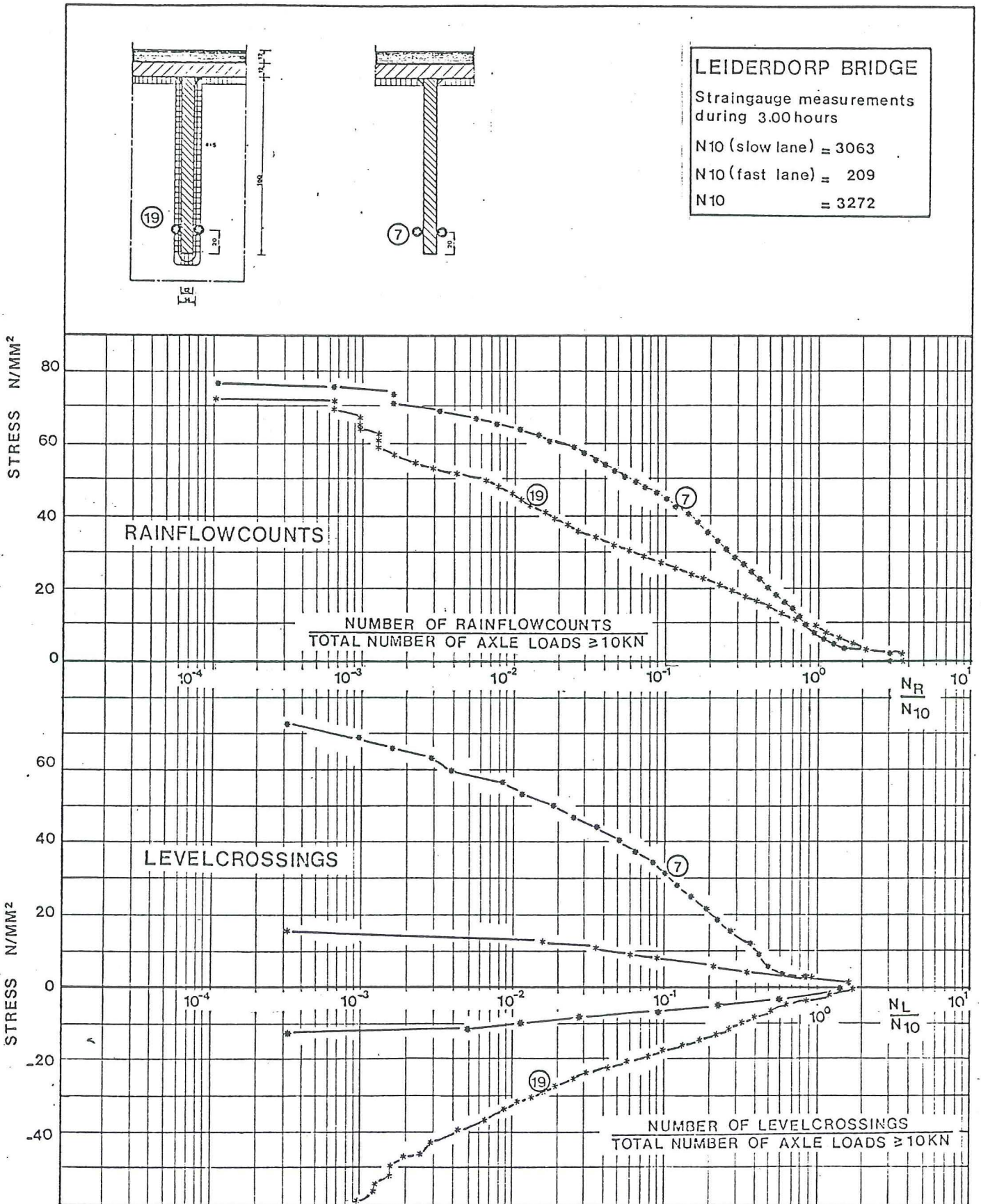


Figure 3.4.5.20.

Figure 3.4.5.21.



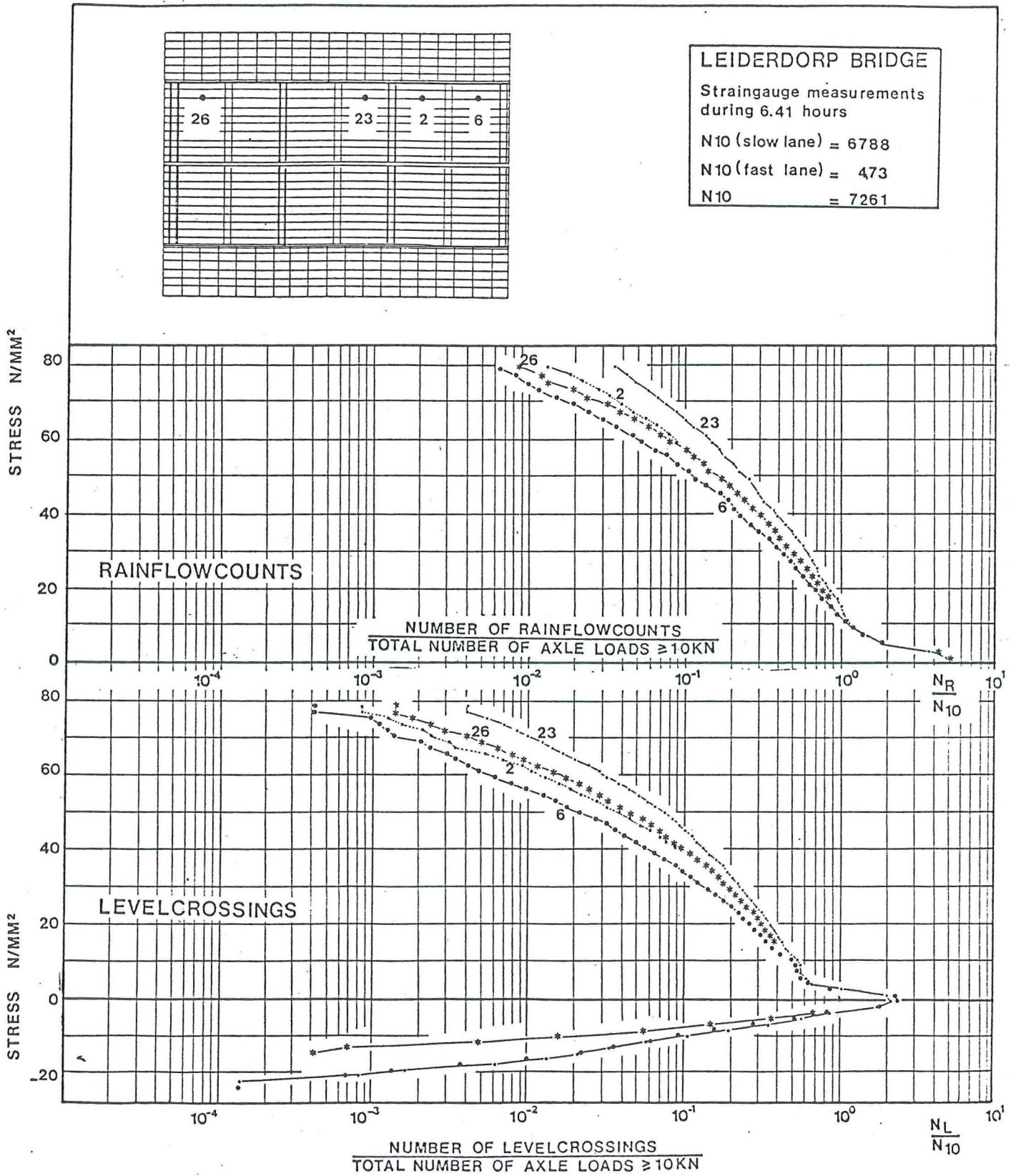


Figure 3.4.5.18.

Figure 3.4.5.19.

### 3.4.6. Comparison with measured stress data on other European bridges

#### 3.4.6.1. Maximum measured stresses

Table III.4.6.1. on page 3-59 shows that the highest stress range ( $90 \text{ N/mm}^2$ ) was measured on the girder anchor of the roadbridge of Monthery (span 12.7 m). On the girder anchor of the bridge of Limburger Bahn (span 45 m)  $50 \text{ N/mm}^2$  was reached during 6 hrs. recording.

#### 3.4.6.2. Some remarks

The extreme stresses measured were moderate, having regard for the level of loads measured on the axles (195 kN at Monthery and 160 kN at Limburger Bahn).

Contrary to wideley held views, there is a need to be concerned with the resistance to fatigue by all the elements of roadbridges i.e. the elements subjected to individual action by the wheels, as well as those that are acted upon by loads distributed (spread) over a large surface of the bridge.

Variations in stresses due to vibration are more important for certain elements of roadbridges.

Railbridges do not appear to be subject to any more fatigue damage (risk) than roadbridges, in so far as the level of stresses and the number of cycles are concerned.

The shape of the histogram-curves of axle weights resembles the shape of histogram-curves of the corresponding stresses, and the number of stress cycles is in the neighbourhood of the number of axles observed during the same period having including vibrations.



E.C.S.C. RESEARCH:  
Measurements and interpretation of dynamic loads on bridges  
**MAX. MEASURED STRESSES**

Bridge	Position	L (m)	$\Delta\sigma$ (N/mm <sup>2</sup> )	
CARONTE	8 (A)	18,6	20	
MONTLHERY	1 (B)	12,7	90	
"	12 (C)	4,5	65	
"	14 (C)	5,5	70	
AUTREVILLE	9 (B)	66	36	
SAINT-NAZAIRE	2 (D)	300	2	
"	3 (D)	160	3	
"	6 (D)	400	15	
HAAGSCHE SCHOUW	2 (A)	11	60	
"	14 (E)	5	60	
RHEDEN	1 (A)	6	44	
"	14 (C)	13	63	
LIMBURGER BAHN	101 (B)	48	50	
"	111 (B)	48	27	
"	151 (A)	12	36	
"	204 (C)	3,4	50	(A) Cross beam
FORT	16 (F)	-	84	(B) Mean beam
MANCHESTER	5 (C)	4,5	64	(C) Stiffner
WYE	5 (C)	-	84	(D) Cable
RIO VERDE	(A)	4,8	60	(E) Longitudinal beam
"	(C)	3,4	37	(F) Deck plate
"	(G)	0,6	60	(G) Sheet

Maximum measured stresses of the E.C.S.C. research  
Table III.4.6.1.

### 3.5. Results of measured stress data in relationship of influence lines

#### 3.5.1. The processing of statical measured data

Influence planes are a well known method of relating the load on the bridgedeck to the stresses in the measuring points. To construct the influence planes from experiments it is necessary to apply very concentrated loads of an appreciable magnitude at a great many points on the bridgedeck.

This presents a lot of practical problems. Instead a set of four points was used, i.e. a dual axle lorry with calibrated wheelloads.

The lorry was placed in a number of fixed positions and at each position the stresses at all the measuring points were taken and recorded.

Using a special algorithm the influence planes of an axle load instead of a single point load could be calculated.

#### 3.5.2. Results of statical measured data

To specify the stress in a measuring point due to an axle load situation in a specific location, for each of the three bridges a coordinate system is used as given in figure 3.5.1. to 3.5.3. on page 3-61 to 3-62.

The results of the influence factors of several measuring points on the bridge structures are given in the appendices.

#### 3.5.3. Dynamical influence factors

To get an indication of the dynamic effects a lorry has been driven with different speeds in the same tracks as used for the static measurements.

Results of the Haagsche Schouw Bridge are presented in table III.5.1. on page 3-63 as ratios between the dynamic influence factor and the static influence factor. An universal ratio cannot be given.

3.5.4. Figures and tables

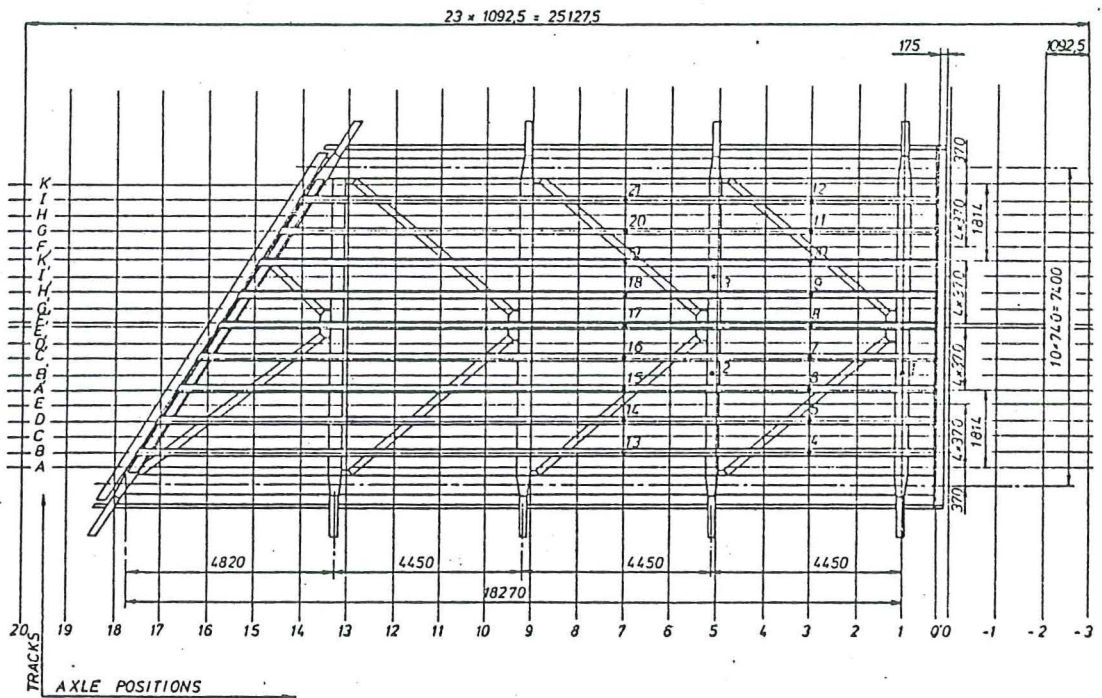
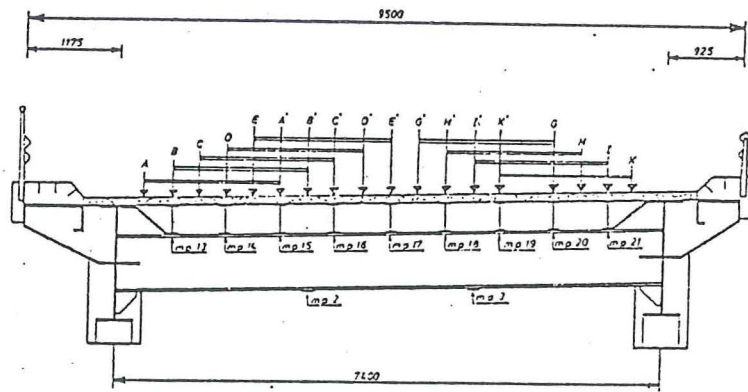
List of figures

Page

- 3.5.1. Coordinate system Haagsche Schouw Bridge 3-61
- 3.5.2. Coordinate system Rheden Bridge 3-62
- 3.5.3. Coordinate system Leiderdorp Bridge 3-62

List of tables

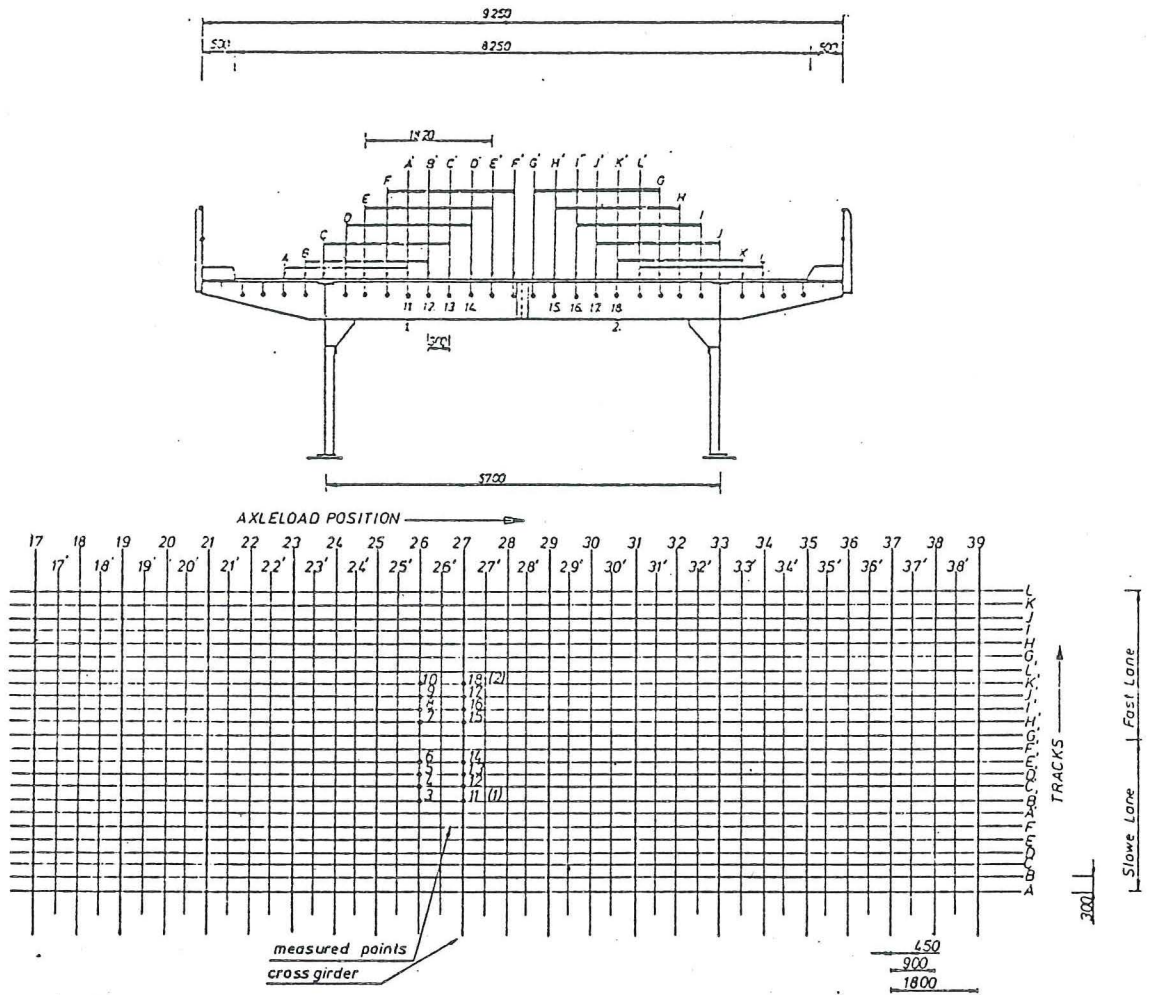
- III.5.1. Dynamic influence factors Haagsche S.B. 3-63



Coordinate system for static measurements on the Haagsche Schouw Bridge

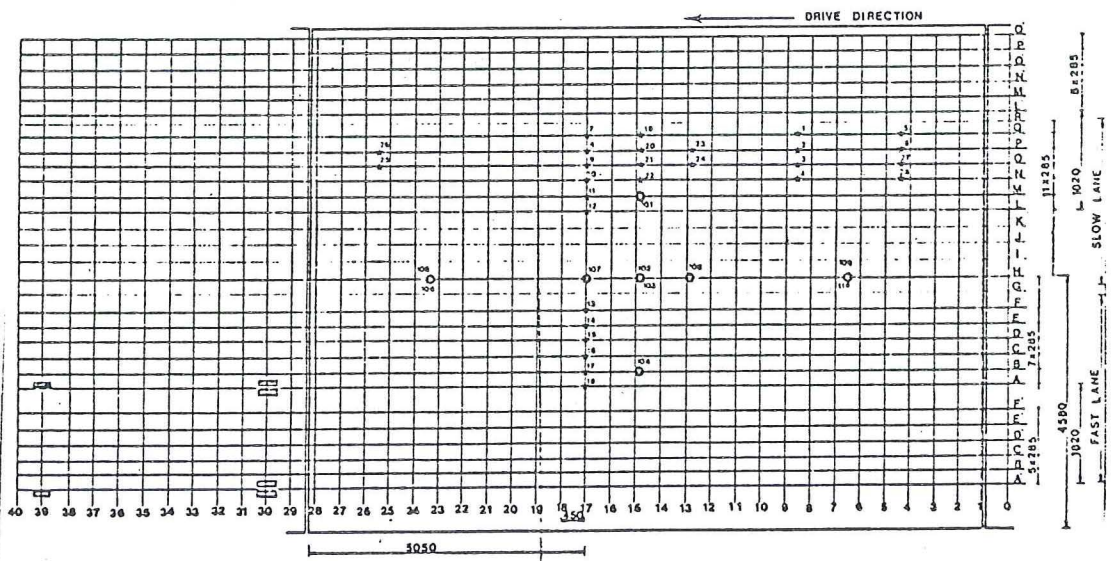
Figure 3.5.1.

3-62



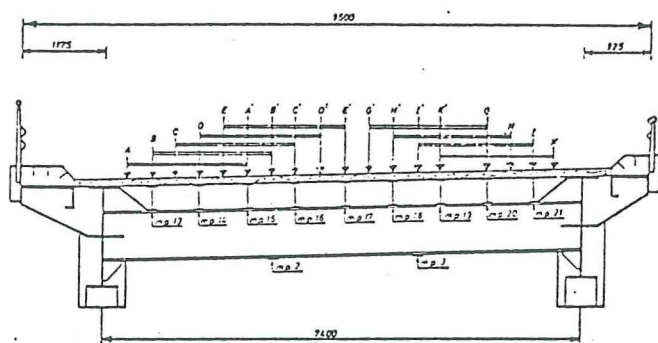
Coordinate system for static measurements on the Rheden Bridge

Figure 3.5.2.



Coordinate system for static measurements on the Leiderdorp Bridge

Figure 3.5.3.



Measured ratios between the dynamic influence factors and the static influence factors.										
		Measuring points								
Track	Speed km/h	2	3	13	14	15	16	18	19	20
B-B <sup>1</sup>	5 -	0,95	1,06	1,03	1,12	0,90	1,09	0,90	-	-
	5	0,87	1,17	1,03	1,09	1,00	1,08	1,00	-	-
	5	0,92	1,08	0,95	1,05	0,92	1,00	0,90	-	-
	25	0,94	1,13	1,02	1,16	0,94	1,18	-	-	-
	30	0,90	1,21	1,08	1,12	1,10	1,14	0,90	-	-
	40	0,90	1,08	1,01	1,04	1,08	0,93	0,75	-	-
	42	0,91	0,97	1,03	1,04	1,04	1,02	0,85	-	-
	45	0,93	0,97	0,95	0,93	0,74	0,92	-	-	-
	45	0,95	1,06	0,95	1,03	0,95	1,08	0,90	-	-
	46	0,94	1,22	0,95	0,95	1,00	0,93	0,80	-	-
47	0,92	0,83	0,95	0,99	0,98	1,02	-	-	-	
I-I <sup>1</sup>	5	0,91	1,02	-	-	-	1,23	0,92	0,92	0,98
	5	-	-	-	-	-	1,17	1,09	1,02	1,08
	5	0,97	1,05	-	-	-	1,30	1,08	0,95	1,05
	25	1,02	1,06	-	-	-	1,23	1,13	0,95	1,07
	25	0,95	1,04	-	-	-	1,10	1,13	0,98	1,07
	25	0,97	1,03	-	-	-	1,10	1,05	1,00	1,03
	41	0,82	0,97	-	-	-	1,13	0,94	1,02	0,97
	41	0,97	1,02	-	-	-	1,44	0,94	0,94	1,05
41	0,92	1,03	-	-	-	1,28	1,03	0,95	1,05	

Measured ratios between dynamic and static influence factors  
Table III.5.1.

### 3.6. Comparison between computed and measured stress data

#### 3.6.1. Simulation of stress-spectra

For the Haagsche Schouw Bridge the axle loads counted in a period of 4.25 hours and the influence lines associated with a measuring point are put together to calculate the theoretical level crossings and rainflow counts.

The cumulative relative distribution curves of the measured axle loads in the fast lane as well as the slow lane are given in figure 3.6.1. on page 3-66. The results of level crossings and rainflow counts measured during 4.25 hours are given in table III.6.1. and III.6.3. on page 3-67.

The theoretical level crossings and rainflow counts for this period are given in table III.6.3. and III.6.4. on page 3-67.

Both, measured and calculated values are plotted in modified cumulative relative distribution curves per measuring point (see i.e. figure 3.6.2. and 3.6.3. on page 3-68).

The measured curves show a remarkable larger number of cycles than the calculated curves, due to the dynamical behaviour of this bridge. This behaviour can be seen in figure 3.6.4. where the analogues recording of a number of measuring points are presented and the position of a lorry indicated with photographs.

A considerable number of cycles occur after the vehicle has left the bridge. So it does not come as a surprise that the empirical values do not coincide with this calculation.

#### 3.6.2. Computed static influence lines

In order to be able to put together design criteria for bridges with respect to fatigue, it is important to assess the actual stresses in relation to the stresses calculated with a design model.

Most design models used in bridge design are simplifications of reality in such a way that the calculated stresses are higher than the actual stresses, so a reducing factor on the calculated stresses can be applied.

To verify this, the Haagsche Schouw Bridge was calculated according to a more advanced model than the model that was used when the bridge was designed.

This calculation was assuming that stringers and cross girders are in the same grating. The reason for this design model was to keep the calculating costs down. A limited investigation showed that the mentioned way of calculation did not cause a great deviation.

As a control-calculation the position of the measuring lorry, as given in figure 3.6.5. on page 3-69 was used.

The results of the Stardyne-program relating to the measured values are given in table III.6.5. on page 3-69.

It appeared that the calculated stresses were about 30% higher than the measured values. Partly this was caused by the theoretical loadingsystem because the axle distance and wheel distance are smaller in practice.

Figure 3.6.6. on page 3-69 shows the stress pattern in longitudinal stringers of a cross section of the bridge.

Taking the wooden deck in account means more stiffness of the longitudinal stringers with a better spreading of the stress patterns. This causes a reduction of the maximum stresses and describes the measured stress pattern better. The deflection on the spot of the lower stresses became greater. So this leveling did not occur in the cross section of the bridge.

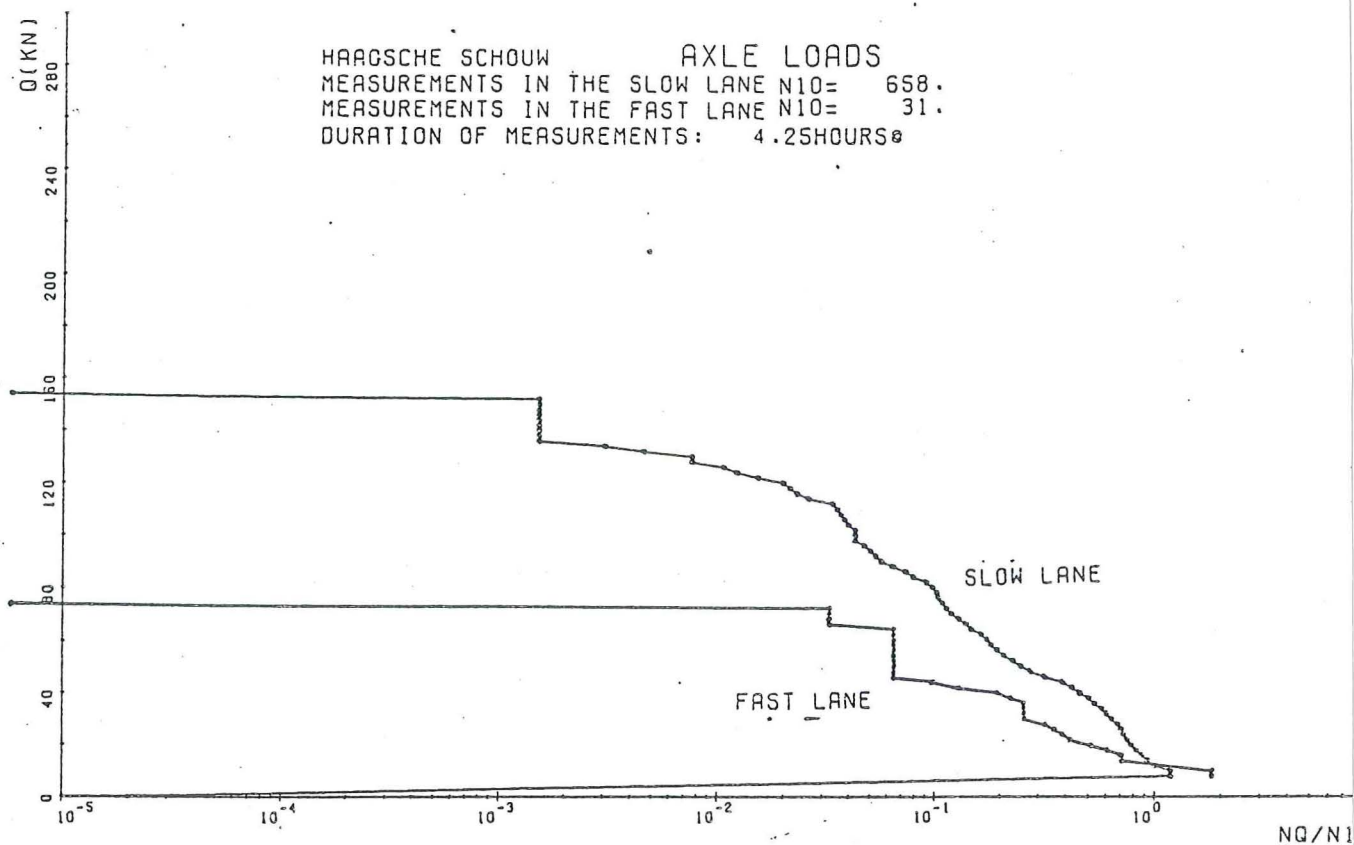
### 3.6.3. Figures and tables

List of figures	Page
3.6.1. Measured axle loads	3-66
3.6.2. Rainflow counts measured and calculated	3-68
3.6.3. Levelcrossings measured and calculated	3-68
3.6.4. Analogue recording of several measuring points	3-68

	Page
3.6.5. Position of the measuring lorry	3-69
3.6.6. Stress pattern in one cross section	3-69

## List of tables

III.6.1. Level crossings measured	3-67
III.6.2. Level crossings calculated	3-67
III.6.3. Rainflow counts measured	3-67
III.6.4. Level crossings calculated	3-67
III.6.5. Results Stardyne-program	3-69



Axle load spectra used for calculating the theoretical levelcrossings and rainflow counts

Figure 3.6.1.



SUM OF THEORETICAL LEVELCROSSINGS OF THE FOLLOWING MEASUREMENTS

Table with columns: CODE NUMBER, NUMBER, DATE, and R. POINTS (2, 3, 13, 14, 15, 16, 18, 19, 20, 21). Rows represent various level crossings from -11.0 to 42.0.

Calculated level-crossings
Table III.6.3

SUM OF LEVELCROSSINGS OF THE FOLLOWING MEASUREMENTS

Table with columns: CODE NUMBER, NUMBER, DATE, and R. POINTS (2, 3, 13, 14, 15, 16, 18, 19, 20, 21). Rows represent measured level crossings from -11.0 to 33.0.

Measured level crossings
Table III.6.1

SUM OF THE THEORETICAL RAINFLOW COUNTS OF THE FOLLOWING MEASUREMENTS

Table with columns: CODE NUMBER, NUMBER, DATE, and R. POINTS (2, 3, 13, 14, 15, 16, 18, 19, 20, 21). Rows represent range N/PM2 from 0.0 to 42.0.

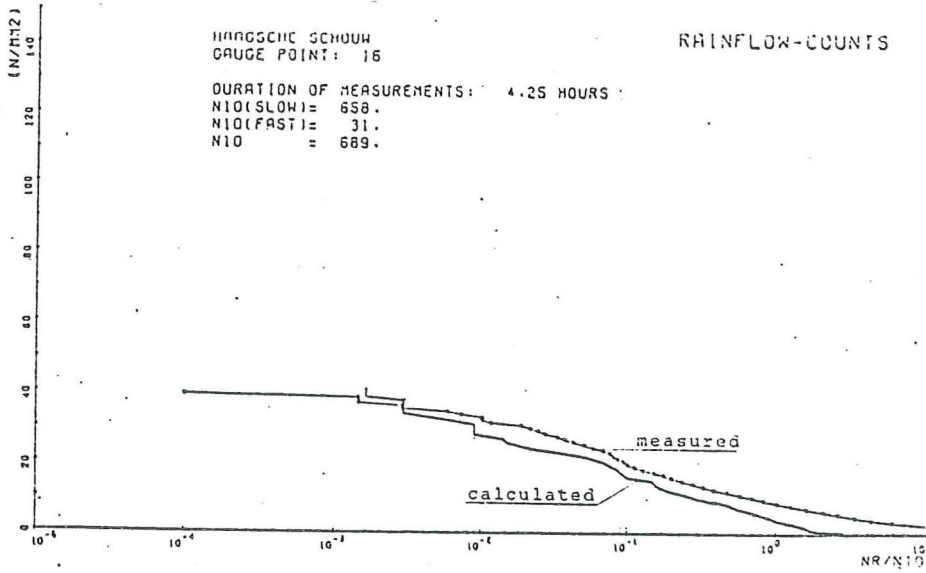
Calculated rain-
flow counts
Table III.6.4

SUM OF THE RAINFLOW COUNTS OF THE FOLLOWING MEASUREMENTS

Table with columns: CODE NUMBER, NUMBER, DATE, and R. POINTS (2, 3, 13, 14, 15, 16, 18, 19, 20, 21). Rows represent measured rainflow counts from 0.0 to 53.0.

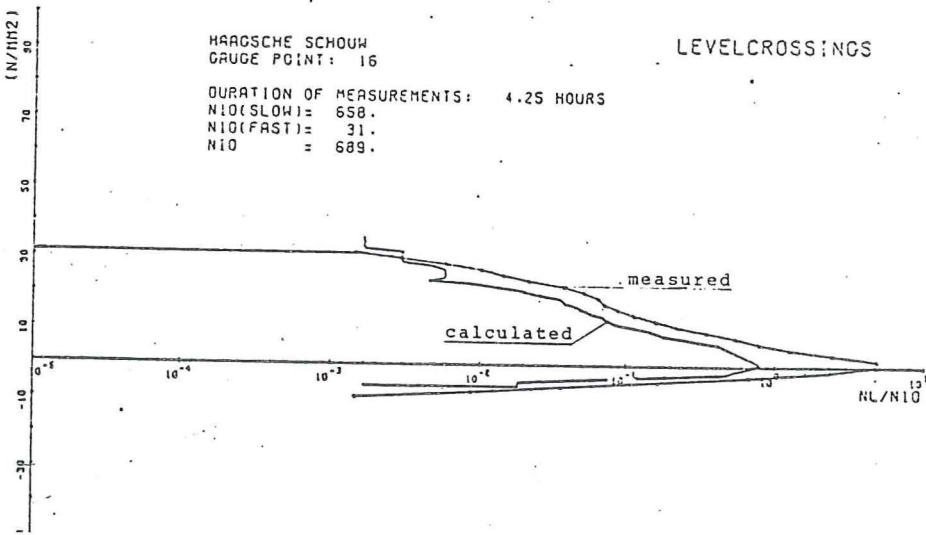
Measured rainflow counts
Table III.6.2

3-67



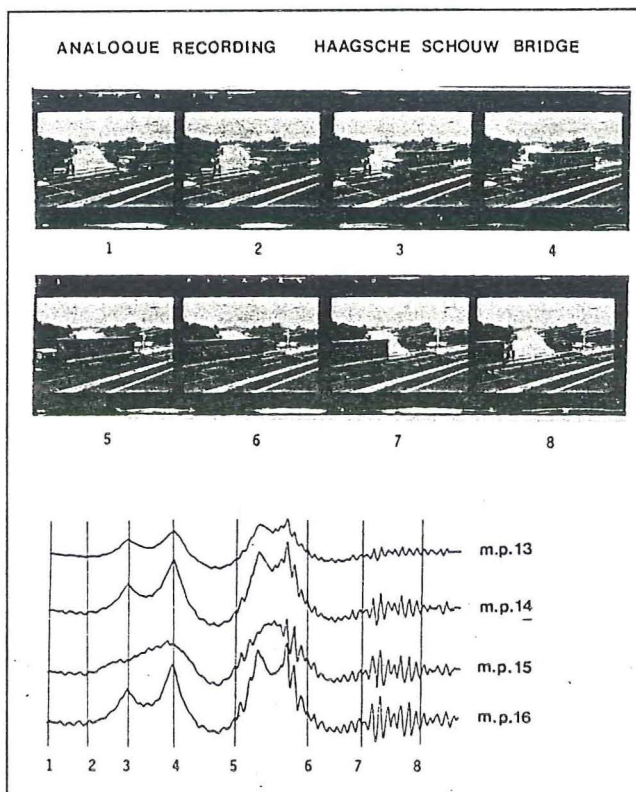
Measured and calculated rainflow counts

Figure 3.6.2



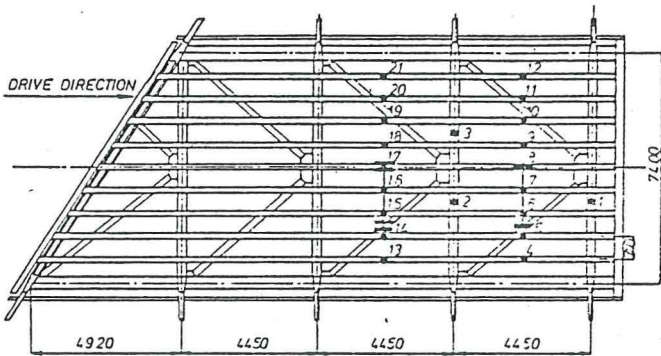
Measured and calculated level crossings

Figure 3.6.3

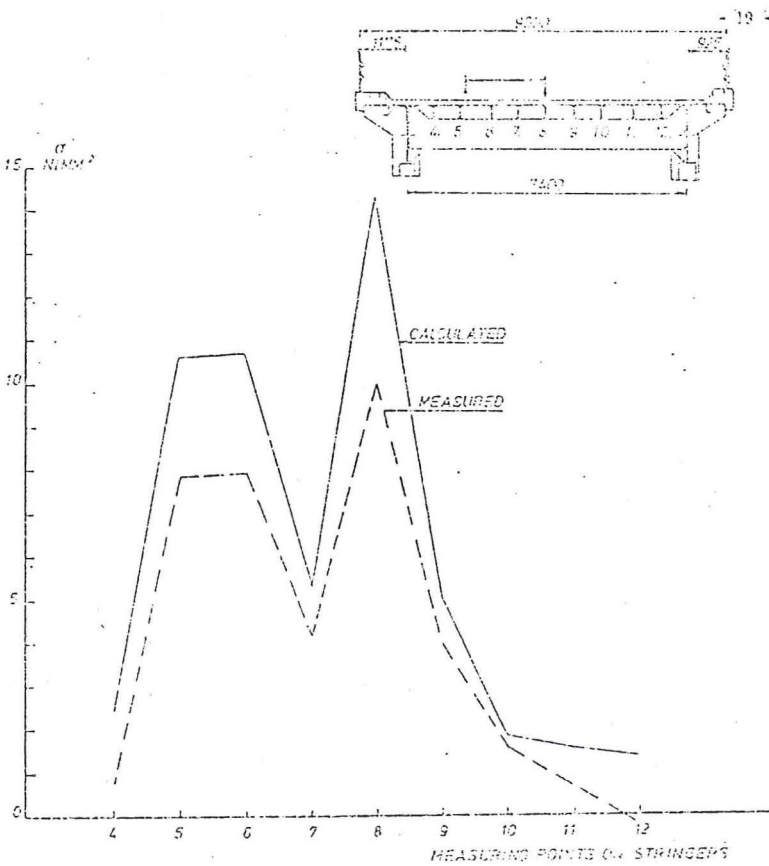


Analogue recording

Figure 3.6.4.



Lorry position for the control-calculation  
Figure 3.6.5.



Comparison between measured and calculated values (1)  
Table III.6.5

Measured point	measured value $\sigma N/mm^2$	calculated value $\sigma N/mm^2$	Deflection %
1	2,04	3,16	54,9
2	5,81	8,60	48,0
3	8,66	11,55	33,4
4	0,71	2,45	
5	7,85	10,60	35,0
6	7,95	10,70	34,6
7	4,18	5,38	28,7
8	9,99	14,35	4,36
9	3,98	4,97	24,9
10	1,63	1,83	12,3
11	0,71	1,52	
12	- 0,20	1,37	
13	1,94	4,26	
14	13,15	18,95	44,1
15	14,27	19,32	35,4
16	9,68	9,93	2,3
17		24,12	

Comparison between measured and calculated values (2)  
Figure 3.6.6

### 3.7. Concluding remarks chapter 3

#### 3.7.1. Measured traffic

The cumulative relative frequency curves of the measured axle loads shows that the traffic distribution on the three Dutch bridges differs much and the heavy weighing commercial vehicles are concentrated in the slow lanes. Leaving the fast lane out of consideration the results for the slow lanes can be summarised as follows:

- 3500 - 6000 axle loads  $\geq$  10 kN are enough to record the cumulative relative frequency curves of axle loads.
- It is not possible to give for each vehicle type unanimous values of axle loads and axle distances which are operative for the three measured bridges.
- Distribution of the vehicle types over the total traffic showed that 10-24% of the traffic consists of commercial vehicles, corresponding 93 - 305 hours.
- Besides type 9, an artic, 2-axle tractor with a 2-axle semi-trailer and type 4, an rigid, 2-axle commercial vehicle with a 2-axle drawbar trailer, the dual-axle lorries are the most frequent types (49 - 80%).
- The frequency of vehicle intervals greater than 50 meter varies between 82 and 96%.

#### 3.7.2. Measured stresses

The modified relative frequency curves of levelcrossings as well as the modified cumulative relative frequency curves of rain flow counts shows that the stress distribution in a cross-section of the bridges differs markedly. The stresses which are exerted in several points, especially where the traffic is not frequent, are not only smaller but also occur less then in the points where most of the heavy traffic runs. Even in the slow lane there is much deviation. It can be concluded that about 60% of the traffic drives in the same track on the bridges and that the stress distribution in a cross-section is dependent on the difference of the influence lines.

About 9000 - 10.000 axle loads  $\geq 10$  kN are enough to construct the frequency curves of the measuring points where 60% of the traffic runs.

Comparison of measured stress spectra in combination of measured influences shows that there is a good correlation between them.

### 3.7.3. Measured and calculated influence lines

An universal ratio between the dynamic influence factors and the static influence factors on the "Haagsche Schouw Bridge" can not be given. Another influence of the dynamic loads of the "Haagsche Schouw Bridge" showed that the number of cycles is larger than the number of cycles that can be calculated with the help of static influence lines.

A limited investigation with computed static influence lines for the "Haagsche Schouw Bridge" showed that the calculated stresses were about 30% higher than the measured values.

More information about dynamic factors will be given in the French final report and the Italian final report will be presenting a comparison of measured and calculated influence lines of several European road bridges.



4. Analysis of the traffic data and stress data in fatigue terms

## 4. ANALYSIS OF TRAFFIC DATA AND STRESS DATA IN FATIGUE TERMS

CONTENTS	Page
4.1. Introduction	4-4
4.2. Traffic data	4-5
4.2.1. Analysing techniques	4-5
4.2.1.1. Standard axle load	4-5
4.2.1.2. Equivalent axle load	4-5
4.2.1.3. Characteristic axle load	4-6
4.2.2. Fatigue loads of measured traffic	4-7
4.2.2.1. CAL of the commercial vehicles	4-7
4.2.2.2. Damaging potential of the population of commercial vehicles	4-7
4.2.3. Fatigue loads of axle load spectra	4-8
4.2.3.1. Actual spectra	4-8
4.2.3.1.1. Characteristic axle load	4-8
4.2.3.1.2. Damaging potential of different axle load classes	4-8
4.2.3.2. Extrapolated spectra	4-9
4.2.3.2.1. Extrapolation of actual axle load spectra	4-9
4.2.3.2.2. Damaging potential of different axle load classes of the extrapolated spectra	4-10
4.2.4. Comparison for the three bridges and other axle load location in the Netherlands	
4.2.5. Conclusions	4-12
4.2.6. Figures and tables	4-12
4.3. Stress data	4-28
4.3.1. Regulations for calculations of fatigue loaded welded joints in the Netherlands	
4.3.2. Actual spectra	4-30
4.3.2.1. Damaging potential of the different stress range classes	4-30
4.3.2.2. Characteristic stress range	4-32



	Page	
4.3.2.3.	Fatigue life expectance calculations	4-33
4.3.2.3.1.	Stiffner of the bridgedeck of the Rheden Bridge - crossing of the stiffner and a cross girder	4-33
4.3.2.3.2.	Stiffner of the bridgedeck of the Rheden Bridge - crossing of the stiffner and a cross girder	4-35
4.3.3.	Extrapolated spectra	4-35
4.3.3.1.	Extrapolation of stress-spectra	4-35
4.3.3.2.	Damaging potential of the extra- polated spectra	4-36
4.3.3.3.	Characteristic stress range	4-37
4.3.3.4.	Assumptions for further analysis	4-37
4.3.3.5.	Analysis in fatigue terms	4-38
4.3.4.	Conclusions	4-39
4.3.5.	Figures and tables	4-40
4.4.	Relationship traffic data to stress data	4-53
4.4.1.	Relating stress-spectra to axle load spectra	4-53
4.4.2.	The effect of temperature of asphalt surfacing	4-53
4.4.3.	Relative contribution of front and rear wheels to fatigue damaging	4-54
4.4.4.	Figures and tables	4-55

#### 4. SOME ANALYSIS OF THE TRAFFIC DATA AND STRESS DATA

##### 4.1. Introduction

This chapter of the final report contains results of the analysis of the traffic data and stress data of chapter 3 in fatigue terms.

Using a standard axle load of 100 kN, the "equivalent axle load method" and the "characteristic axle load method" the measured and extrapolated axle load spectra are worked out in a way they are relevant to fatigue.

The damaging potential of different axle load classes of the measured and extrapolated spectra and the damaging potential of the commercial vehicles have been calculated using a fifth power relationship.

Comparison for the three bridges have been made using measurements of the Government Laboratory for highway designs of ten axle load locations in The Netherlands.

Fatigue life expectancy calculations are made using the regulations for calculations of fatigue loaded welded joints in The Netherlands. The damaging potential of different stress range classes of the measured and extrapolated spectra have been calculated.

Besides some attention has been paid to the relationship of traffic data to stress data; the relative contribution of front and rear wheels to fatigue damage and the effect of temperature of asphalt surfacing.

## 4.2. Traffic data

### 4.2.1. Analysing techniques

#### 4.2.1.1. Standard axle load

One of the methods to describe an axle load spectrum in a way it is relevant to fatigue, is the "standard axle load method".

Figure 4.2.1. on page 4-14 shows cumulative axle load spectra related to a 100 kN standard axle of measured traffic on three bridges. In this figure the number of axles occurring in each loadrange have been converted to an equivalent number of 100 kN standard axles using a fourth power relationship.

$$\frac{n_i \left(\frac{Q_i}{100}\right)^4}{\sum \left\{n_i \left(\frac{Q_i}{100}\right)^4\right\}}$$

$n_i$  = number of axles in a loadrange  
 $Q_i$  = midvalue of that load-range

From this figure it appears that the curves are significantly different, except the phenomenon that only a very small percentage of the total damage is caused by the large proportion of axles weighing less than 30 - 40 kN.

The contribution of high axle loads and axle loads < 40 kN to fatigue damage potential, could perhaps be ignored without introducing great errors.

#### 4.2.1.2. Equivalent axle load (see ref. 6-5)

Another method to describe an axle load spectrum in a way it is relevant to fatigue, is the equivalent axle load method. The equivalent axle load  $Q_m$  and its associated number of cycles  $n_m$  can be fixed by calculating the centre of gravity of the distribution of damaging potential of axle loads, as follows:

$$Q_m = \frac{\sum n_i Q_i^4}{\sum n_i Q_i^3} \quad n_m = \frac{\sum n_i Q_i^3}{Q_m^3}$$

The equivalent axle load  $Q_m$  gives a value close to the load class which gives the largest damage in fatigue.

The number  $n_m$ , corresponding to  $Q_m$  as well as  $Q_m$  itself are independent from the slope of the fatigue life curve 3 and 4.

For the three bridges values of  $Q_m$ ,  $n_m$  and the distribution of damaging potential of measured axle loads in the slow lane and fast lane have been calculated. Results as given in figure 4.2.2. on page 4-15 shows that the equivalent axle load  $Q_m$  for the slow lanes varies from 85 - 94.4 kN and its associated number of cycles  $n_m$  from 3752 to 8939 cycles. For the fast lanes  $Q_m$  varies from 56,5 - 73,4 kN and  $n_m$  from 286 - 1342 cycles.

#### 4.2.1.3. Characteristic axle load (see ref. 6-6)

The characteristic axle load method is a method to calculate an axle load such that N-axles of that load has the same fatigue damage potential as the N-axles of the axle load spectrum.

If fatigue damage potential is proportional to the a'th power of axle load then:

$$CAL = \sqrt[a]{\frac{\sum n_i Q_i^a}{\sum n_i}} \quad a = \text{shape of the fatigue life curve.}$$

Characteristic axle loads have been calculated for the Rheden Bridge, Haagsche Schouw Bridge and the Leiderdorp Bridge using a fifth power relationship.

This method will be used in the following chapters to describe an axle load spectrum in a way it is relevant to fatigue.

#### 4.2.2. Fatigue loads of measured traffic

##### 4.2.2.1. CAL of the commercial vehicles

The values of CAL, calculated for the different vehicle types and axles in the slow lane of each bridge are given in table IV.2.1. and IV.2.2. on page 4-16 and IV.2.3.a on page 4-17. In table IV.2.3b values of CAL have been calculated using a third, fourth and fifth power relationship.

With respect to the most damaging types, it appears that;

- for the Rheden Bridge it are type 3, 9 and 7.
- for the Leiderdorp Bridge it are type 7 and 13, both vehicles with 6 axles,
- and for the Haagsche Schouw Bridge it are type 10 and 12, both an artic, tractor with a semi-trailer.

A review of the values of CAL including mean values and the standard deviation for the different vehicle types in slow lane of the three bridges, is given in table IV.2.4. on page 4-18. It appears that type 7, a rigid 3-axle commercial vehicle with a 3-axle drawbar trailer and type 10 an artic, 2-axle tractor with a 3-axle semi-trailer are the most damaging commercial vehicles.

##### 4.2.2.2. Damaging potential of the population of commercial vehicles

Using the characteristic axle load per vehicle type the fatigue damaging potential of the population of each vehicle type has been calculated on the assumption that it is proportional to the fifth power of axle load.

In table IV.2.5. on page 4-18/the commercial vehicle types have been listed according to the damaging potential and the results have been normalised so that the total has a value of one.

It appears that the two most damaging types of the population of vehicles on the Rheden Bridge and the Leiderdorp Bridge are type 9 and 10, both an artic, 2-axle tractor with a 2 or 3-axle semi-trailer. For the Haagsche Schouw Bridge it appeared to be type 9 and type 2 a 3-axle lorry.

Mentioned vehicle types produce together 40 - 50% of the total fatigue damage.

#### 4.2.3. Fatigue loads of axle load spectra

##### 4.2.3.1. Actual spectra

##### 4.2.3.1.1. Characteristic axle loads

For the slow lane as well the fast lane it is possible to calculate a value of CAL for the total measured axle load spectra. Values of CAL for the two lanes of the three bridges are given in table IV.2.6. on page 4-19, and it appeared that;

- the characteristic axle load for the slow lanes varies between 66 - 70 kN and for the fast lane between 40 - 52 kN.
- the characteristic axle loads of two almost similar spectra are the same, independent of the number of axle loads.

##### 4.2.3.1.2. Damaging potential of different axle load classes

Using a fifth power relationship, it is possible to calculate the damaging potential of the load classes of the measured axle load spectra. Results for the slow lane of the three bridges are given in table IV.2.7. on page 4-19.

The measured axle loads are divided over eight axle load classes and for each class the percentage of damaging potential and the percentage of the number of axles are given.

In table IV.2.7. one reads:

- less than 1% of the total damage is caused by axle loads < 40 kN
- over 99% of the total damage is caused by 37 - 43% of the total number of axle loads > 8 kN
- 4 - 10% of the total number of axle loads > 8 kN causes 54 - 64% of the total damage. These axle loads amounts 80 - 120 kN on the Rheden Bridge and the Leiderdorp Bridge and 100 - 140 kN on the Haagsche Schouw Bridge.
- the highest axle loads class 140 - 160 kN causes on the Rheden Bridge and the Leiderdorp Bridge less than 5% of the total damage. For the Haagsche Schouw Bridge this percentage amounts 16.6% (Extrapolation seems to be necessary)

#### 4.2.3.2. Extrapolated spectra

##### 4.2.3.2.1. Extrapolation of actual axle load spectra

In chapter 3 of these report, only results of measurements between 07.00 - 19.00 hours have been given. Extrapolating measured spectra, it is necessary to know the distribution of the traffic through the day (07.00 - 0.700 hours).

For the Rheden Bridge 24 hours of continuous measurements have been analysed and compared with not-continuous measurements. Results as given in appendix D of this report showed that for the Rheden Bridge 18750 vehicles with 12227 axle loads  $\geq 10$  kN were registered in 24 hours continuous measurements (09.00 - 09.00 hours). These measurements took place in 1978.

Results of measurements carried out by RWS<sup>1)</sup> are given in figure 4.2.3. on page 4-20. This figure shows the average number of vehicles per annum or a months in 1978 (based on the average number of vehicles a working day).

Taking into consideration above mentioned measurements and 250 working days a year, the number of axle loads  $\geq 10$  kN in one hundred years amounts  $3.10^8$ .

That means extrapolating the measured axle load spectra, a maximum axle load of about 187 kN (see figure 4.2.4. on page 4-20).

The same extrapolation are made for the Haagsche Schouw Bridge and the Leiderdorp Bridge. For these two bridges the traffic counts of RWS are given in figure 4.2.5. and 4.2.6. on page 4-21/4-22 and the extrapolated spectra for one hundred years in figure 4.2.6. and 4.2.8. on page 4-21/4-22. The maximum axle load of the extrapolated axle load spectra for the Haagsche Schouw Bridge amounts 240 kN and for the Leiderdorp Bridge 230 kN. The characteristic axle loads of the extrapolated spectra varies between 72 - 79 kN.

---

1) Traffic countings of the "Dienst Verkeerskunde of Rijks-waterstaat".

#### 4.2.3.2.2. Damaging potential of different axle load classes of the extrapolated axle load spectra

Calculating the damaging potential of each axle load class of the extrapolated axle load spectra for the Rheden Bridge it appears that 92.4% of the total damage is caused by 26.6% of the total number of axle loads  $\geq 10$  kN which have a value of 60 - 140 kN (see table IV.2.8. on page 4-23).

Even when the total number of axle loads  $\geq 10$  kN amounts 1.10" ( $\pm$  300 years) the highest axle load classes can be ignored because the damaging potential is neglectable small (see table IV.2.8 on page 4-23).

Figure 4.2.9. and 4.2.10. on page 4-24 shows the different axle load spectra, damaging potential of axle load classes and characteristic axle loads for above mentioned periods.

The same calculations are made for the Haagsche Schouw Bridge and the Leiderdorp Bridge. Results of the damaging potential of each axle load class of the extrapolated axle load spectra are given in table IV.2.9. and IV.2.10. on page 4-23.

The axle load spectra for 100 years and the damaging potential of axle loads for the three Dutch Bridges are compared in figure 4.2.11. on page 4-25 and table IV.2.11 on page 4-25. For these bridges it can be concluded that axle loads  $< 40$  kN are not important with respect to the damaging potential of the axle load spectrum in the total life of the bridge. Axle loads  $> 160$  kN can be ignored at the Rheden Bridge and the Leiderdorp Bridge and axle loads  $> 200$  kN at the Haagsche Schouw Bridge.

#### 4.2.4. Comparison for the three bridges and other axle load locations in the Netherlands

The Government laboratory for highway designs is among other things in charge of measuring axle loads in the slow lane of several highway locations.

In this chapter the damaging potential of measured axle load spectra at the locations will be compared with the results of the three bridges as given in the previous chapters.



The date of used measurements and code of the locations are indicated in table IV.2.12 on page 4-26. At each location axle loads 20 kN have been measured and grouped over seven axle load classes. The total number of axles and the proportionally division of the axles over the seven axle load classes are given in table IV.2.13. on page 4-26.

Tabel IV.2.14. on page 4-26 gives for each of the ten locations the damaging potential of the different axle load classes also proportionally.

The mean values including the standard deviation of the damaging potential of each axle load class and the values concerning the three bridges are given in Table IV.2.15 on page 4-27.

The grouping of the measured axle loads by the Government Laboratory is not the same as the classification used for the three bridges, but still it is possible comparing them together.

- For the ten locations of the Government laboratory it appeared that 42.9 - 55.8% of the total damage is caused by the number of axle loads in two axle load classes. For eight locations these axle loads amounts 100 - 135 kN and for the other two 80 - 120 kN, just as for the actual and extrapolated axle load spectra at the Rheden Bridge and the Leiderdorp Bridge they caused 54.0 - 63.4% of the total damage.

For the Haagsche Schouw Bridge 56% of the total damage of the actual spectra is caused by axle loads between 100 - 140 kN and for the extrapolated spectra the percentage amounts 43,9% and axle loads between 120 - 160 kN.

- The highest axle loads class of the Government laboratory (> 150 kN) causes on the ten locations 6.6 - 21.1% of the total damage and for the highest axle loads classe (140 - 160 kN) of the actual spectra at the three bridges it is 5 - 16.6% of the total damage.

Extrapolation of the actual spectra showed that dependent on the spectra, the damaging potential of higher axle load classes (> 180 kN or > 200 kN) is neglectable small.

#### 4.2.5. Conclusions

Results showed that about 92% of the total damage is caused by 23 - 37% of the total number of axle loads. The axle loads amounts 60 - 140/160 or 180 kN and the number of axles  $2 \cdot 10^7$  -  $1,2 \cdot 10^8$  dependent on the different axle load spectra. Due to the high number of axle loads it is reasonable to concluded that the fatigue damage potential is proportional to the fifth power of axle load or stress range.

Assuming that the fatigue damage is proportional to the fifth power of axle load, an axle load of 73 kN for the Rheden Bridge and an axle load of 79 kN for the Haagsche Schouw Bridge and the Leiderdorp Bridge is calculated, such that N-axles of that load has the same fatigue damage potential as the N-cycles of the load spectra.

Furthermore it appeared that two vehicle types, mostly the artic, 2-axle trailer with a 2 or 3-axle semi-trailer produce together 40 - 50% of the total fatigue damage of the population of commercial vehicles.

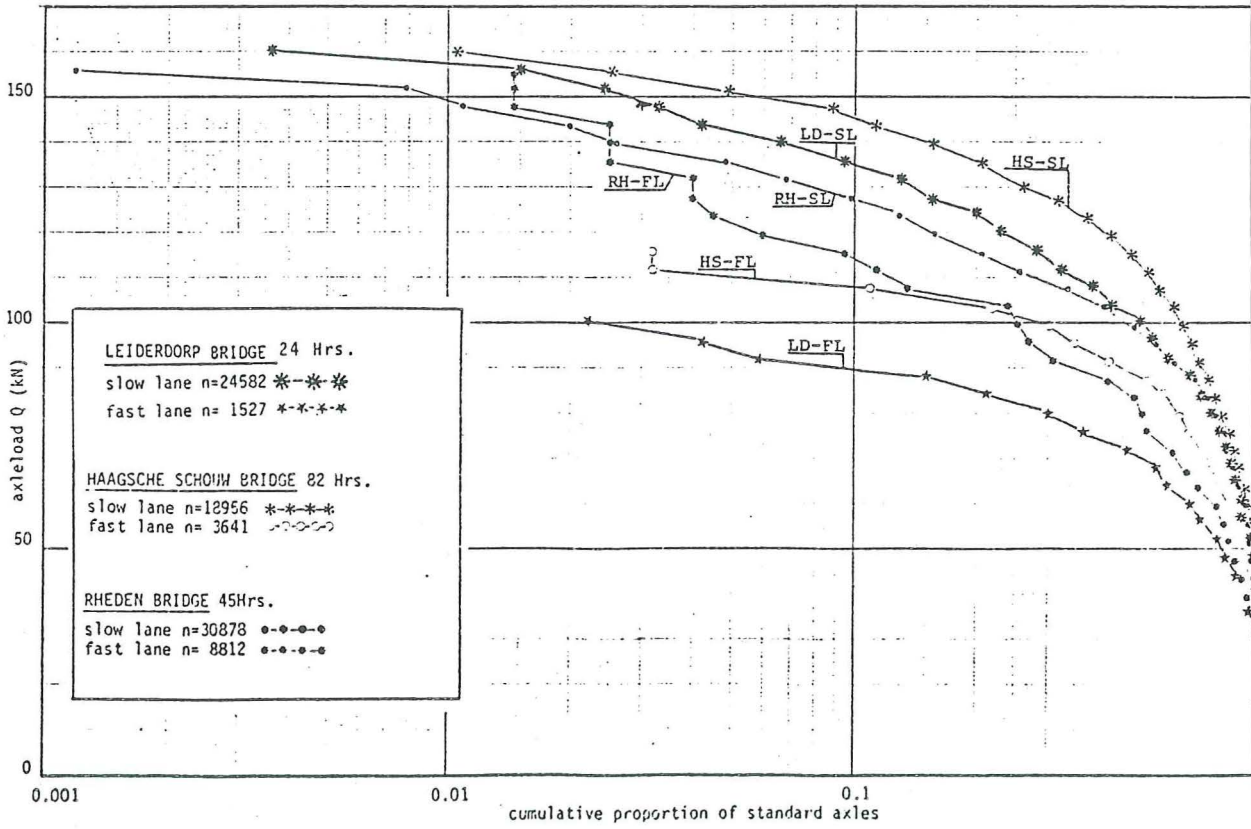
#### 4.2.6. Figures and tables

List of figures	Page
4.2.1. Cumulative axle load spectra related to a 100 kN standard axle	4-14
4.2.2. Equivalent axle loads $Q_m$ and its associated number of cycles $n_m$	4-15
4.2.3. Counted vehicles on the Rheden Bridge by RWS	4-20
4.2.4. Measured and extrapolated axle load spectra on the Rheden Bridge	4-20
4.2.5. Counted vehicles on the Haagsche Schouw Bridge by RWS	4-21
4.2.6. Measured and extrapolated axle load spectra on the Haagsche Schouw Bridge	4-21
4.2.7. Counted vehicles on the Leiderdorp Bridge by RWS	4-22
4.2.8. Measured and extrapolated axle load spectra on the Leiderdorp Bridge	4-22

	Page
4.2.9.- Axle load spectra on the Rheden Bridge	4-24
4.2.10.	
4.2.11. Axle load spectra for three Dutch Bridges (100 years)	4-25

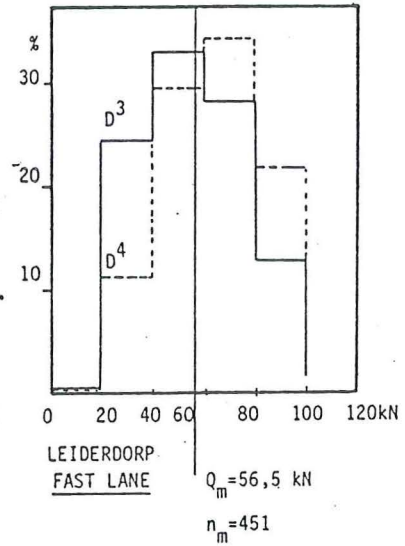
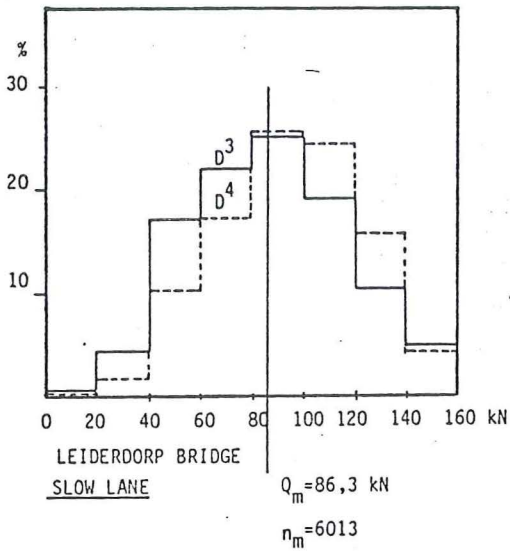
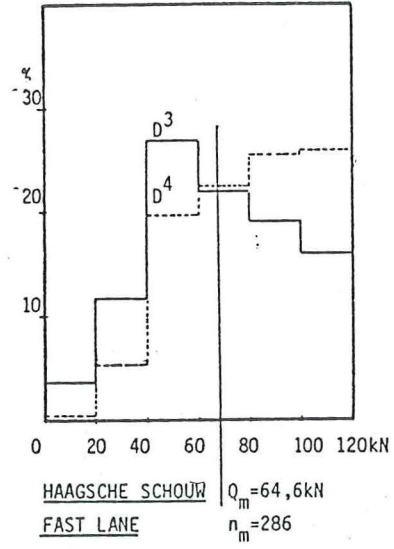
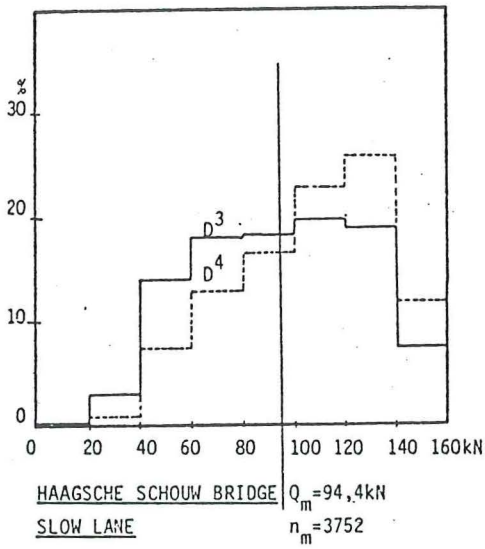
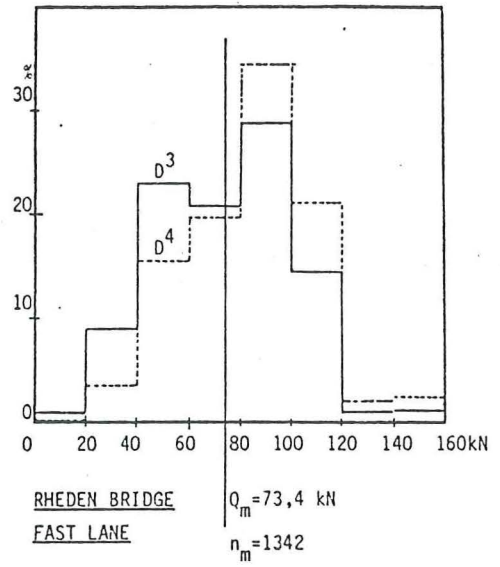
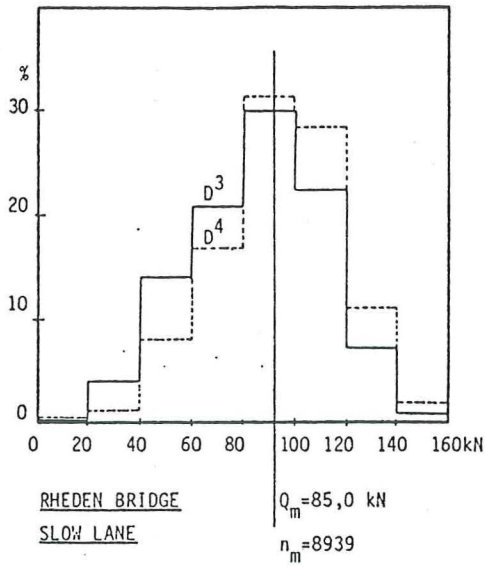
## List of tables

IV.2.1. Characteristic axle loads Haagsche Schouw Bridge	4-16
IV.2.2. Idem for the Rheden Bridge	4-16
IV.2.3.a- IV.2.3.b Idem for the Leiderdorp Bridge	4-17
IV.2.4. Mean values for the different vehicle types in the slow lane of three Dutch bridges	4-18
IV.2.5. Damaging potential of the population of vehicles	4-18
IV.2.6. CAL for the total axle load spectra	4-19
IV.2.7. Damaging potential of different axle load classes of the measured axle load spectra	4-19
IV.2.8.- Idem for the extrapolated axle load IV.2.9.- IV.2.10. spectra	4-23
IV.2.11. Idem for the three Dutch Bridges (100 years)	4-25
IV.2.12. Date of measurements of the Government Laboratory for highway designs	4-26
IV.2.13. The propotionally division of the number of axle loads 20 kN	4-26
IV.2.14. The propotionally devision of the damaging potential of the different axle load classes	4-16
IV.2.15. Damaging potential of axle loads (13 locations)	4-27



Cumulative axle load spectra related to a 100 kN standard axle

Figure 4.2.1.



Equivalent axleloads  $Q_m$  and there associated number of cycles  $n_m$   
Figure 4.2.2.

Haagsche Schouw Bridge slow lane 82 hours $CAL = \sqrt[5]{\frac{EnL^5}{Ln}}$								
Vehicle type	number of vehicles	Type	characteristic axle load (kN)					
			Axle 1	Axle 2	Axle 3	Axle 4	Axle 5	Axle 6
1.								
2.	295	90.9	63.4	103.4	89.8			
3.	9	51.7	56.5	56.6	33.4	48.7		
4.	245	73.1	54.8	83.1	75.8	67.7		
5.	24	80.5	66.1	54.1	70.8	90.5	93.9	81.9
6.	47	84.5	61.5	107.3	74.8	78.2	64.3	
7.	3	90.7	56.2	116.9	72.0	93.3	70.3	
8.	211	78.8	46.4	79.6	89.3			
9.	314	91.3	59.8	105.6	87.6	91.4		
10.	73	100.7	53.3	124.2	83.9	84.5	82.2	
11.	2	41.6	51.2	33.2	33.2	36.9		
12.	23	99.8	67.2	113.8	76.0	87.9	116.1	
13.	35	94.3	65.9	94.7	83.6	93.8	90.3	113.0
16.	517	26.2	28.2	23.2				
17.	1313	22.1	17.8	24.5				
18.	885	41.4	30.3	46.5				
19.	1163	56.9	38.9	64.3				
20.	1551	69.8	49.6	78.6				
21.	3076	30.2						

Characteristic axle loads for the Haagsche Schouw Bridge  
Table IV.2.1.

Rheden bridge slow lane 45 hours $CAL = \sqrt[5]{\frac{EnL^5}{Ln}}$								
vehicle type	number of vehicles	characteristic axle load (kN)*						
		Type	Axle 1	Axle 2	Axle 3	Axle 4	Axle 5	Axle 6
1.	166	66.6						
2.	539	66.5	49	71	71			
3.	6	87.7	64.1	95.4	88.7	97.5		
4.	711	62.9	48	76.1	62.6	64.0		
5.	140	71.7	56.7	77.8	63.2	75.8	76.1	
6.	338	69.8	54.5	85.8	66.9	61.1	62.9	
7.	95	77.8	61.9	91.8	70.8	84.6	70.8	70.7
8.	379	69.0	43.7	74.8	82.3			
9.	1097	78.1	51.7	86	75.3	83.9		
10.	641	75.3	54	93.5	67.9	65.7	71.2	
11.	19	70.4	61.1	50.6	70.9	83.0		
12.	106	75.0	52.7	72.1	66.7	83.6	83.7	
13.	120	72.6	57.3	71.9	71.3	76.2	71.6	80.0
16.	561	33.2	33.7	32.6				
17.	951	35.1	22.4	43				
18.	631	47.3	32.6	53.4				
19.	1276	62.0	37.8	70.6				
20.	1364	58.0	42.1	65.2				
21.	2777	26.8						

Characteristic axle loads for the Rheden Bridge

Table IV.2.2

LEIDERDORP BRIDGE SLOW LANE 24 HOURS $CAL = \sqrt{\frac{5 \sum nL^5}{\sum n}}$								
Vehicle type	Number of vehicles	Type	Characteristic axle loads					
			Axle 1	Axle 2	Axle 3	Axle 4	Axle 5	Axle 6
1								
2	621	64.2	49.7	68.0	68.6			
3	57	60.5	57.2	66.2	61.5	54.3		
4	309	68.5	55.2	79.8	61.5	67.7		
5	83	85.3	67.9	86.0	82.6	87.0	94.7	
6	158	84.2	68.2	81.3	68.3	64.3	106.2	
7	74	98.4	92.5	97.8	105.2	106.6	81.0	99.1
8	136	66.5	45.6	66.3	75.4			
9	752	74.6	49.2	81.1	75.9	78.3		
10	310	86.1	54.1	86.8	68.6	73.9	107.8	
11	5	50.9	45.0	32.0	64.0	37.3		
12	40	82.4	50.6	72.6	88.7	83.5	93.4	
13	60	90.7	61.8	78.3	69.2	96.0	93.5	110.0
16	408	64.3	43.6	72.8				
17	832	44.7	39.5	48.1				
18	560	47.6	29.6	54.1				
19	807	57.7	41.7	64.9				
20	741	67.3	50.8	75.3				
21	1783	18.3						

Table IV.2.3.a.

LEIDERDORP BRIDGE SLOW LANE 24 HOURS				
Vehicle type	Number of vehicles	CAL <sup>5</sup>	CAL <sup>4</sup>	CAL <sup>3</sup>
2	621	64.2	57.3	50.4
3	57	60.5	56.5	52.1
4	309	68.5	64.3	59.2
5	83	85.3	81.2	76.6
6	158	84.2	75.3	65.6
7	74	98.4	92.4	85.6
8	136	66.5	61.1	55.4
9	752	74.6	69.4	63.3
10	310	86.1	78.3	69.7
11	5	50.9	47.2	43.0
12	40	82.4	74.5	65.7
13	60	90.7	84.9	78.5
16	408	64.3	52.0	37.0
17	832	44.7	33.3	23.2
18	560	47.6	39.5	31.7
19	807	57.7	52.2	46.4
20	741	67.3	62.5	57.5
21	1783	18.3	16.1	14.7

Table IV.2.3.b.

Characteristic axle loads for the Leiderdorp Bridge  
Table IV.2.3.

Vehicle Type	Characteristic Axle Loads (kN)				
	Leiderdorp	Haagsche Schouw	Rheden	Mean values	Standard deviation
2	64.2	90.0	66.5	73.9	14.8
3	60.5	51.7	87.7	66.6	18.8
4	68.5	73.1	62.9	68.2	5.1
5	85.3	80.5	71.7	79.2	6.9
6	84.3	84.5	69.8	79.5	8.4
7	98.4	90.7	77.8	89.0	10.4
8	66.5	78.8	69.0	71.4	6.5
9	74.6	91.3	78.1	81.3	8.8
10	86.1	100.7	75.3	87.4	12.8
11	50.9	41.6	70.4	54.3	14.7
12	82.4	99.8	75.0	85.7	12.7
13	90.7	94.3	72.6	85.9	11.6
16	64.3	26.2	33.2	41.2	20.3
17	44.7	22.1	35.1	34.0	11.3
18	47.6	41.4	47.3	45.4	3.5
19	57.7	56.9	62.0	58.9	2.7
20	67.3	69.8	58.0	65.0	6.2
21	18.3	30.2	26.8	25.1	6.1

Comparison of the Characteristic axle loads on three Dutch bridges  
Table IV.2.4.

Vehicle type.	Rheden Bridge 45 hours	Vehicle type	Haagsche Schouw Bridge 82 hours	Vehicle type	Leiderdorp Bridge 24,7 hours
9	0.3114	9	0.2480	10	0.2050
10	0.1879	2	0.1710	9	0.1948
6	0.0689	20	0.1592	7	0.1146
4	0.0680	10	0.1174	6	0.0933
19	0.0571	4	0.0637	13	0.0617
2	0.0512	8	0.0558	20	0.0573
8	0.0445	13	0.0485	2	0.0569
20	0.0437	19	0.0430 91%	5	0.0524
7	0.0406	12	0.0353	4	0.0522
13	0.0352 91%	6	0.0314	19	0.0288 91%
5	0.0331	5	0.0126	16	0.0250
12	0.0312	18	0.0067	12	0.0213
21	0.0094	7	0.0034	8	0.0149
18	0.0072	21	0.0024	17	0.0083
11	0.0038	3	0.0004	18	0.0076
3	0.0031	16	0.0004	3	0.0057
17	0.0025	17	0.0004	11	0.0002
16	0.0013	11	0.0003	11	1

Damaging potential of the population of vehicles on three Dutch bridges

Table IV.2.5.



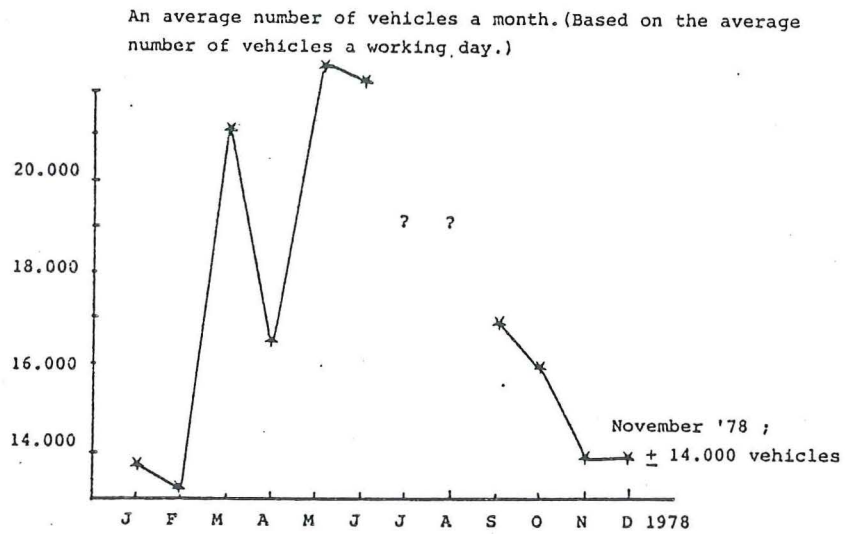
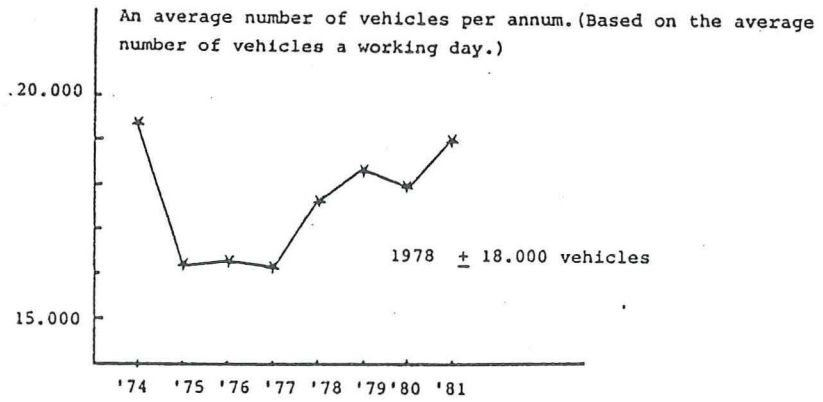
Lane	Rheden		Haagsche Schouw		Leiderdorp	
	CAL	hrs.	CAL	hrs.	CAL	hrs.
Slow	68	45	70	82	66	24
	68	62	70	66		
Fast	52	45	40	82	44	24
	51	62	40	66		

Characteristic axle loads for the total axle load spectra  
Table IV.2.6.

Axleload Q kN - kN	Haagsche Schouw		Rheden		Leiderdorp	
	Slow lane 82 hrs.		Slow lane 45 hrs.		Slow lane 24 hrs.	
	D.pot %	$N_i$ %	D.pot %	$N_i$ %	D.pot %	$N_i$ %
8 - 20	0.0026	44.63	0.01	30.02	0.0054	32.04
20 - 40	0.27	18.81	0.63	26.98	0.885	27.24
40 - 60	3.51	19.05	4.56	20.66	6.81	22.30
60 - 80	8.81	8.88	13.09	11.01	16.59	9.80
80 - 100	14.87	4.27	31.59	7.57	27.21	5.55
100 - 120	23.95	2.52	32.24	3.08	26.61	2.21
120 - 140	32.01	1.46	14.7	0.61	17.3	0.76
140 - 160	16.59	0.37	3.8	0.068	4.6	0.10
$D_{tot}$	1.		1.		1.	
$N_{tot}$		19147		30787		26571

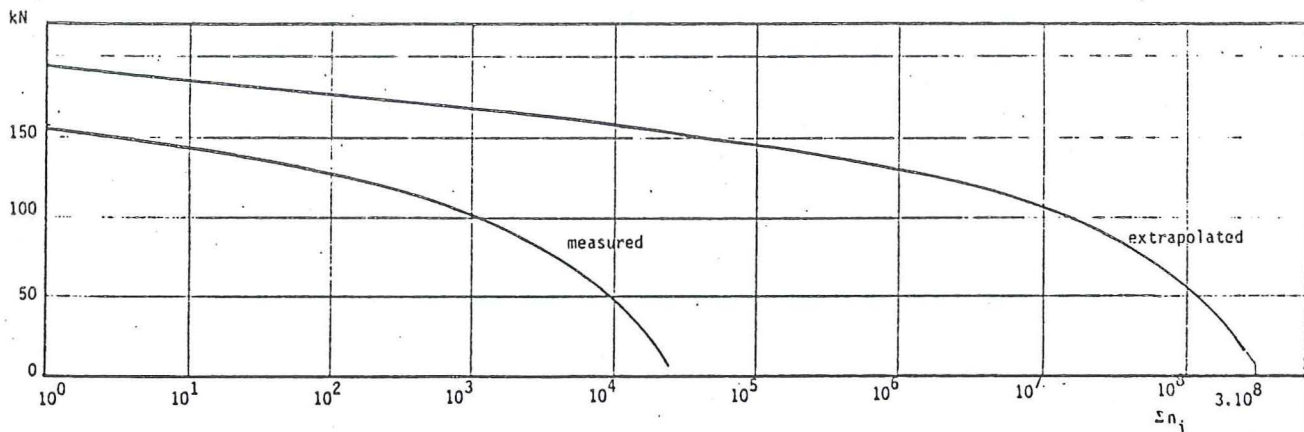
Damaging potential of different axle load classes  
of the measured axle load spectra

Table IV.2.7.

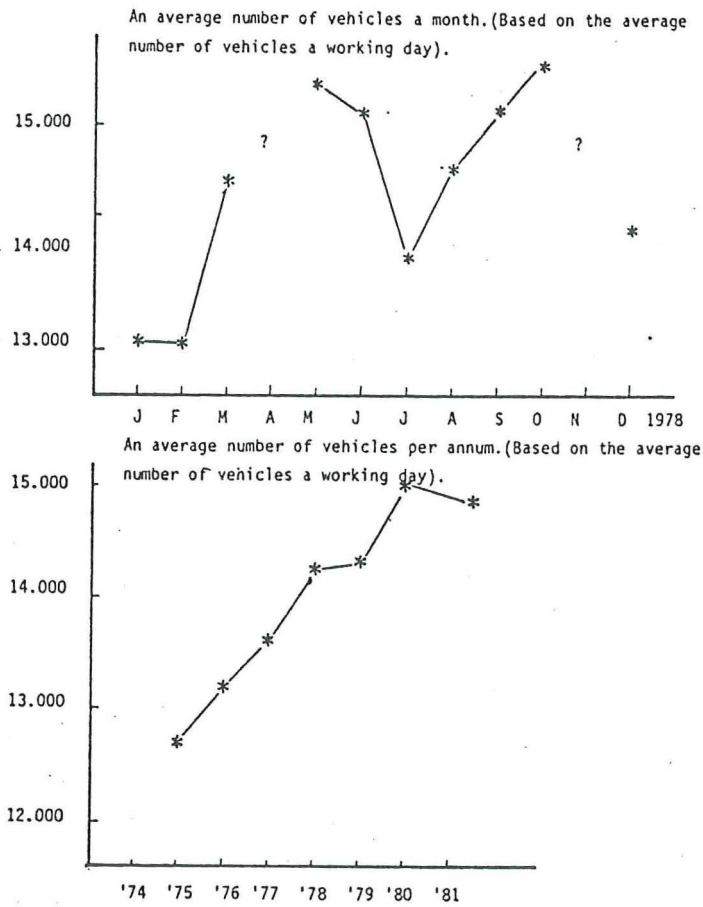


Counted vehicles on the Rheden Bridge by the "Dienst Verkeers- van Rijkswaterstaat"

Figure 4.2.3.

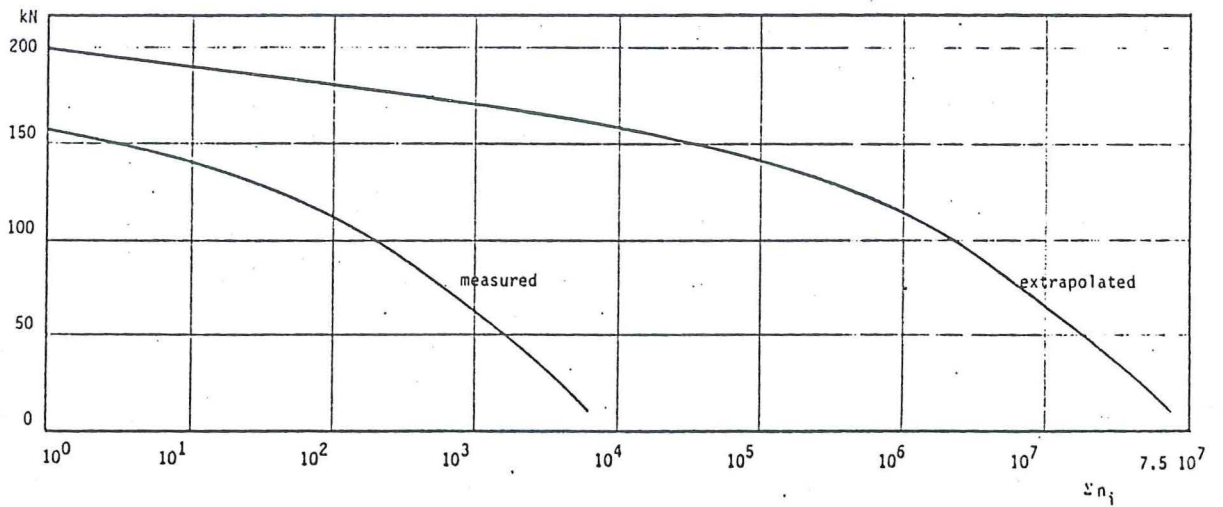


Measured and extrapolated axle load spectra on the Rheden Bridge  
Figure 4.2.4.



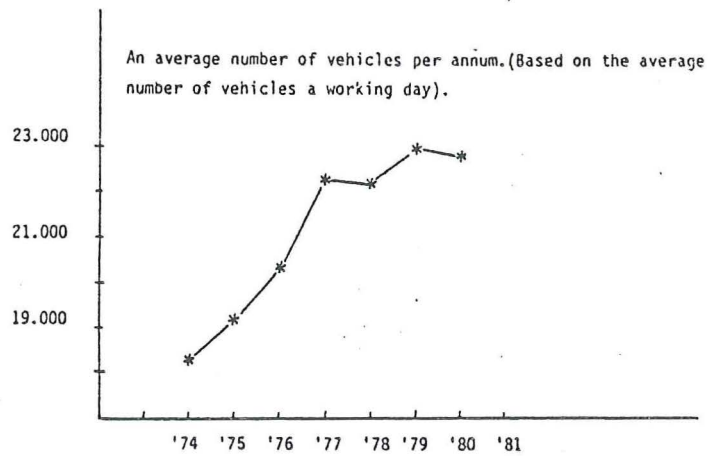
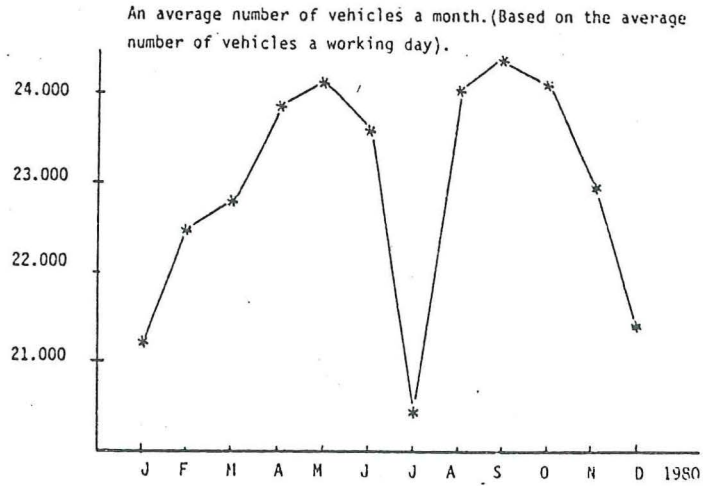
Counted vehicles on the Haagsche Schouw Bridge by the "Dienst Verkeerskunde van Rijkswaterstaat"

Figure 4.2.5.



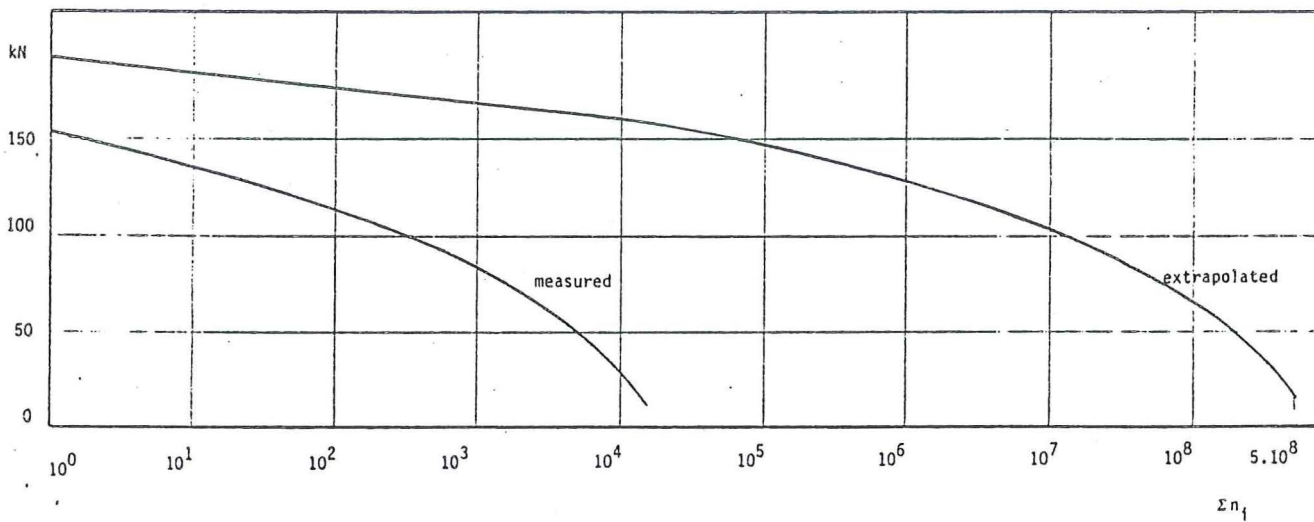
Measured and extrapolated axle load spectra on the Haagsche Schouw Bridge.

Figure 4.2.6.



Counted vehicles on the Leiderdorp Bridge by the "Dienst Verkeerskunde van Rijkswaterstaat

Figure 4.2.7.



Measured and extrapolated axle load spectra on the Leiderdorp Bridge

Figure 4.2.8.

$Q_i$ kN - kN	$EN_{10} = 3.10^8$ (100 years)		$EN_{10} = 1.10^{11}$ (300 years)	
	Damaging potential of axles in % *)	$N_i$	Damaging potential of axles in % *)	$N_i$
0 - 20	0.0012	$0.7 \times 10^8$	0.0007	$1.5 \times 10^{10}$
20 - 40	0.3391	$0.8 \times 10^8$	0.3571	$3 \times 10^{10}$
40 - 60	3.8284	$0.7 \times 10^8$	3.8	$2.5 \times 10^{10}$
60 - 80	11.1705	$3.8 \times 10^7$	12.4	$1.5 \times 10^{10}$
80 - 100	26.9210	$2.6 \times 10^7$	27.2	$9.4 \times 10^9$
100 - 120	36.5356	$1.3 \times 10^7$	36.3	$4.6 \times 10^9$
120 - 140	17.8302	$2.8 \times 10^6$	16.6	$9.1 \times 10^8$
140 - 160	3.2340	$2.4 \times 10^5$	3.3	$8.8 \times 10^7$
160 - 180	0.1383	5570	0.1386	$1.99 \times 10^6$
180 - 200 (187)	0.0011	30	0.012	$1.0 \times 10^2$
200 - 220	-	-	0.000019987	

Damaging potential for the extrapolated axle load spectra of the Rheden Bridge.

Table IV.2.8.

$Q_i$ kN - kN	$EN_{10} = 2.6 \times 10^4$		$EN_{10} = 5 \times 10^8$ (100 years)	
	Damaging potential of axles in % *)	$N_i$	Damaging potential of axles in % *)	$N_i$
0 - 20	0.0054	8513	0.0027	$1.6 \times 10^8$
20 - 40	0.8849	7239	0.5649	$1.4 \times 10^8$
40 - 60	6.8132	5924	5.7151	$1.1 \times 10^8$
60 - 80	16.5895	2604	13.956	$5.0 \times 10^7$
80 - 100	27.2124	1474	25.5851	$2.6 \times 10^7$
100 - 120	26.61	586	28.4094	$1.06 \times 10^7$
120 - 140	17.3	201	17.2782	$2.8 \times 10^7$
140 - 160	4.6	30	6.5624	$5.2 \times 10^5$
160 - 180			1.8441	$7.8 \times 10^4$
180 - 200			0.0819	$1.99 \times 10^3$
200 - 220			0.0007	10
220 - 230			0.0001	1

Damaging potential for the measured and extrapolated axle load spectra of the Leiderdorp Bridge

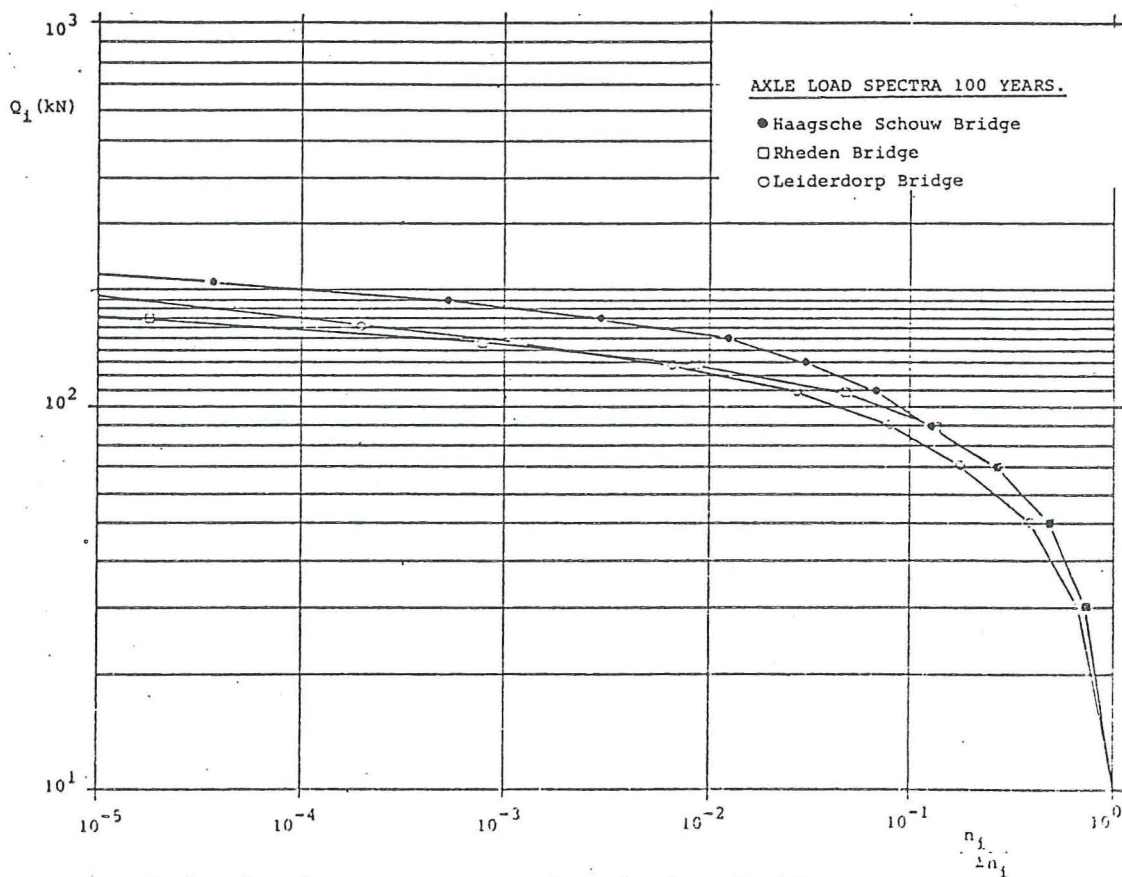
Table IV.2.9.

$Q_i$ kN - kN	$EN_{10} = 1.6 \times 10^4$ (5 days)		$EN_{10} = 7.5 \times 10^7$ (100 years)	
	Damaging potential of axles in % *)	$N_i$	Damaging potential of axles in % *)	$N_i$
0 - 20	0.0026	8546	0.0008	$1.9 \times 10^7$
20 - 40	0.27	3601	0.2104	$2.0 \times 10^7$
40 - 60	3.5080	3648	2.1645	$1.6 \times 10^7$
60 - 80	8.8027	1701	7.2727	$1.0 \times 10^7$
80 - 100	14.8662	818	12.7706	$5.0 \times 10^6$
100 - 120	23.95	483	19.5238	$2.8 \times 10^6$
120 - 140	32.01	279	20.9691	$1.3 \times 10^6$
140 - 160	16.59	71	23.0303	$7.0 \times 10^5$
160 - 180			9.8268	$1.6 \times 10^5$
180 - 200			4.0087	$3.74 \times 10^4$
200 - 220			0.4502	$2.54 \times 10^3$
220 - 240			0.0167	$6.10^1$

Damaging potential for the measured and extrapolated axle load spectra of the Haagsche Schouw Bridge

Table IV.2.10.

$$*) \frac{N_i Q_i^5}{EN_i Q_i^5} \times 100\%$$

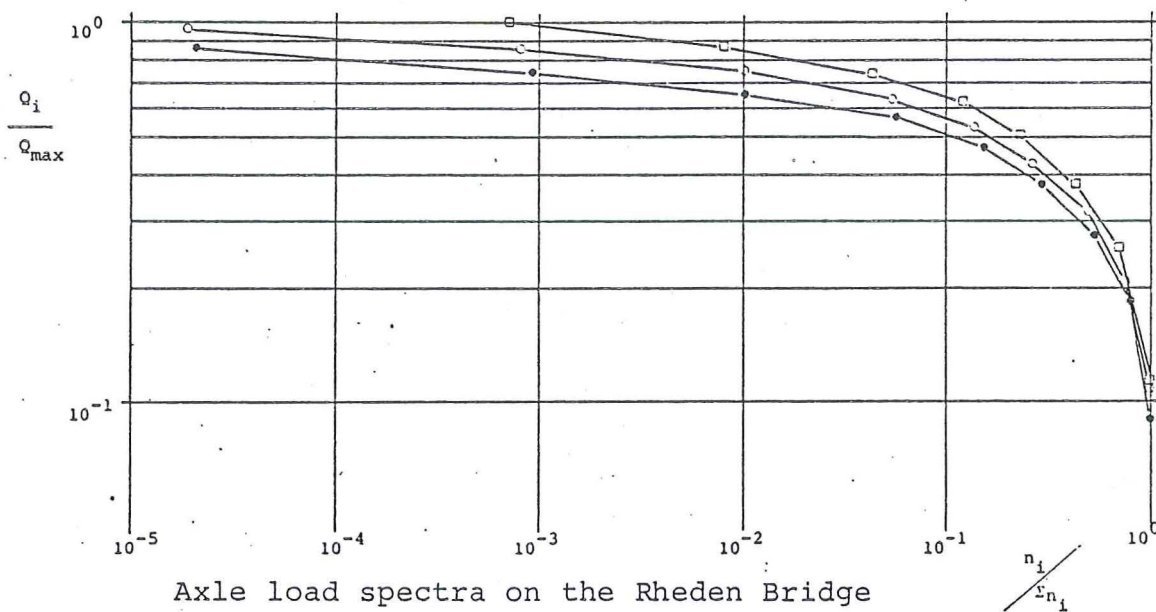


Axle load spectra on the Rheden Bridge

Figure 4.2.9.

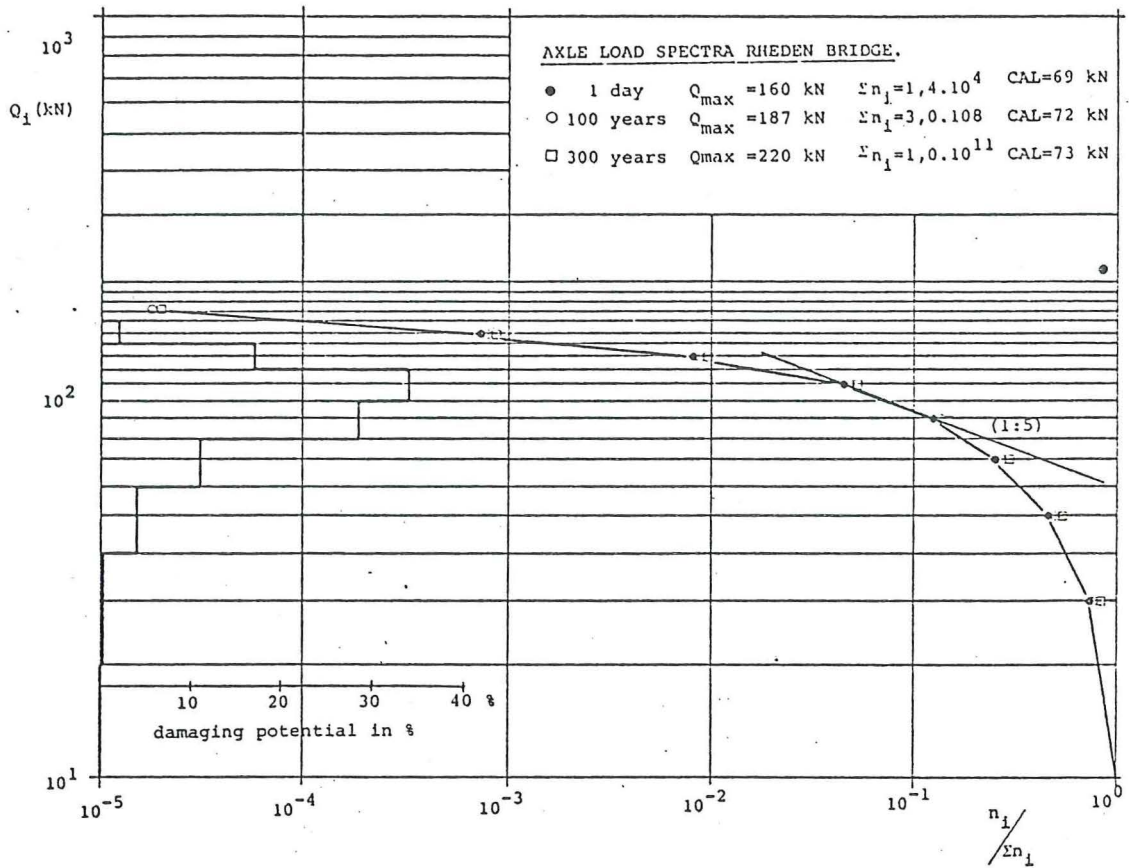
AXLE LOAD SPECTRA RHEDEN BRIDGE

- 1 day  $Q_{max} = 160 \text{ kN}$   $\sum n_i = 1,4 \cdot 10^4$
- 100 years  $Q_{max} = 187 \text{ kN}$   $\sum n_i = 3,0 \cdot 10^8$
- 300 years  $Q_{max} = 220 \text{ kN}$   $\sum n_i = 1,0 \cdot 10^{11}$



Axle load spectra on the Rheden Bridge

Figure 4.2.10.



Axle load spectra for three Dutch Bridges (100 years)  
Figure 4.2.11.

$Q_i$ kN - kN	Rheden Bridge $\Sigma N_{10} = 3 \cdot 10^8$	Haagsche Schouw Bridge $\Sigma N_{10} = 7.5 \cdot 10^5$	Leiderdorp Bridge $\Sigma N_{10} = 5 \cdot 10^8$
0 - 20	0.0012	0.0008	0.0027
20 - 40	0.34	0.21	0.57
40 - 60	3.83	2.17	5.72
60 - 80	11.17	7.27	13.96
80 - 100	26.92	12.77	25.59
100 - 120	36.54	19.52	28.41
120 - 140	17.83	20.91	17.28
140 - 160	3.23	23.03	6.56
160 - 180	0.14	9.83	1.84
180 - 200	0.0011 (-137 kN)	4.01	0.08
200 - 220		0.45	0.0007
220 - 240		0.017	0.0001 (230 kN)

Damaging potential of axle loads for three Dutch Bridges (100 years).

Table IV.2.11.

Highway nr.	Location		Code	Date of measurements
15	Echteveld	-ZB-	A-1	11-12-1978 - 17-12-1978
		-NB-	A-2	6-11-1978 - 12-11-1978
12	Veenendaal	-NB-	B-1	24- 4-1978 - 30- 4-1978
		-ZB-	B-2	10- 4-1978 - 16- 4-1978
28	Harderwijk	-ZOB-	C-1	12- 6-1978 - 18- 6-1978
		-NWB-	C-2	22- 5-1978 - 28- 5-1978
47	Ruurlo	-NOB-	D-1	9- 4-1979 - 15- 4-1979
		-ZWB-	D-2	7- 5-1979 - 13- 5-1979
16		-WB-	E-1	26-11-1979 - 2-12-1979
		-OB-	E-2	17-12-1979 - 23-12-1979

Date of measurements of the Government Laboratory for Highway designs  
Table IV.2.12.

Location code	Number of Axle loads $\geq 20$ kN	Axle load classes ( %-division)						
		20-50 kN	50-80 kN	80-100 kN	100-120 kN	120-135 kN	135-150 kN	$>150$ kN
A-1	38898	39.5	36.1	13.8	7.8	2.0	0.6	0.2
A-2	38296	44.1	32.5	11.6	7.9	2.9	0.8	0.2
B-1	42439	47.7	32.0	11.8	6.4	1.6	0.4	0.2
B-2	39172	39.2	30.7	12.3	9.1	4.9	2.6	1.3
C-1	35760	40.1	33.3	13.1	9.3	3.0	0.9	.4
C-2	38172	44.7	32.3	11.3	7.5	2.5	1.0	0.7
D-1	5658	55.1	28.0	9.5	5.3	1.5	0.4	0.2
D-2	5830	38.9	32.9	11.9	10.0	4.3	1.4	0.5
E-1	79301	38.7	32.2	12.7	10.6	4.0	1.4	0.5
E-2	83843	36.9	34.9	11.6	9.4	4.5	1.9	0.8

The proportionally division of the number of axle loads  $\geq 20$  kN  
Table IV.2.13.

Location code	Axle load classes ( %-division of damaging potential)						
	20-50 kN	50-80 kN	80-100 kN	100-120 kN	120-135 kN	135-150 kN	$>150$ kN
A-1	0.6	11.0	21.4	32.8	17.8	9.7	6.6
A-2	0.6	9.2	16.7	31.1	23.6	11.9	6.9
B-1	0.8	12.0	22.4	33.4	17.1	7.5	6.8
B-2	0.3	4.9	10.0	20.0	22.9	20.9	21.1
C-1	0.6	8.3	16.6	32.1	21.9	10.9	9.8
C-2	0.5	8.2	14.7	26.4	18.3	12.5	19.4
D-1	1.1	11.9	20.4	31.2	18.9	9.5	7.1
D-2	0.4	6.8	12.5	28.6	25.9	15.0	10.8
E-1	0.4	6.8	13.5	30.8	24.0	14.7	9.9
E-2	0.3	6.4	10.9	24.1	24.2	17.7	16.4

The proportionally division of the damaging potential of the different axle load classes

Table IV.2.14.



Axle load classes (kN)		50-60	50-80	80-100	100-120	120-135	135-150	>150 kN				
Mean values of A-1 - E2 (%)		0.56	8.6	15.9	29.1	21.5	13.0	11.5				
Standard deviation of A-1 - E-2 (%)		0.25	2.5	4.4	4.3	3.2	4.1	5.5				
Axle load classes (kN)		8-20	20-40	40-60	60-80	80-100	100-120	120-140	140-160	160-180	180-200	>200k
Rheden	45 hrs.	0.01	0.63	4.56	13.09	31.59	32.24	14.7	3.8			
	100 years	0.0012	0.34	3.83	11.17	26.92	36.54	17.83	3.23	0.14	0.0011	
Leiderdorp	24 hrs.	0.0054	0.89	6.81	16.59	27.21	26.61	17.3	4.6			
	100 years	0.0027	0.57	5.72	13.96	25.59	28.41	17.28	6.56	1.84	0.08	0.0007
Haagsche Schouw	82 hrs.	0.0026	0.27	3.51	8.81	14.87	23.95	32.01	16.59			
	100 years	0.0008	0.21	2.17	7.27	12.77	19.52	20.91	23.03	9.83	4.01	0.45

Damaging potential of axle loads (13 locations)

Table IV.2.15.

### 4.3. Stress data

#### 4.3.1. Regulations for calculations of fatigue loaded welded joints in the Netherlands (= draft report)

In 1977 the regulations for calculation of welded joints in unalloyed and low alloy steel up to and including Fe 510, which are predominantly statically loaded, has been published. The part concerning the fatigue loaded welded joints is still in preparation.

In the draft report of the regulations it is started from the stress range concept, so the R-value is leaving out of consideration.

In the regulations a difference will be made between structures used for offshore and other structures. What the difference exactly will be is still under discussion, perhaps the cutt off stress will be lower than  $0,55 \Delta\sigma_k$ .<sup>1)</sup>

As the new regulations will concern fatigue loaded welded joints in general, special load spectra will not be mentioned. These spectra must be given in the regulations concerning special structures, as there are railway bridges, highway bridges, crane girders etc.

The design method mentioned in the new rules starts from a stress spectrum which will be translated in a design spectrum (see figure 4.3.2. on page 4-41). By means of the use of the damage rule of Palmgren-Miner

$$\sum \frac{n_i}{N_i} < 1$$

the maximum fatigue stress can be calculated.

---

1)  $\Delta\sigma_k$  is the characteristic stress range at  $10^7$  cycles for the given type of welded joints; see figure 4.3.1. on page 4-41 showing the standard  $\Delta\sigma$ -N curve:

The determination of the potential fatigue damage starts from a standard  $\Delta\sigma$ -N curve, with a shape like given in figure 4.3.1. on page 4-41.

- If  $\Delta\sigma$  is smaller than the value of the stress range exceeded once in one hundredth of the life of the structure, than the damage  $D_3 = 0$ .
- If  $\Delta\sigma > \Delta\sigma_k$  the damage  $D_3$  can be calculated as follows:

$$D_3 = \frac{n_1}{N_1} + \frac{n_2}{N_2} \dots\dots\dots + \frac{n_i}{N_i} \quad N_i = \frac{10^A}{\Delta\sigma_i^3} \quad \text{or}$$

$$\log N_i = A - 3 \log \Delta\sigma_i$$

A: Depends on the type of welding joints.

- If  $0,55 \Delta\sigma_k < \Delta\sigma < \Delta\sigma_k$ , the damage  $D_5$  can be calculated as follows:

$$D_5 = \frac{n_1}{N_1} + \frac{n_2}{N_2} \dots\dots\dots + \frac{n_j}{N_j} \quad N_j = \frac{10^B}{\Delta\sigma_j^5} \quad \text{or}$$

$$\log N_j = B - 5 \log \Delta\sigma_j$$

$$B = \frac{5A - 14}{3}$$

- If  $D_3 \geq 0,25 D_5$  than  $D_{tot} = D_3 + D_5$  and

$$\text{if } D_3 < 0,25 D_5 \text{ than } D_{tot} = D_3 + 5 \frac{D_3 \cdot D_5}{D_3 + D_5}$$

In the regulations a number of  $\Delta\sigma$ -N curves are given for various welded joints. These  $\Delta\sigma$ -N curves give the characteristic values, that is to say values with a probability of 95% and a confidence level of 95% (see figure 4.3.3. on page 4-42).

### 4.3.2. Actual spectra

#### 4.3.2.1. Damaging potential of the different stress range classes

Using a fifth power relationship it is possible to calculate the damaging potential of each stress range class.

Results of the measuring points 3, 4 5 and 6 situated on several longitudinal stiffeners of the orthotropic steel deck in one cross section of the Rheden Bridge on the spot of the slow lane are given in table IV.3.1. on page 4-43.

The following conclusions can be made:

- 1. The division of the damaging potential of the eight stress range classes corresponds with the differences between the cumulative relative frequency curves of rainflow counts as given in chapter 3.
- 2. Concerning the heaviest stress spectrum (mp5) it appears that 90% of the total damage is concentrated in the highest stress range classes 40 - 80 N/mm<sup>2</sup>, so extrapolation seems to be necessary. Mentioned stress range classes presents 9% of the total number of stress cycles.
- 3. For the measuring points 3 - 6 it holds, that the number of stresses in the lowest class 0 - 10 N/mm<sup>2</sup> varies between 62 - 85,6%, the damaging potential of this class varies between 0,007 - 0,13% and seems to be neglectable small.

Results of measuring points on several longitudinal stiffeners of the orthotropic steeldeck in several cross sections of the Leiderdorp Bridge are given in table IV.3.2. on page 4-43 and shows:

- 1. Concerning the measuring points at a midspan location of various longitudinal stiffeners it appears that 76 - 87% of the total damage is concentrated in the three highest stress range classes namely 50 - 80 N/mm<sup>2</sup>. These classes presents 1 - 4½% of the total number of stress ranges.
- 2. Concerning measuring points at a crossing of cross stiffener and longitudinal stiffener (20 and 21) is

- uniformly divided over the six stress range classes 20 - 80 N/mm<sup>2</sup>. These classes presents 5 - 7% of the total number of stress ranges.
- 3. For the given measuring points it holds that the number of stresses in the lowest stress range class 0 - 10 N/mm<sup>2</sup> varies between 76 - 91%, the damaging potential of this class varies between 0,004 - 0,086%.

Results of the measuring points 13 to 21 on several longitudinal girders and measuring points 2 and 3 on a cross girder all situated in the same cross section of the Haagsche Schouw Bridge, are given in table IV.3.3. on page 4-44.

The following conclusions can be made.

- 1. Concerning the division of the damaging potential over the stress range classes it appears that 60 - 75% of the total damage is concentrated in two classes 20 - 40 N/mm<sup>2</sup> (max. 60 N/mm<sup>2</sup>).
- 2. Extrapolation of these spectra is not necessary, taking into account the damage of the highest stress range class 50 - 60 N/mm<sup>2</sup> which causes about 4 - 5% of the total damage.
- 3. It appears that for the given measuring points the number of stress ranges in its lowest stress range class 0 - 10 N/mm<sup>2</sup> varies between 93,9 - 99,5%, the damaging potential of this class varies between 1 - 2%.
- 4. The division of the damaging potential over the different stress range classes do not change if the 0 - 10 N/mm<sup>2</sup> class is to be neglected.

Summarising previous results it can be concluded that:

- 1. For the bridge structure with an orthotropic deck the damaging potential of the 0 - 10 N/mm<sup>2</sup> stress range classes is neglectable small (0.004 - 0.13%) the number of stress cycles in this class varies between 62 - 91%. The damage of the highest measured stress range class (70 - 80 N/mm<sup>2</sup>) for the heaviest stress spectrum amounts 18,7 - 48% so extrapolation seems to be necessary.

- 2. For the bridge structure with longitudinal girders and a deck of wooden boards the damaging potential of the 0 - 10 N/mm<sup>2</sup> stress range class is neglectable small (1 - 2%), the number of stress cycles in this class varies between 93,9 - 99,5%. The damage of the highest measured stress range class (50 - 60 N/mm<sup>2</sup>) varies between 4 - 5% so extrapolation seems to be not necessary.

#### 4.3.2.2. Characteristic stress range

In the same way as the value of CAL of an axle load spectrum has been calculated (see chapter 3), a stress range can be determined such that N-cycles of that stress range has the same fatigue damaging potential as N-cycles of the stress spectrum. Using a fifth power relationship the values of the characteristic stress range CSR<sup>1)</sup> for several measuring points situated on one of the three bridges are tabulated in table IV.3.4. on page 4-44.

It appears that for:

##### -1. Rheden Bridge

For several measuring points situated on several longitudinal stiffeners of the orthotropic steeldeck in one cross section on the spot of the slow lane, values of CSR varies between 18 - 35 N/mm<sup>2</sup>.

##### -2. Leiderdorp Bridge

For the measuring points at a midspan location on the longitudinal stiffeners of the orthotropic steeldeck the characteristic stress range varies between 25 - 47 N/mm<sup>2</sup>. For the measuring points at the crossing of the longitudinal stiffener and the cross stiffener CSR amounts about 20 N/mm<sup>2</sup>.

---

1)  

$$CSR = \sqrt[5]{\frac{\sum n \sigma_r^5}{\sum n}}$$

### -3. Haagsche Schouw Bridge

The characteristic stress ranges of the measuring points on the longitudinal girder as well as the cross girder varies between 11 - 13 N/mm<sup>2</sup>.

#### 4.3.2.3. Fatigue life expectance calculations

The determination of the potential fatigue damage of a welded joints starts from a standard  $\Delta\sigma$ -N curve. By means of the use of the damage rule of Palgrem-Miner  $\sum n_i/N_i < 1$  the fatigue damage can be calculated.

In the following sections the fatigue life expectance calculations will be made for several stress spectra.

##### 4.3.2.3.1. Stiffner of the bridge deck of the Rheden Bridge at a "midspan" location

For this detail of the structure we have used the maximum stress spectrum of straingauge 5. The situation of this straingauge is given in figure 4.3.4. on page 4-45. Using the measured stress spectrum of figure 4.3.5. on page 4-45 and the  $\Delta\sigma$ -N curve of class 85 with  $\Delta\sigma_k = 85$  N/mm<sup>2</sup> the required design spectrum can be constructed (see figure 4.3.6. on page 4-45). From this figure it appears that all counted stress ranges are smaller than  $\Delta\sigma_k$ <sup>1)</sup> so for each class

$$N_i = \left(\frac{\Delta\sigma_k}{\Delta\sigma_i}\right)^5 \cdot 10^7$$

---

#### 1) Remark:

The Dutch code states that of all stress ranges are smaller than  $\Delta\sigma_k$ , no fatigue damage will occur.

However if some stress ranges are larger than  $\Delta\sigma_k$  (even if the fatigue damage of these ranges is small) the mentioned calculation has to be made. This illustrates the importance of the lower part of the S-N curve on the fatigue life expectance calculations.

In the measured period of 45 hours  $\sum n_i/N_i = 1,2155 \cdot 10^{-4}$ .  
Using the measured axle load spectrum of this period and the period of 24 hours continuous measurements the total damage for one day can be calculated.

$$\left( \frac{N_{10_{45 \text{ hrs}}}}{N_{10_{24 \text{ hrs}}}} \right)^{-1} * \sum n_i/N_i$$

So,  $(\sum n_i/N_i)_{\text{day}} = (26891/11261)^{-1} * 1,2155 \cdot 10^{-4} = 5.0858 \cdot 10^{-5}$ ,  
that means a fatigue life expectancy of 19.662 days  
( $= 1/\sum n_i/N_i$ ) or with 250 days a year  $\rightarrow$  78,65 years.

Using the characteristic stress range of gauge point 5 (see table IV.3.4.:  $CSR_5 = 34.47 \text{ N/mm}^2$ ) and the  $\Delta\sigma$ -N curve of class 85 with  $\Delta\sigma_k = 85 \text{ N/mm}^2$  it is possible to calculate a value

$$N_{CSR} = \left( \frac{\Delta\sigma_k}{CSR} \right)^5 * 10^7$$

$N_{CSR_5} = (85/34.47)^5 * 10^7 = 9,12 \cdot 10^8$ , that is the number of measured stress ranges in a period of 45 hours.

$$- n_{\text{day}} = (26891/11261)^{-1} * 9,12 \cdot 10^8 = 5,1089 \cdot 10^4$$

$$- n_{\text{year}} = 250 * 5,1089 \cdot 10^4 = 1,2772 \cdot 10^7$$

That means a fatigue life expectancy of  $9,12 \cdot 10^8 / 1,28 \cdot 10^7 = 71,4$  year.

If welded joints of class 60 or 30 with  $\Delta\sigma_k = 60$  or  $30 \text{ N/mm}^2$  were situated in the same location the design spectra changes (see figure 4.3.7. and 4.3.8. on page 4-46). The fatigue life expectancy would than be 11,69 years in the case of class 65 or 1.24 years in the case of class 30.

In both cases these values are not very realistic but they give a very clear insight into the necessity of a good fatigue design of the bridge structure.



#### 4.3.2.3.2. Stiffner of the bridge deck of the Rheden Bridge crossing of the stiffner and a cross girder

For this detail of the structure we have used the maximum stress spectrum of strain gauge 13. The situation of this strain gauge is given in figure 4.3.9. on page 4-47.

Using the stress spectrum of gauge point 13 and the  $\Delta\sigma$ -N curve of class 40 with  $\Delta\sigma_k = 40 \text{ N/mm}^2$  the design spectrum can be constructed (see figure 4.3.10. on page 4-47.

Calculations, which method is already given in section 4.3.2.3.1. give a fatigue life expectancy for this detail of the structures of 57,92 years.

#### 4.3.3. Extrapolated spectra

##### 4.3.3.1. Extrapolation of stress spectra

For the Rheden Bridge axle loads and stresses have been measured in several periods. For these periods (see chapter 3), the number of stresses of gauge point 5 have been expressed in the number of axle loads  $> 10 \text{ kN}$ .

Using the number of axle loads counted in section 4.2. for the total life of the bridge (100 years), the number of cycles of gauge point 5 amounts  $1.10^9$ . Extrapolation of the measured spectrum for  $1.10^9$  cycles gives a maximum stress range of  $110 \text{ N/mm}^2$  (measured maximum amounts  $80 \text{ N/mm}^2$ ). See figure 4.3.11. on page 4.48.

Just as for the Rheden Bridge the measured stress spectra of three measuring points on the Leiderdorp Bridge have been extrapolated for a total number of stress cycles of  $1.10^9$ . These number of stress cycles can probably occur in the total life of the Bridge which amounts 100 years.

Extrapolation of the measured stress spectrum for measuring point 7 and 9 gives a maximum stress range of  $120 \text{ N/mm}^2$  and for measuring point 23 a value of  $160 \text{ N/mm}^2$ . See figure 4.3.12-4.3.13 on page 4.49.

#### 4.3.3.2. Damaging potential of the extrapolated spectra

Using the fifth power relationship the damaging potential of each stress range class has been calculated.

For the Rheden Bridge results of measuring point 5 are given in figure 4.3.11. on page 4-48 and table IV.3.5. on page 4.48. The following conclusions can be made.

- 1. stress ranges smaller than  $30 \text{ N/mm}^2$  are not important
  - 2. stress ranges between  $90 - 100 \text{ N/mm}^2$  are less important
  - 3. stress ranges between  $100 - 110 \text{ N/mm}^2$  are not important
- So extrapolation into higher stresses does not have any case.

For the Leiderdorp Bridge results are given in figures 4.3.12 up to 4.3.14. on page 4-49 and table IV.3.6. on page 4.50. The following conclusions can be made.

- 1. Concerning measurement point 23.
  - stress ranges smaller than  $40 \text{ N/mm}^2$  are not important
  - stress ranges between  $110 - 120 \text{ N/mm}^2$  are less important
  - stress ranges between  $120 - 160 \text{ N/mm}^2$  are not important
  - stress ranges between  $40 - 110 \text{ N/mm}^2$  causes 97% of the total damage; the number of cycles amounts  $8 \cdot 10^7$ .
- 2. Concerning measuring point 7
  - stress ranges smaller than  $30 \text{ N/mm}^2$  are not important
  - stress ranges between  $90 - 120 \text{ N/mm}^2$  are not important
  - stress ranges between  $30 - 90 \text{ N/mm}^2$  causes 98% of the total damage; the number of cycles amounts  $8 \cdot 10^7$ .
- 3. Concerning measuring point 9
  - stress ranges smaller than  $30 \text{ N/mm}^2$  are not important
  - stress ranges between  $100 - 120 \text{ N/mm}^2$  are not important
  - stress ranges between  $30 - 100 \text{ N/mm}^2$  causes 97% of the total damage; the number of cycles amounts  $3.8 \cdot 10^7$ .

Summarising previous conclusions it appears that depend on the measuring point:

- 1. stress ranges smaller than 30 or 40 N/mm<sup>2</sup> and stress ranges higher than 90, 100 or 120 N/mm<sup>2</sup> are not important in relationship of fatigue damage.
- 2. the intermediate stress range classes causes 97 - 98% of the total damage.
- 3. the number of stress cycles in these intermediate stress range classes amounts  $3.8 \cdot 10^7$  -  $8 \cdot 10^7$  so fifth power relationship of the fatigue damage seems to be reasonable.

#### 4.3.3.3. Characteristic stress range

Just as we have done for the actual stress spectra it is possible to calculate values of CSR for the extrapolated spectra. Results as given in table IV.3.7. on page 4-51 shows that the difference between a value of CSR of the extrapolated spectra and the actual spectra is small.

#### 4.3.3.4. Assumptions for further analysis

For further analysis of the spectra the following assumptions are made:

- 1. the slope of the S-N curve amounts 1:5
- 2.  $\Delta\sigma_k$  is the admissible value of the stress range  $\Delta\sigma_k$  at  $10^7$  cycles
- 3. the relationship between the stress range  $\Delta\sigma$  and number of cycles N is:

$$N = \left(\frac{\Delta\sigma_k}{\Delta\sigma}\right)^5 \cdot 10^7$$

Using above mentioned assumptions graphs have been plotted which give for several CSR-values the relationship between  $\Delta\sigma$  and N ( $N > 10^7$ ) (see figure 4.3.15 on page 4-51).

In this way it is easy to calculate a minimum value for  $\Delta\sigma_k$  if the number of stress range cycles during the lifetime and the characteristic stress range are known.

4.3.3.5. Further analysis in fatigue terms

- A. For the Rheden Bridge the characteristic stress range of the extrapolated stress spectra of gauge point 5 in the total life of the bridge seemed to be  $37,6 \text{ N/mm}^2$ .

Using the characteristic stress range of  $37,6 \text{ N/mm}^2$  and a total number of cycles, which amounts  $1 \cdot 10^9$  in one hundred years the following conclusions can be made:

- 1. If  $N_{\text{CSR}}^{2)} = 1 \cdot 10^9$  cycles  $\rightarrow \Delta\sigma_k = 94.4 \text{ N/mm}^2$
- 2.  $\Delta\sigma_k = 90 \text{ N/mm}^2$  gives a fatigue life expectancy of 79 years
- 3.  $\Delta\sigma_k = 100 \text{ N/mm}^2$  gives a fatigue life expectancy of 133 years
- 4.  $\Delta\sigma_k = 110 \text{ N/mm}^2$  gives a fatigue life expectancy of 214 years

Assuming that a lifetime of 75 years will be the minimum to be wished,  $\Delta\sigma_k$  must have a minimum of  $90 \text{ N/mm}^2$ . That means according to conclusions mentioned before, all damaging stresses are situated in an area where  $N > 10^7$ . That means for the Dutch code in the area where the slope of the S-N curve is 1:5 (see figure 4.3.16 on page 4.52). For the new Eurocode it is even more clear that it must be in that area (see figure 4.3.17 on page 4-52).

Much more important are:

- a. the situation of the S-N curve itself
- b. the reasonableness of the slope 1:5
- c. the point under which no fatigue damage will occur

Concerning the last item:

According to the Dutch rules no fatigue damage will occur when  $\Delta\sigma < 0,55 \Delta\sigma_k (N > 2 \cdot 10^8)$ .

The Eurocode says it must be  $< 0.63 \Delta\sigma_k (N > 10^8)$ .

For  $\Delta\sigma_k = 90 \text{ N/mm}^2$  it will be  $50 \text{ N/mm}^2$  respectively  $57 \text{ N/mm}^2$   
 For  $\Delta\sigma_k = 100 \text{ N/mm}^2$  it will be  $55 \text{ N/mm}^2$  respectively  $63 \text{ N/mm}^2$   
 For  $\Delta\sigma_k = 110 \text{ N/mm}^2$  it will be  $61 \text{ N/mm}^2$  respectively  $69 \text{ N/mm}^2$

---

2) 
$$N_{\text{CSR}} = \left(\frac{\Delta\sigma_k}{\text{CSR}}\right)^5 \cdot 10^7$$

#### 4.3.4. Conclusions

##### Actual spectra

- 1. For the bridge structure with an orthotropic deck the damaging potential of the 0 - 10 N/mm<sup>2</sup> stress range class is neglectable small (0.004 - 0.13%) the number of stress cycles in this class varies between 62 - 91%. The damage of the highest measured stress range class (70 - 80 N/mm<sup>2</sup>) for the heaviest stress spectrum amounts 18,7 - 48% so extrapolation seems to be necessary.
- 2. For the bridge structures with longitudinal girders and a deck of wooden boards, the damaging potential of the 0 - 10 N/mm<sup>2</sup> stress range class is neglectable small (1 - 2%), the number of stress cycles in this class varies between 93,9 - 99,5%. The damage of the highest measured stress range class (50 - 60 N/mm<sup>2</sup>) varies between 4 - 5% so extrapolation seems to be not necessary.
- 3. The Dutch fatigue code states that if all stress ranges are smaller than  $\Delta\sigma_k$ , no fatigue damage will occur. However, if some stress ranges are larger than  $\Delta\sigma_k$  (even if the fatigue damage of these stress ranges is small) the mentioned calculation has to be made. This means for the Rheden Bridge a fatigue life expectancy of about 75 years. This illustrates the importance of the lower part of the S-N curve on the fatigue life expectancy calculations.

##### Extrapolated spectra

- 1. Stress ranges smaller than 30 - 40 N/mm<sup>2</sup> and stress ranges higher than 90, 100 or 120 N/mm<sup>2</sup> (dependent on the spectra) are not important in relationship to fatigue damage.
- 2. The intermediate stress range classes causes 97 - 98% of the total damage. The number of stress cycles in these stress range classes still amounts  $3,8 \cdot 10^7$  -  $8 \cdot 10^7$  cycles. So a fifth power relationship of the fatigue damage according to the Dutch fatigue code and the Eurocode seems to be reasonable.



-3. Calculating a minimum value for  $\Delta\sigma_k$ , that is the admissible value of the stress range at  $10^7$  cycles, it appeared that the maximum stress range must be close to the value of  $\Delta\sigma_k$  of the welded detail if lifetime of 75 - 100 years will be the minimum to be wished. Therefore the part of the S-N curve with a slope 1:3 is not important for bridge components with a great number of cycles.

- 4. Important are:
- a. the situation of the S-N curve itself
  - b. the reasonableness of the slope 1:5
  - c. the point under which no fatigue damage will occur.

#### 4.3.5. Figures and tables

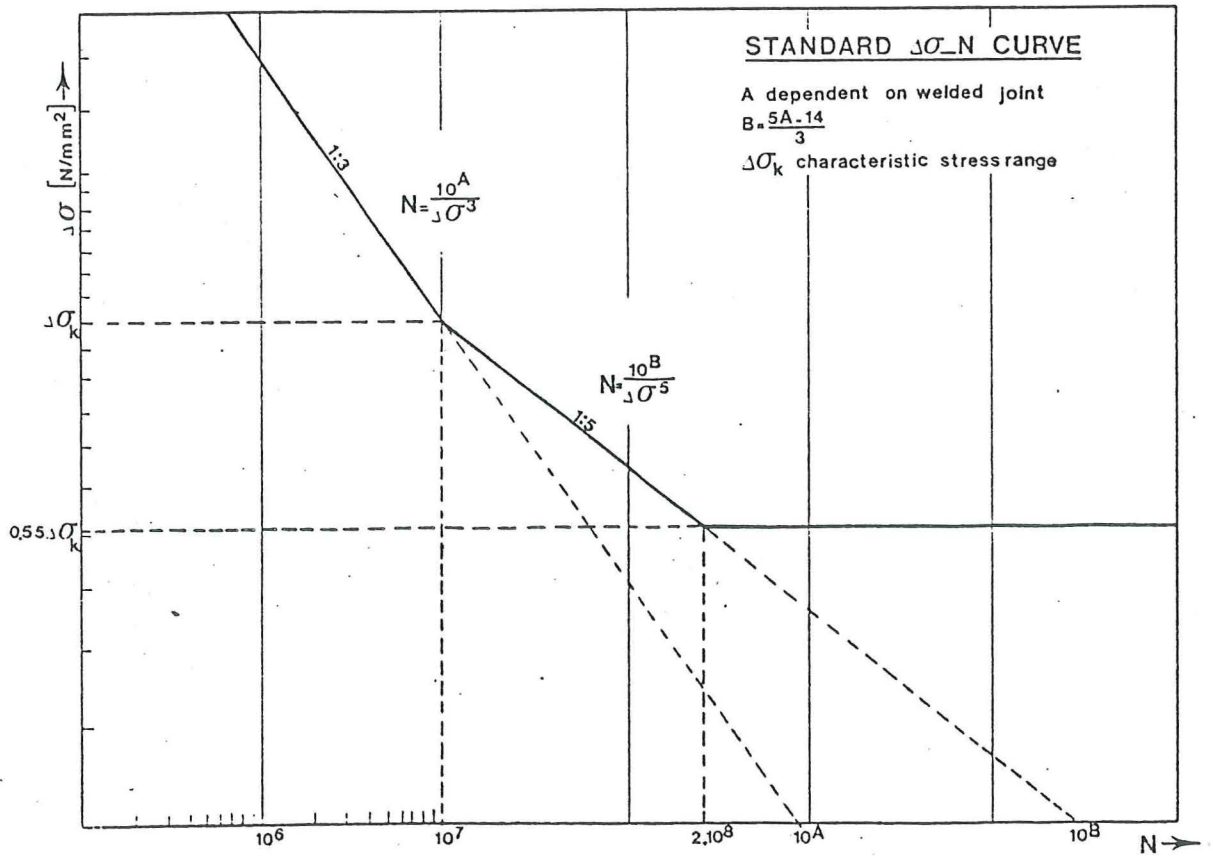
List of figures	Page
4.3.1. $\Delta\sigma$ -N curve slope 1:3 → 1:5	4-41
4.3.2. Stress spectrum - Design spectrum - Palgrem-Miner	4-41
4.3.3. Characteristic $\Delta\sigma$ -N curves - 95% survival	4-42
4.3.4. Situation mp5 on the Rheden Bridge	4-45
4.3.5. Measured stress spectrum mp5 Rheden B.	4-45
4.3.6. Design spectrum mp5 using class 85	4-45
4.3.7. Design spectrum mp5 using class 60	4-46
4.3.8. Design spectrum mp5 using class 30	4.46
4.3.9. Situation mp13 on the Rheden Bridge	4.47
4.3.10. Design spectrum mp13 using class 40	4-47
4.3.11. Stress spectrum mp5, 100 years	4-48
4.3.12. Extrapolated stress spectrum mp7 Leiderdorp Bridge	4-49

	Page
4.3.13. Extrapolated stress spectrum mp9 Leiderdorp Bridge	4-49
4.3.14. Extrapolated stress spectrum mp23 Leiderdorp Bridge	4-50
4.3.15. Relationship $\Delta\sigma_k$ , $\Sigma_n$ and CRS using a fifth power relationship	4-51
4.3.16. $\Delta\sigma$ -N curve, Dutch code	4-52
4.3.17. $\Delta\sigma$ -Ncurve, Eurocode	4-52

## List of tables

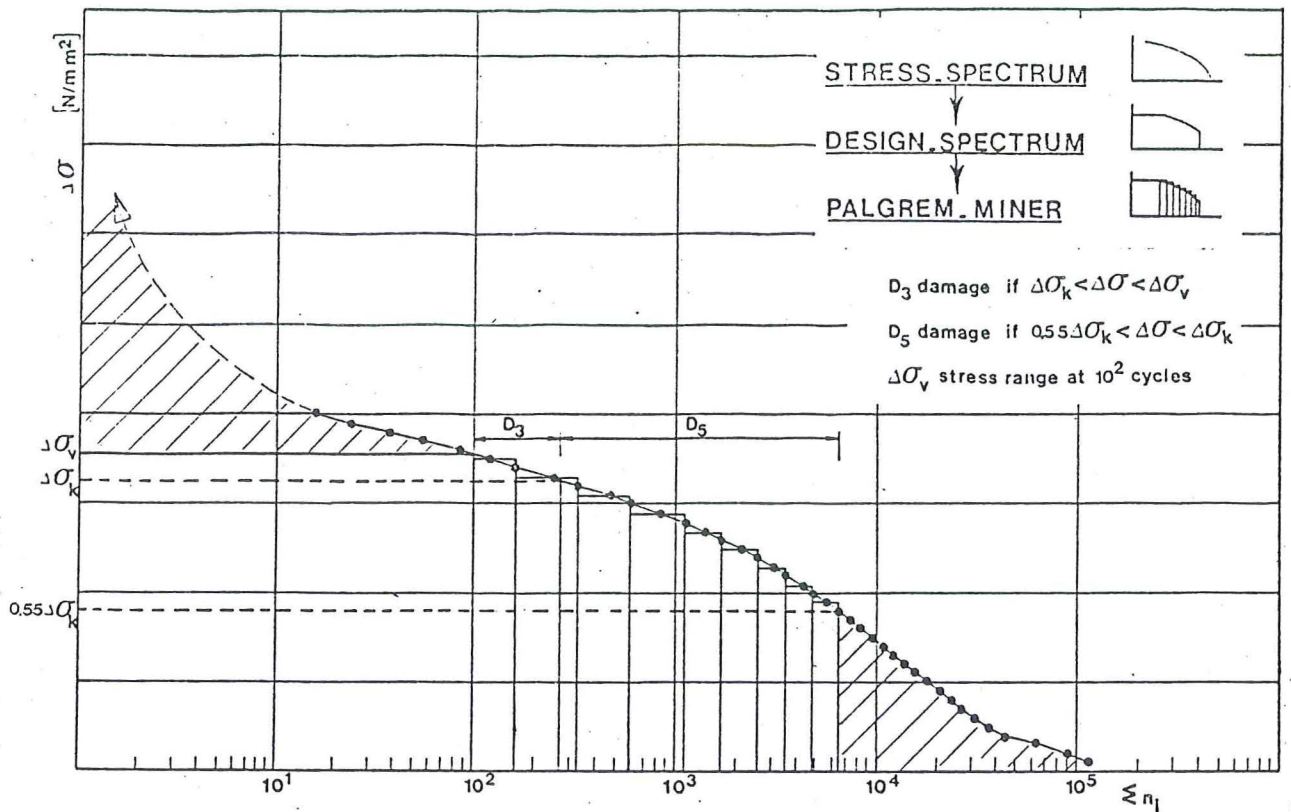
IV.3.1. Rheden Bridge damaging potential actual stress spectra	4-43
IV.3.2. Leiderdorp Bridge damaging potential actual stress spectra	4-43
IV.3.3. Haagsche Schouw Bridge damaging potential actual stress spectra	4-43
IV.3.4. Characteristic stress range - values of actual stress spectra	4-43
IV.3.5. Damaging potential stress spectrum mp5, 100 years Rheden Bridge	4-48
IV.3.6. Damaging potential stress spectra mp7, 9 and 23, Leiderdorp Bridge	4-50
IV.3.7. Characteristic stress range values of actual and extrapolated stress spectra	4-51





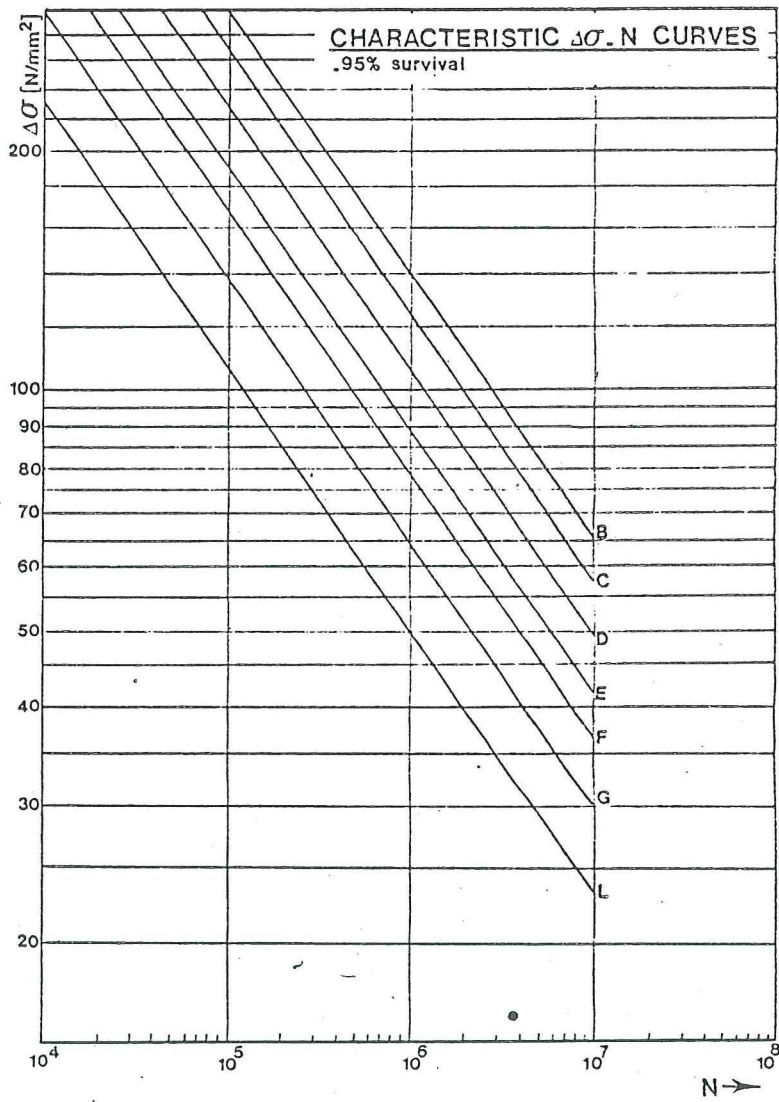
$\Delta\sigma$ -N curve slope 1:3, 1:5

Figure 4.3.1.



Stress spectrum - Design spectrum - Palmgren Miner

Figure 4.3.2.



Characteristic curves - 95% survival  
 Figure 4.3.3.

Stress range classes N/mm <sup>2</sup>	Number of stress ranges in %				Damaging potential in %			
	mp.3	mp.4	mp.5	mp.6	mp.3	mp.4	mp.5	mp.6
0 - 10	85.6	73.2	63.7	62.0	0.13	3.013	0.008	0.007
10 - 20	10.5	13.0	12.0	16.0	3.74	0.559	0.26	0.45
20 - 30	2.6	6.5	9.1	10.8	12.14	3.59	2.00	3.87
30 - 40	0.8	3.5	6.4	5.9	20.60	10.50	7.24	11.29
40 - 50	0.3	2.3	4.8	3.3	26.64	23.85	18.34	22.43
50 - 60	0.1	1.0	2.6	1.4	22.65	29.39	26.20	26.18
60 - 70	0.02	0.3	1.2	0.5	9.79	22.08	27.17	21.72
70 - 80	0.004	0.08	0.4	0.2	4.30	19.01	18.69	14.06
Total number of stress ranges	77765	115116	121877	92369				

Rheden Bridge damaging potential actual stress spectra  
Table IV-3-1

Stress range classes N/mm <sup>2</sup>	Number of stress in % (actual spectra)									
	6.41 hours					3.00 hours			5.01 hours	
	mp.6	mp.23	mp.24	mp.9	mp.26	mp.19	mp.21	mp.9	mp.7	mp.9
0 - 10	79.02	76.16	86.89	88.82	78.6	78.55	83.03	90.62	76.01	86.75
10 - 20	8.11	6.80	5.48	5.32	7.15	14.52	11.74	4.75	10.09	6.34
20 - 30	5.13	5.53	3.05	2.55	5.48	5.37	3.74	1.95	6.02	3.06
30 - 40	3.42	3.83	1.80	1.42	3.27	1.08	1.03	1.14	3.68	1.71
40 - 50	2.18	3.19	1.24	0.97	2.68	0.29	0.28	0.77	2.48	0.98
50 - 60	1.17	1.74	0.71	0.49	1.46	0.15	0.11	0.38	1.10	0.55
60 - 70	0.66	1.43	0.43	0.29	0.92	0.02	0.05	0.19	0.54	0.34
70 - 80	0.30	1.33	0.41	0.14	0.45	0.03	0.01	0.20	0.09	0.26
$\sum n_i$	35579	34259	44763	50417	35769	11620	14424	25761	17631	30491
Stress range classes N/mm <sup>2</sup>	Damaging potential in % (actual spectra)									
	6.41 hours					3.00 hours			5.01 hours	
	mp.6	mp.23	mp.24	mp.9	mp.26	mp.19	mp.21	mp.9	mp.7	mp.9
0 - 10	0.009	0.004	0.013	0.02	0.007	0.07	0.086	0.03	0.01	0.017
10 - 20	0.23	0.08	0.19	0.34	0.15	3.15	3.00	0.33	0.37	0.303
20 - 30	1.86	0.83	1.36	2.10	1.49	15.0	12.26	1.72	2.81	1.88
30 - 40	6.63	3.07	4.31	6.28	4.80	16.2	18.25	5.25	9.20	5.65
40 - 50	14.50	9.00	10.42	15.06	13.80	15.44	17.65	12.6	21.81	11.34
50 - 60	21.74	13.37	16.35	20.66	20.43	21.08	18.77	17.43	26.41	17.54
60 - 70	27.96	25.41	22.99	28.66	29.71	5.7	18.93	20.3	29.76	25.15
70 - 80	26.92	48.14	44.34	26.82	29.63	23.4	11.07	42.35	9.63	38.13
CSR (N/mm <sup>2</sup> )	30.67	36.57	46.55	26.01	24.83	20.36	19.71	25.64	29.13	27.56

Leiderdorp Bridge damaging potential actual stress spectra  
Table IV-3-2

Stress range classes N/mm <sup>2</sup>	Number of stress ranges in % (actual spectra)									
	mp.13	mp.14	mp.15	mp.16	mp.17	mp.18	mp.20	mp.21	mp.2	mp.3
0 - 10	93.9	94.45	95.41	93.95	96.2	98.5	99.48	98.9	96.9	98.18
10 - 20	5.1	4.93	3.91	4.90	3.4	1.4	0.43	0.93	2.43	1.71
20 - 30	0.96	0.51	0.57	0.89	0.3	0.11	0.08	0.12	0.64	0.11
30 - 40	0.03	0.10	0.11	0.25	0.05	0.02	0.007	0.01	0.03	0.0014
40 - 50	-.-	0.01	0.059	0.01	0.01	-.-	-.-	-.-	0.006	-.-
50 - 60	-.-	0.002	-.-	0.002	0.0009	-.-	-.-	-.-	-.-	-.-
$n_i$	38453	132512	118085	133220	116527	98240	55917	18938	65877	69139

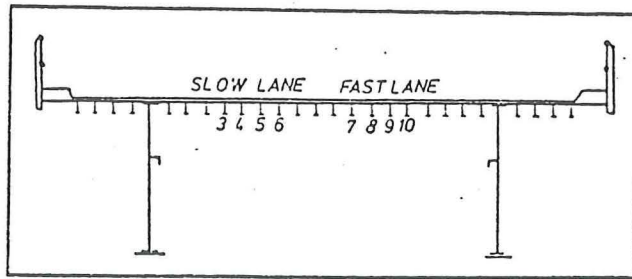
  

Stress range classes N/mm <sup>2</sup>	Damaging potential in %		
	mp.14	mp.15	mp.16
0 - 10	1.75	1.9	1.01
10 - 20	22.24	18.92	12.87
20 - 30	29.55	35.62	29.85
30 - 40	30.40	36.65	45.16
40 - 50	11.57	6.97	7.19
50 - 60	4.48	-.-	3.92
CSR (N/mm <sup>2</sup> )	11,1	10,9	12,4

Haagsche Schouw Bridge damaging potential actual stress spectra  
Table IV-3-3

Characteristic Stress Range		
<u>Rheden:</u>	mp 3	18,44 N/mm <sup>2</sup>
	mp 4	30,48 "
	mp 5	34,47 "
	mp 6	30,69 "
<u>Leiderdorp:</u>	mp 6	30,67 "
	mp 23	36,57 "
	mp 24	46,55 "
	mp 9	26,01/25,61/27,56 N/mm <sup>2</sup>
	mp 26	24,83 N/mm <sup>2</sup>
	mp 19	20,36 "
	mp 21	19,71 "
mp 7	29,13 "	
<u>Haagsche_Schouw:</u>	mp 14	11,1 "
	mp 15	10,9 "
	mp 16	12,4 "

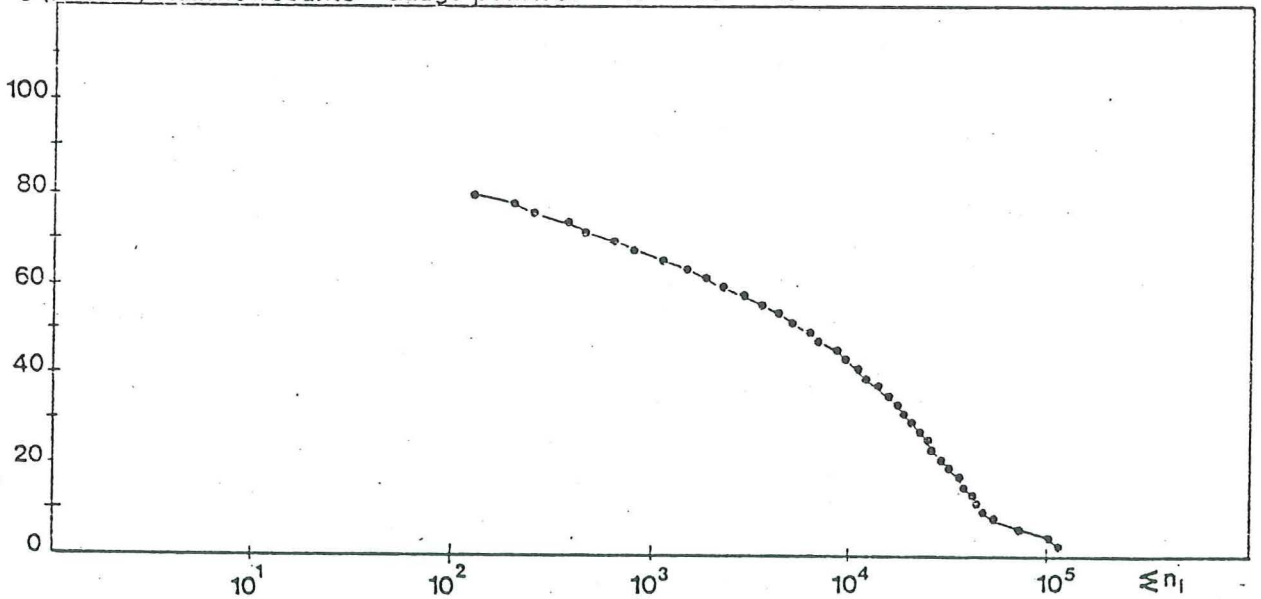
Characteristic Stress Range - values of actual stress spectra  
Table IV-3-4



Situation mp 5 on the Rheden Bridge  
Figure 4.3.4.

RHEDEN BRIDGE

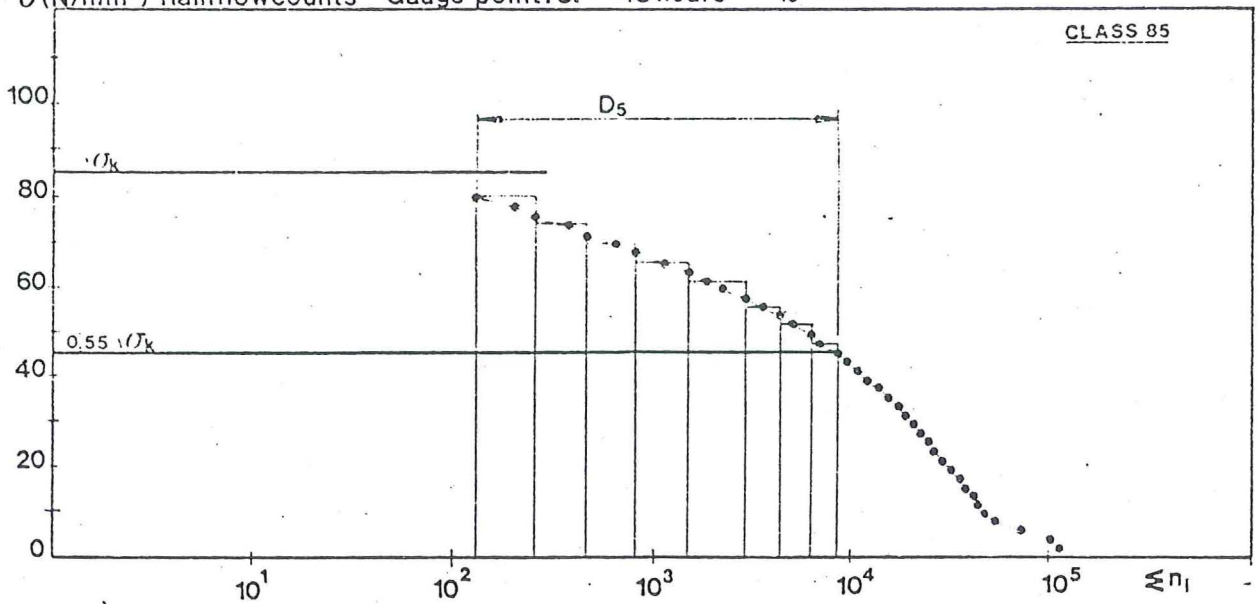
$\sigma$  (N/mm<sup>2</sup>) Rainflowcounts Gauge point: 5. 45 hours  $n_{10}$  32741



Measured stress spectrum measuring point 5 Rheden Brige  
Figure 4.3.5.

RHEDEN BRIDGE

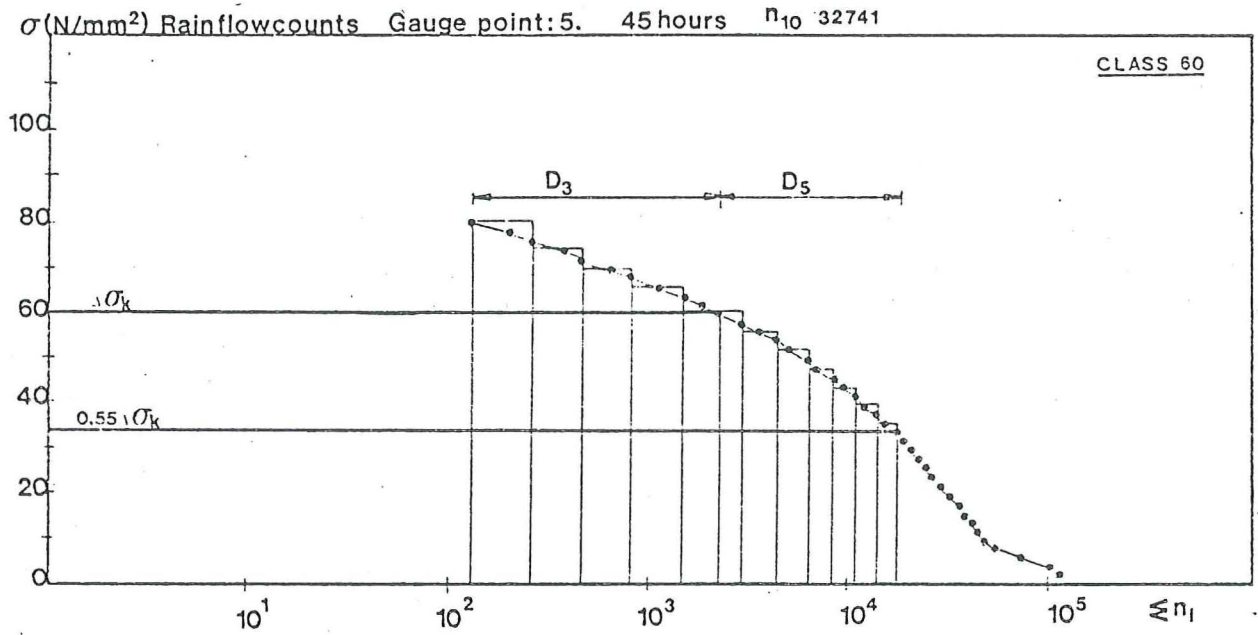
$\sigma$  (N/mm<sup>2</sup>) Rainflowcounts Gauge point: 5. 45 hours  $n_{10}$  32741



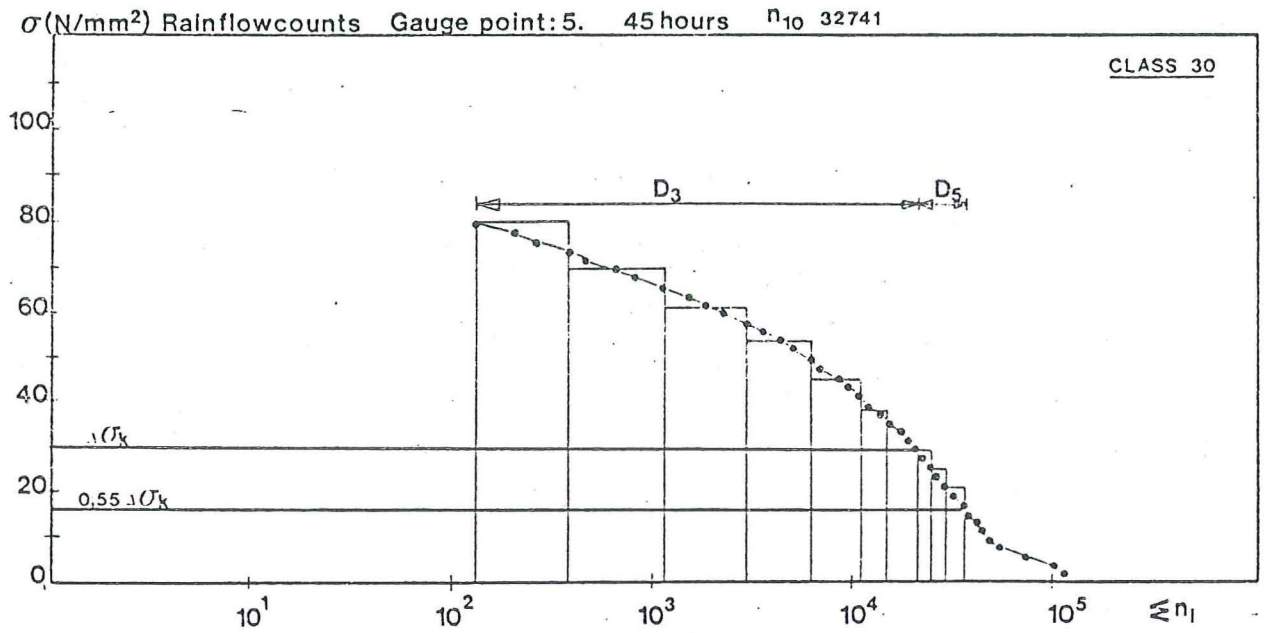
Design spectrum mp 5 using class 85

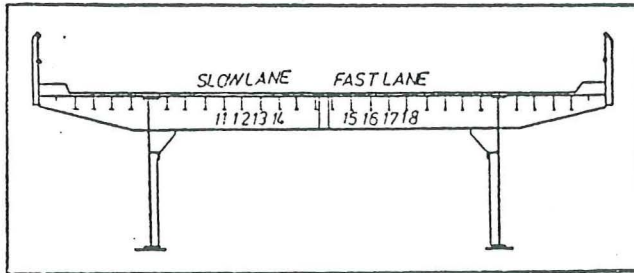
Figure 4.3.6.

RHEDEN BRIDGE



RHEDEN BRIDGE

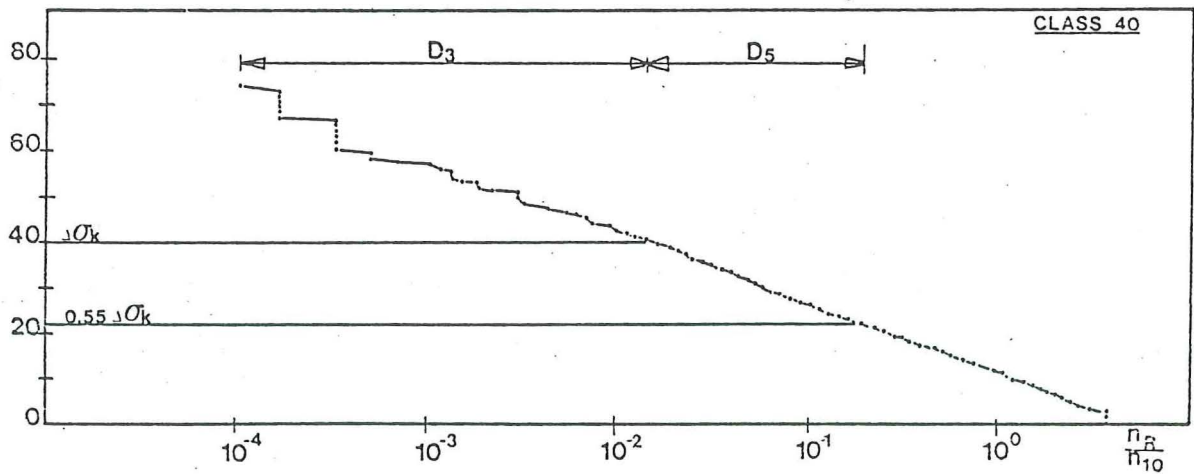




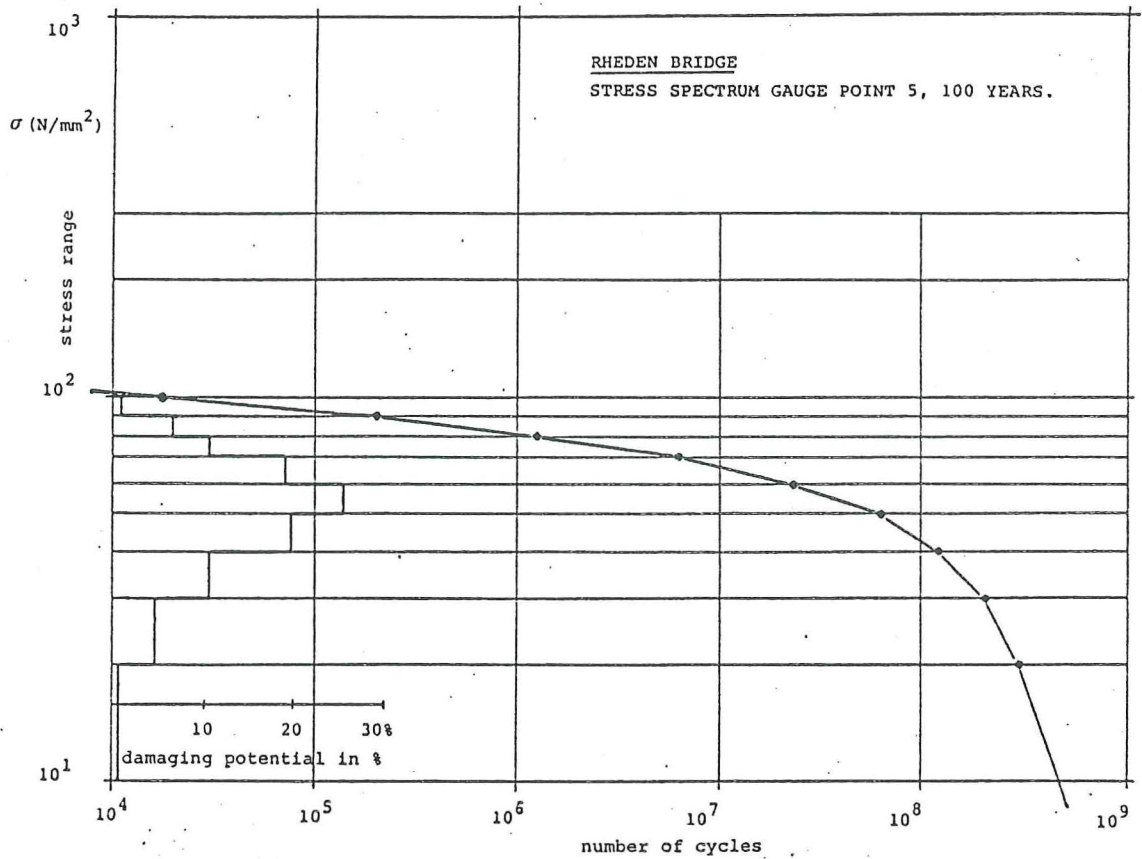
Situation mp 13 on the Rheden Bridge  
Figure 4.3.9.

RHEDEN BRIDGE

$\sigma(N/mm^2)$  Rainflowcounts Gauge point:13. 7.96 hours  $n_{10}=6103$



Design spectrum mp 13 using class 40  
Figure 4.3.10



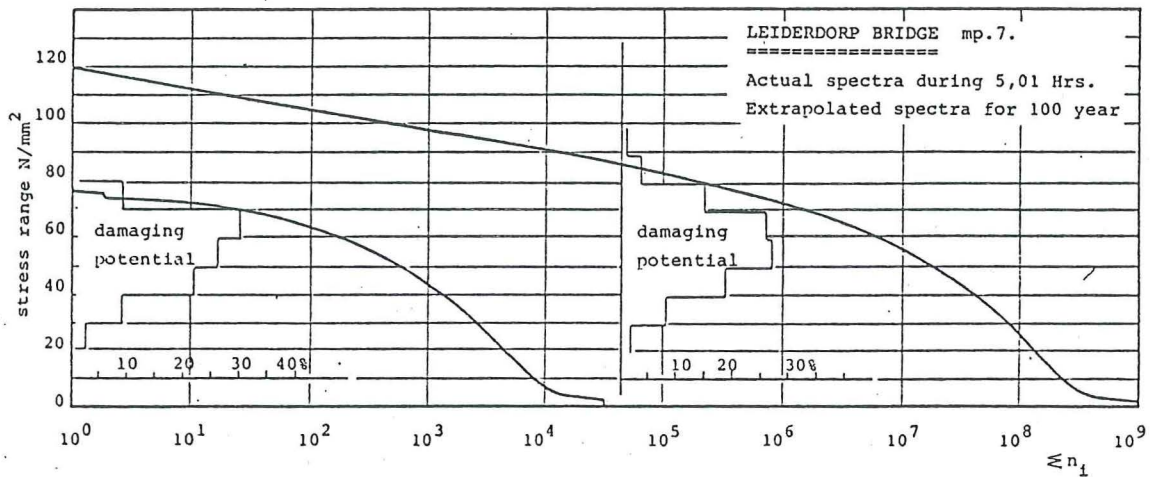
Stress spectrum measuring point 5, 100 years  
Figure 4.3.11.

$\sigma_{r_i}$ N/mm <sup>2</sup> - N/mm <sup>2</sup>	$\Sigma N_i = 1 \times 10^9$ (100 years) Damaging potential <sup>*)</sup> of stress ranges in %	$N_i$
0 - 10	0.002	$5 \times 10^8$
10 - 20	0.2	$2 \times 10^8$
20 - 30	1.3	$1 \times 10^8$
30 - 40	5.6	$8 \times 10^7$
40 - 50	14.7	$6 \times 10^7$
50 - 60	26.8	$4 \times 10^7$
60 - 70	21.6	$1.4 \times 10^7$
70 - 80	15.8	$5 \times 10^6$
80 - 90	10.6	$1.8 \times 10^6$
90 - 100	3.0	$2.9 \times 10^5$
100 - 110	0.3	$2 \times 10^4$

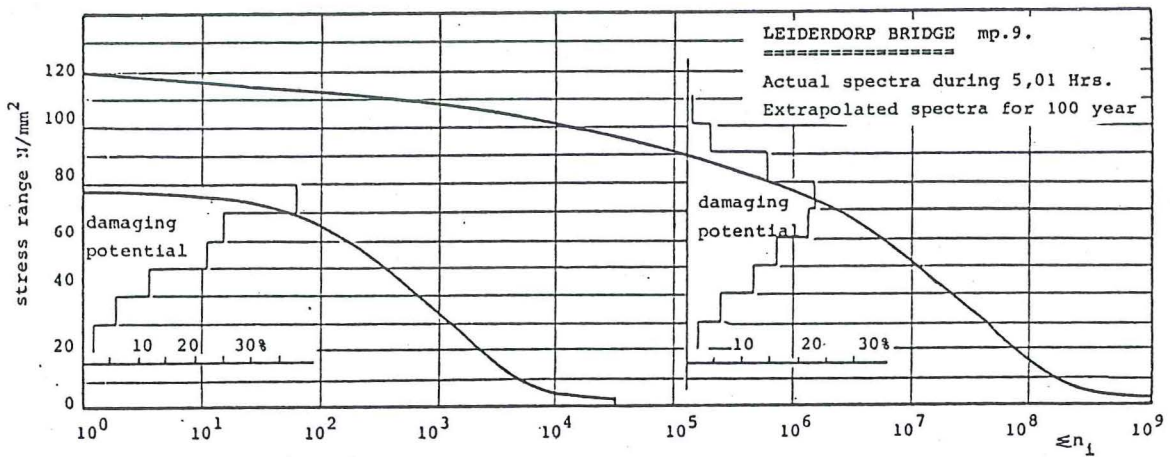
$$*) \frac{N_i \sigma_{r_i}^5}{\Sigma N_i \sigma_{r_i}^5} \times 100\%$$

Damaging potential stress spectrum mp 5, 100 years  
Table IV-3-5

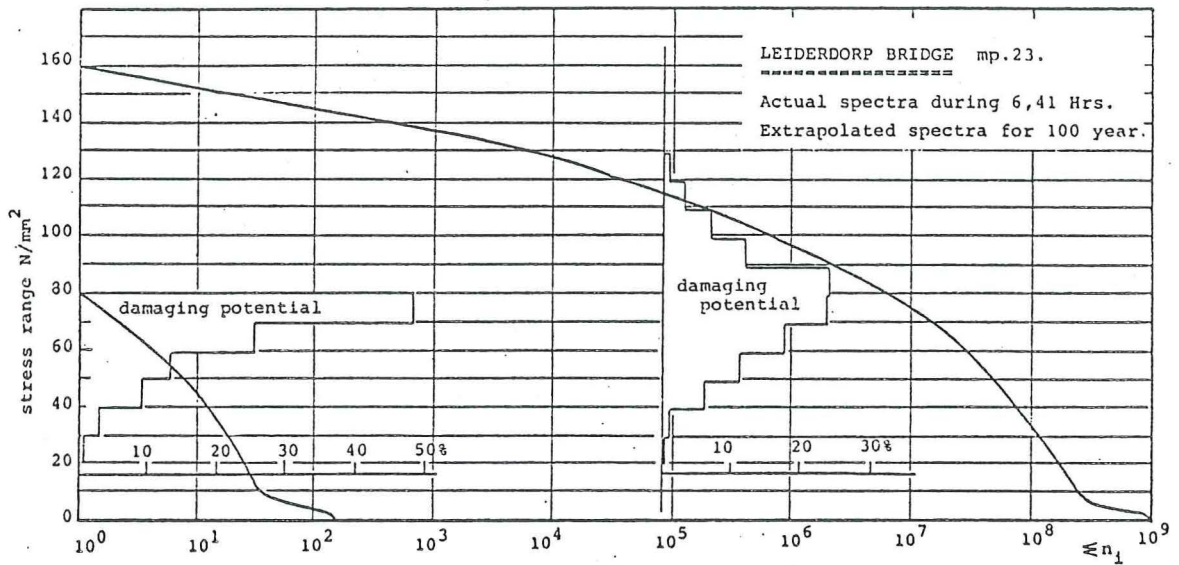




Extrapolated stress spectrum mp.7, Leiderdorp Bridge  
Figure 4.3.12.



Extrapolated stress spectrum mp.9, Leiderdorp Bridge  
Figure 4.3.13.



Extrapolated stress spectrum mp.23, Leiderdorp Bridge

Figure 4.3.14

Stress range classes N/mm <sup>2</sup>	Number of stress ranges in %			Damaging potential in %		
	mp.7	mp.9	mp.23	mp.7	mp.9	mp.23
0 - 10	79.0	89.0	78.0	0.01	0.02	0.003
10 - 20	9.0	4.0	6.0	0.29	0.19	0.05
20 - 30	4.0	3.2	5.9	1.63	2.00	0.58
30 - 40	3.6	1.8	2.1	7.89	6.04	1.11
40 - 50	2.4	1.0	3.0	18.50	11.83	5.59
50 - 60	1.3	0.5	2.0	27.31	16.12	11.09
60 - 70	0.53	0.29	1.4	25.69	21.55	16.34
70 - 80	0.15	0.15	0.9	14.79	22.77	21.58
80 - 90	0.02	0.05	0.49	3.56	14.20	21.88
90 - 100	0.002	0.009	0.14	0.57	4.45	10.89
100 - 110	3.8x10 <sup>-5</sup>	0.001	0.052	0.0002	0.80	6.70
110 - 120	2.0x10 <sup>-6</sup>	2.2x10 <sup>-5</sup>	0.014	0.0017	0.03	2.84
120 - 130	-.-	-.-	0.0033	-.-	-.-	1.02
130 - 140	-.-	-.-	0.0006	-.-	-.-	0.29
140 - 150	-.-	-.-	0.0001	-.-	-.-	0.037
150 - 160	-.-	-.-	2.8x10 <sup>-7</sup>	-.-	-.-	0.025
CSR (n/mm <sup>2</sup> )				29.9	27.46	38.98
≤ n <sub>i</sub>	1.10 <sup>9</sup>	1.10 <sup>9</sup>	1.10 <sup>9</sup>			

Damaging potential stress spectra mp.7, 9 and 23, Leiderdorp

Table IV-3-6

Characteristic Stress Range $N/mm^2$		
Rheden:	actual spectra	extrapolated spectra
mp 5	34,47	
<u>Leiderdorp:</u>		
mp 7	29,13	29,9
mp 9	± 26,00	27,46
mp 23	36,57	38,98

Characteristic Stress Range values of actual and extrapolated stress spectra

Table IV-3-7

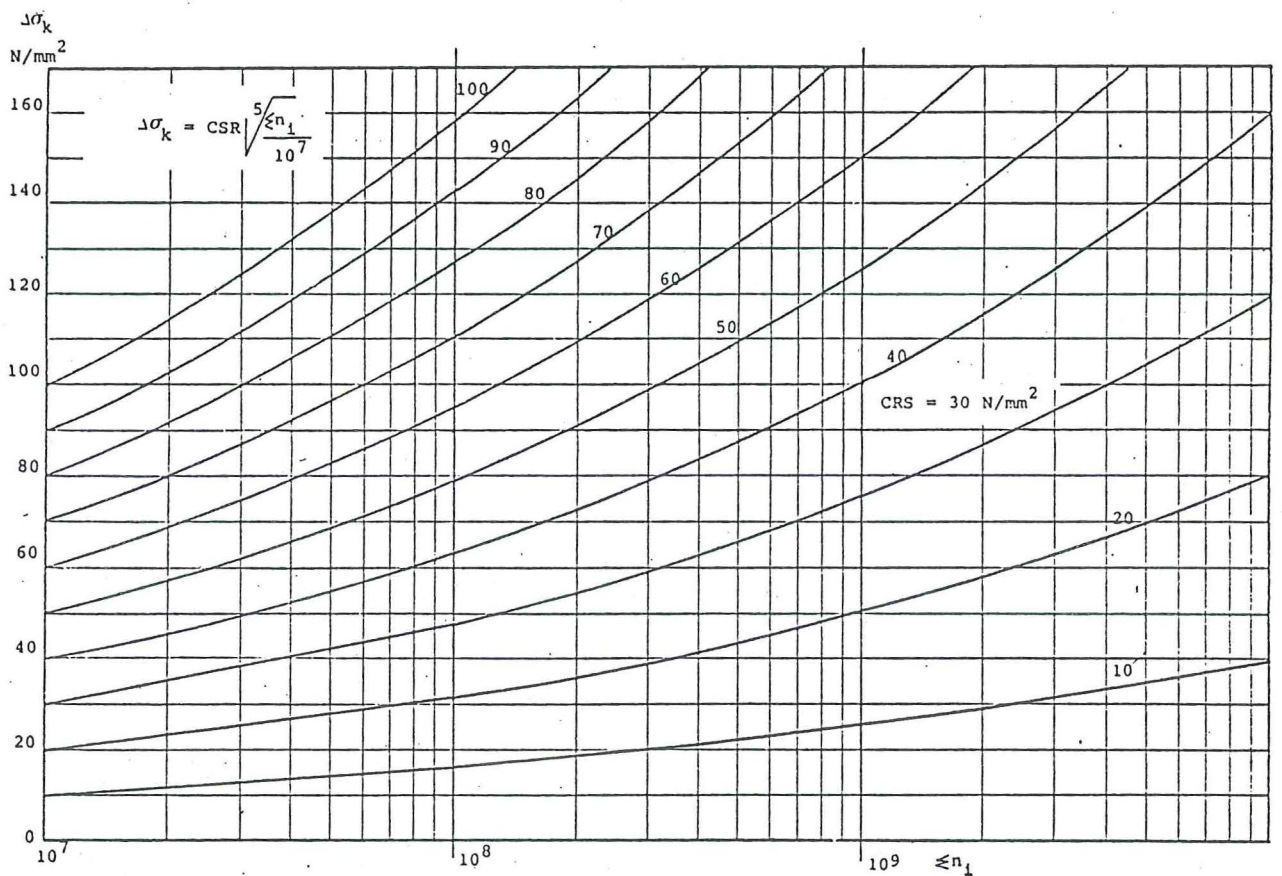


Figure 4.3.15.

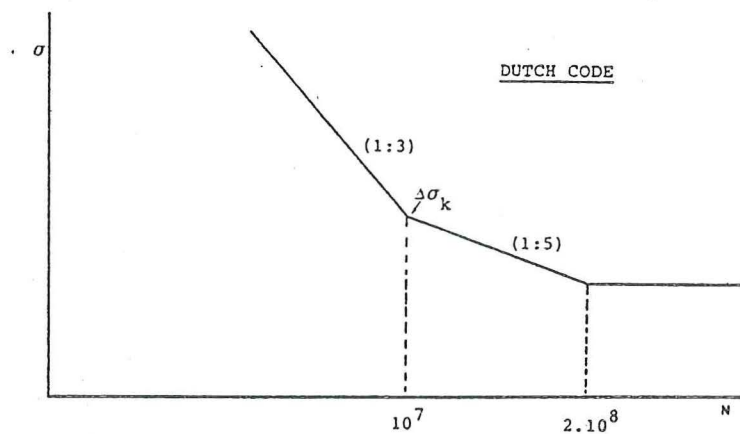
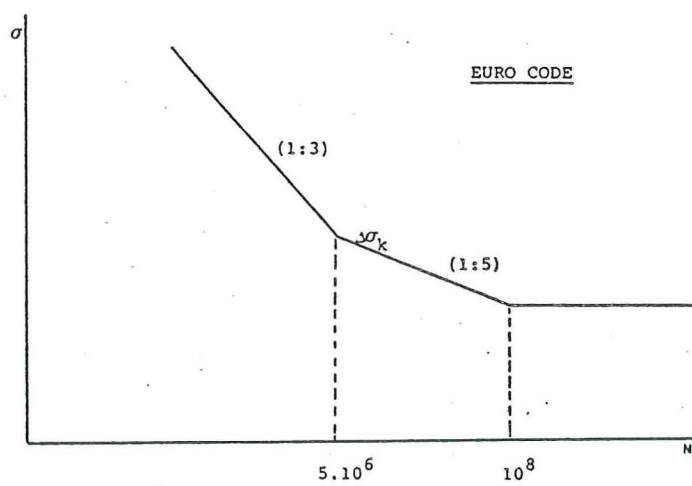


Figure 4.3.16



#### 4.4. Relationship traffic data to stress data

##### 4.4.1. Relating stress spectra to axle load spectra

Chapter 4.3.1. showed that in regulations for calculations of fatigue loaded welded joints in The Netherlands the slope of  $\Delta\sigma$ -N curve have a value of 3 hanging to 5 for  $N > 10^7$  at the characteristic stress range  $\Delta\sigma_k$ .

To obtain the intended life it is likely that nearly all stress ranges must be below  $\Delta\sigma_k$ .

A number  $\Sigma n\sigma_r^5$  may therefore be calculated for a stress spectrum that is proportional to its fatigue damage potential.

A smimilar number  $\Sigma nL^5$  may be calculated for an axle load spectrum; if stress range is proportional to axle load then  $\Sigma nL^5$  for the axle load spectrum that procuded it.

Values of  $\Sigma n\sigma_r^5$  have been calculated obtained during various periods of measurements at the Rheden Bridge.

These values and the relationship between them is plotted in figure 4.4.1. on page 4-56.

The results suggest that the hypothesis that  $\Sigma n\sigma_r^5$  is proportional to  $\Sigma nL^5$  is reasonable.

##### 4.4.2. The effect of asphalt surfacing

In Ref. 6-7 is suggested that the contribution of an asphalt surfacing provides a factor of safety whose value is unknown and not yet taken into account during design. At normal traffic speeds and lower temperatures its contribution to compisite action could cause lower stresses and hence longer fatigue life for welds.

Static and dynamic tests on a orthotropic steeldeck of the Willebrug in Rotterdam (ref. 6-8) were carried out at our laboratory to investigate the stress distribution of an orthotropic steeldeck and the influence of the asphalt surfacing upon this.

Figure 4.4.2. and 4.4.3. on page 4-56 and 4-57 shows testingmachines and testspecimen. Figure 4.4.4. on page 4-58 gives the location of the measured points. The loading statical as well as dynamical amounts 50 kN on a loadsurface from  $25 \times 32 \text{ cm}^2$ .

In figure 4.4.5./4.4.6. on page 4-58/59 the magnitude defined as the ratio between elasticity percentage at a point of the deckplate with an asphalt surfacing of 50 mm and the elasticity percentage in the same point but know without asphalt-surfacing is plotted against the temperature of the asphalt.

In the first place it appears that increasing temperature and dynamic loading the contribution of asphalt surfacing decreases according to loss of stiffness.

Second, at constant temperature but stopped traffic these contribution also decreases, but in this case due to plastic deformation.

#### 4.4.3. Relative contribution of front and rear wheels to fatigue damage

The loading configuration may be important for welds in a steeldeck; front wheels have single tyres and rear wheels normally haven twin types. This difference means that a front wheel may produce higher stresses than a rear wheel although it is more highly loaded.

Using measured influence line data it is possible to assess the relative contribution of front and rear axles to potential fatigue damage.

Comparison of the maximum value of stress produced by the front and rear wheels, per unit of wheelload has been done for the Rheden Bridge in table IV.4.4.1. on page 4-59.

Except for the gauges 1 and 2 the front wheel produces a significantly higher peak stress than the rear wheel per unit wheelload.

Using stress and axle load spectra it is possible to calculate the relative contribution of front and rear axles to potential fatigue damage.

In section 4.4.5. it seems to be reasonable suggesting that  $\sum \sigma_r^5$  is proportional to  $\sum nL^5$ .

If the axle load spectrum is split into two, one for front and one for rear wheels, the following relation may then be proposed:

$$\Sigma n \sigma_r^5 = k_F \Sigma n_F L_F^5 + k_R \Sigma n_R L_R^5$$

The values of  $k_F$  and  $k_R$  obtained from a multiple linear regression analysis will reflect the relative contributions of front and rear wheels to potential fatigue damage. Some results are given in table IV.4.4.2. on page 4-59.

#### 4.4.4. Figures and tables

List of figures	Page
4.4.1. $\Sigma n \sigma_r^5$ and $\Sigma n L^5$ relationship	4-56
4.4.2. Photo of testing machine and test specimen in the cooling box	4-56
4.4.3. Testing machine and test specimen	4-57
4.4.4. Location of the measured points	4-58
4.4.5. Strain as function of the temperature of 12y and 12y'	4-58
4.4.6. Deflection as function of the temperature midway between rib I and II	4-59
List of tables	
IV.4.4.1. Peak values - Rheden Bridge	4-59
IV.4.4.2. Relative contribution of front and rear axles to potential fatigue damage	4-59

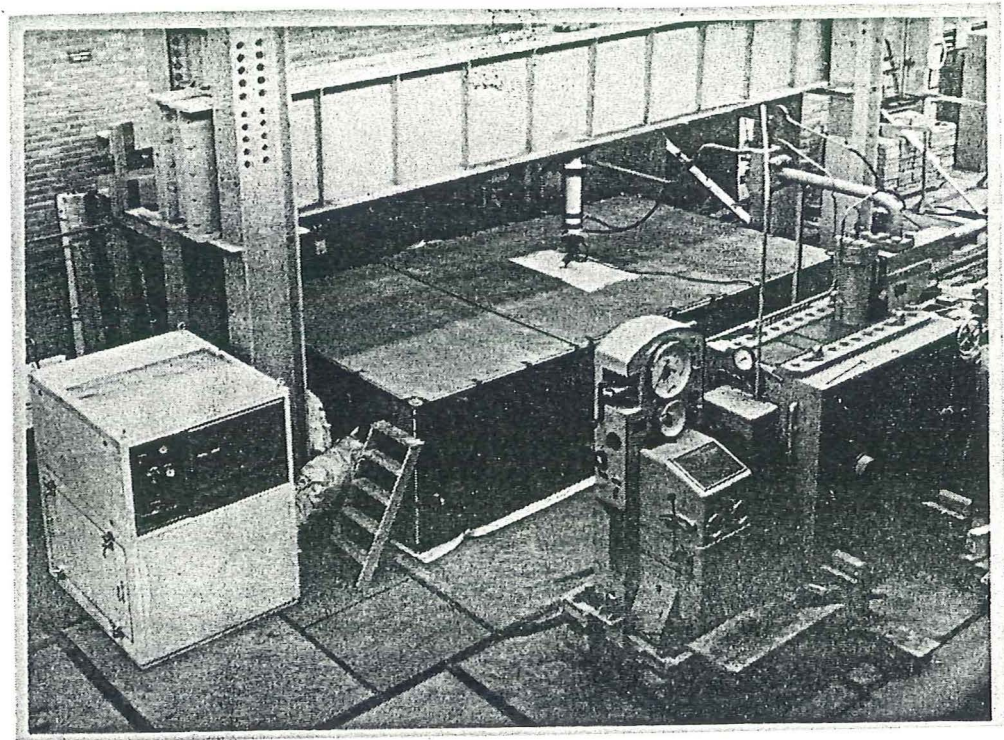
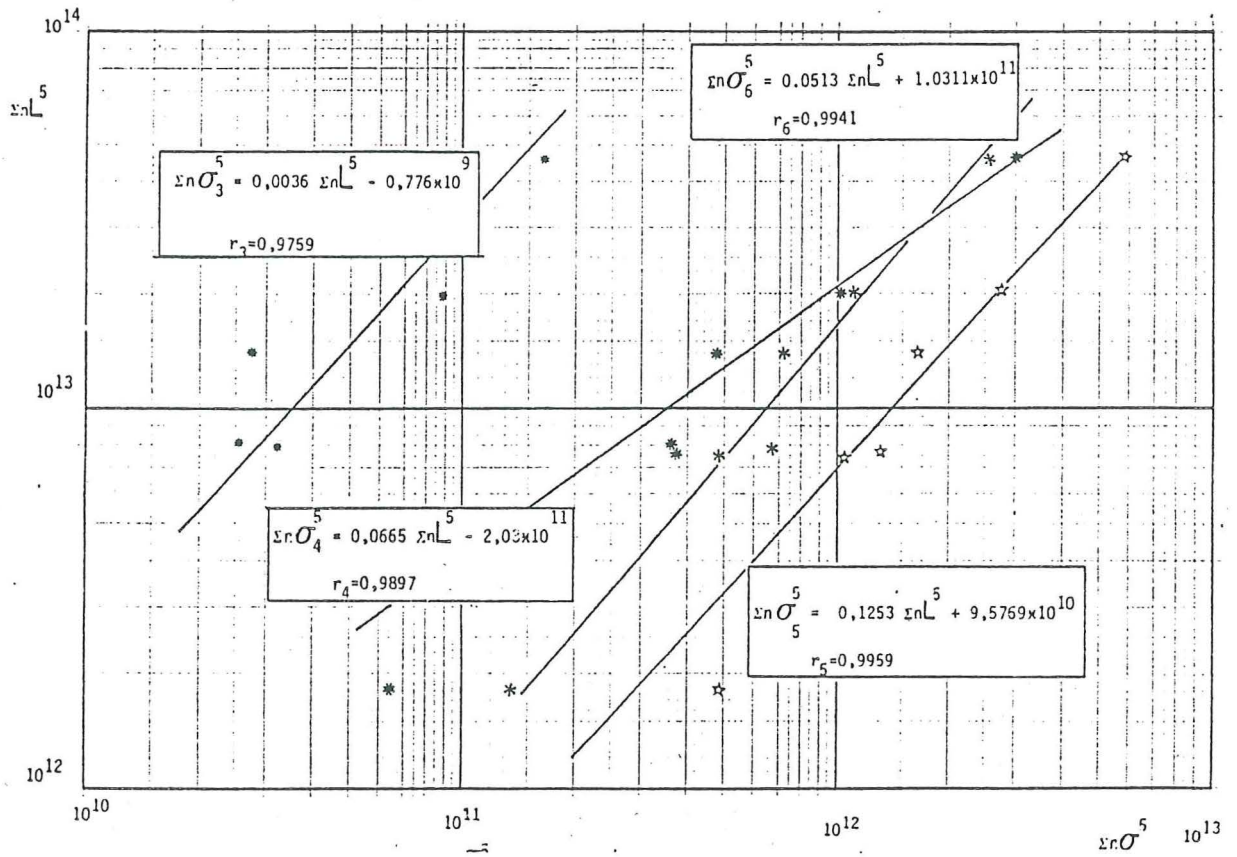
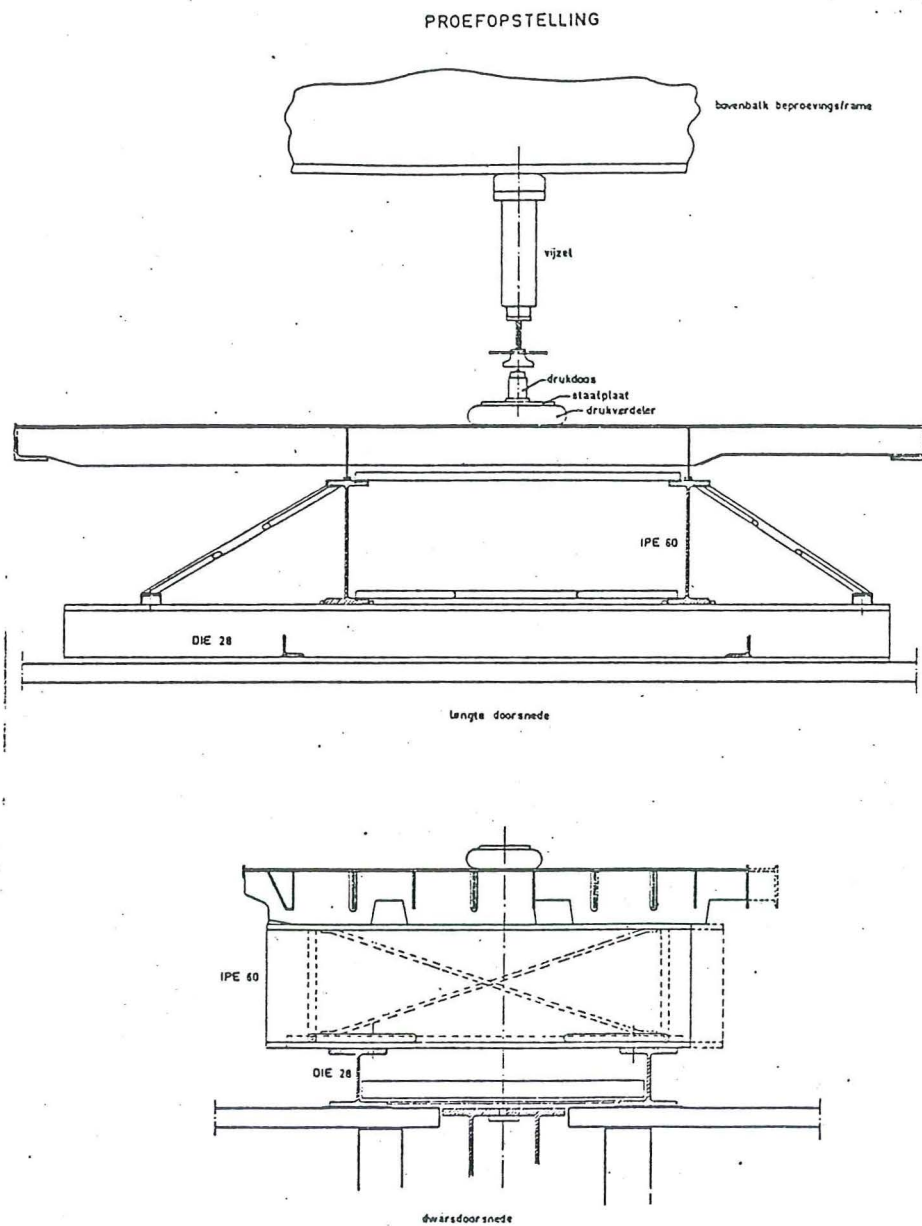
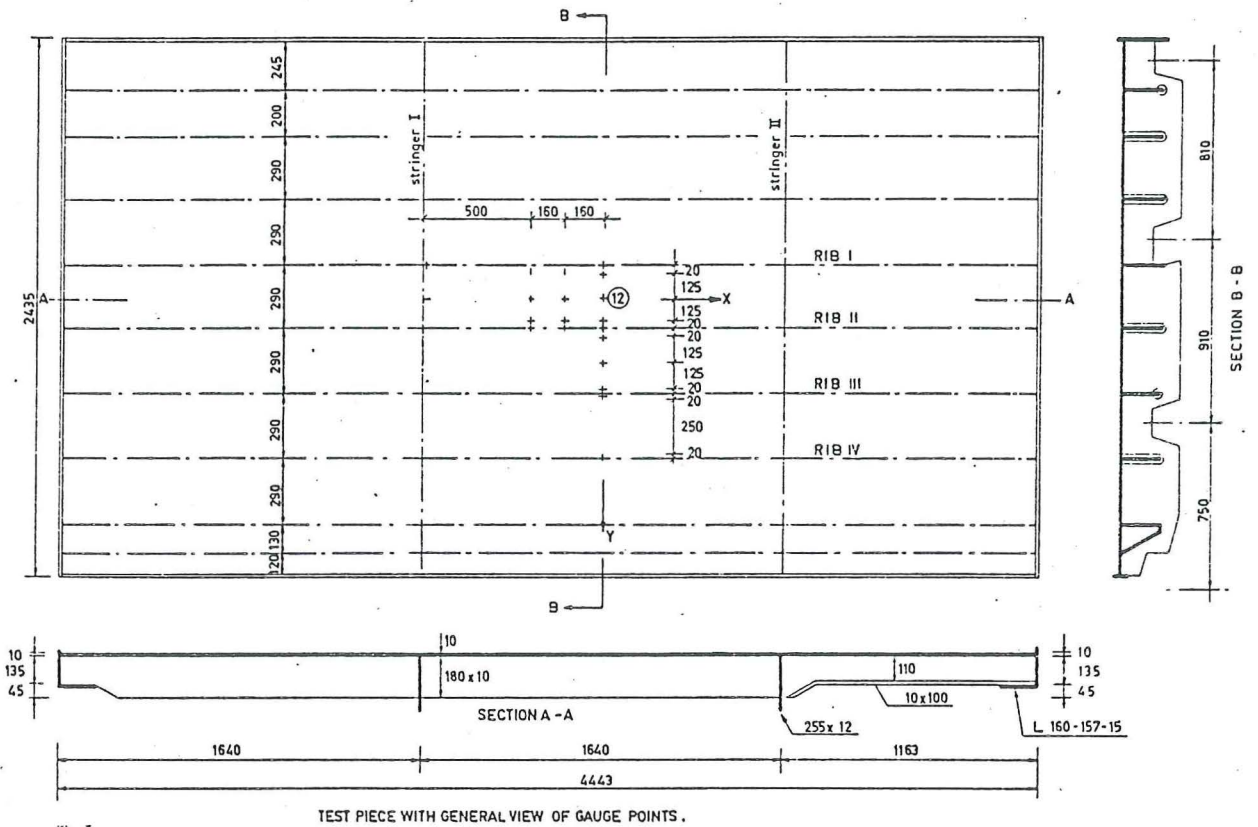


Photo of testing machine and test specimen in the cooling box  
 Figure 4.2.2.

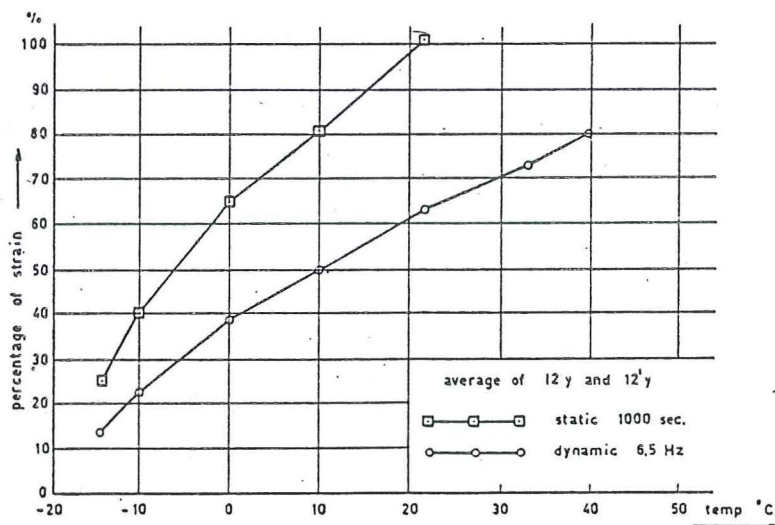




Testingmachine and testspecimen  
Figure 4.4.3.

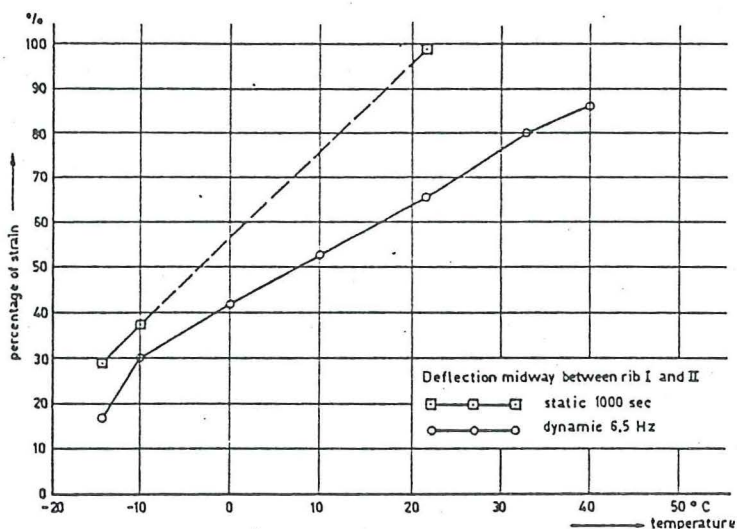


Location of the measured points  
Figure 4.4.4



STRAIN AS FUNCTION OF THE TEMPERATURE, (in % with respect to plate without wearing surface, under static load.)

Strain as function of the temperature of 12y and 12y  
Figure 4.4.5.



DEFLECTION AS FUNCTION OF THE TEMPERATURE (in % with respect to plate without wearing surface, under static and dynamic load.)

Deflection as function of the temperature midway between rib I and II

Figure 4.4.6.

Gauge number	Front wheel-load (kN)	Rear wheel-load (kN)	$P_F = \frac{\text{peak stress}}{\text{wheel load}}$ - front wheel (N/mm <sup>2</sup> / kN)	$P_R = \frac{\text{peak stress}}{\text{wheel load}}$ - rear wheel (N/mm <sup>2</sup> / kN)	$\frac{P_F}{P_R}$
1	17.6	51.0	0.2	0.19	1.05
2	18.2	51.8	0.25	0.29	0.86
6	18.4	52.6	1.14	0.93	1.23
7	18.2	51.8	1.54	1.14	1.35
11	17.6	51.0	0.47	0.32	1.47
12	17.6	51.0	0.46	0.32	1.44
13	18.4	52.6	0.55	0.34	1.62
15	18.2	51.8	0.79	0.40	1.98
16	18.2	51.8	0.4	0.29	1.38
17	18.2	51.8	0.73	0.43	1.70
18	18.2	51.8	0.69	0.45	1.53

Peakvalues static measurements at the Rheden Bridge  
Table IV.4.4.1.

Gauge point	A ±10 <sup>10</sup>	k <sub>F</sub>	k <sub>R</sub>
3	- 8.34	0.1375	0.00131
4	-152.71	2.5006	0.2414
5	-298.00	4.8892	0.4705
6	-127.00	2.0928	0.2003

Relative contribution of front and rear axles to potential fatigue damage

Table IV.4.4.2.



5. General discussion of the results



## 5. GENERAL DISCUSSION OF THE RESULTS

Conclusions so far can be summarized as follows:

- From frequency distribution curves of axle loads it appears that after about 8000 axle loads larger than 10 kN the shape of the curve does not change very much. The number of axle loads needed for a reliable shape of a frequency distribution curve of stresses depend on the lateral distribution of the axle loads. The results indicate that about 12.000 axle loads larger than 10 kN will be sufficient to get a curve reliable enough to extrapolate for fatigue life estimate calculations.
- There seems to be a good correlation between the shapes of distribution curves of axle loads and those of induced stresses. Relating stress spectra to axle load spectra it appeared that the hypothesis that  $\sum \sigma_r^5$  is proportional to  $\sum nL^5$  is reasonable. So it may be expected that knowledge of the axle load frequency distributions, lateral distribution (60% of the traffic drives in the same track of about 300 mm) of these axle loads and the influence planes will be sufficient for a computer simulation of the frequency distribution curves of the stresses.
- This is only true of the dynamic behaviour of the bridge does not influence the number of cycles. In this investigation one of the bridges, a movable bridge, showed a far larger number of cycles that could be expected from calculation. Analysis of these stresses into fatigue terms showed however that the damaging potential of these small stress cycles is neglectable.
- Analysis of the extrapolated stress spectra, for one hundred years showed that stress ranges smaller than  $40 \text{ N/mm}^2$  (axle load about 60 kN) and higher than  $90 \text{ N/mm}^2$  (axle load about 140 kN) are not important in relationship to fatigue life estimates because the damaging potential of these stress range classes are small. The intermediate stress range classes (axle loads between 40 kN and 140 kN) cause over 95% of the damage of the total stress spectrum.

The number of cycles in these classes amounts still  $\sim 3 \cdot 10^7$  -  $\sim 10^8$  cycles, so a fifth power relationship of the fatigue damage seems to be reasonable knowing the design S-N curves of the different fatigue codes.

- Calculating a minimum value for  $\Delta\sigma_k$ , that is the admissible value of the stress range  $\Delta\sigma$  at  $10^7$  cycles, it appeared that the maximum stress range of the spectra must be close to the value of  $\Delta\sigma_k$  of the welded detail if a life time of 75 - 100 years will be the minimum. Therefore the part of the S-N curve with a slope 1:3 is not important for bridge components with a great number of cycles. More important is the position of the S-N curve itself, the correctness of the assumption of slope 1:5 and the point under which fatigue damage will not occur (fatigue limit).
- Assuming that the fatigue damage is proportional to the fifth power of axle loads, an axle load of 73 - 79 kN (characteristic axle load) is calculated, such that N-axles of that load has the same fatigue damage potential as N-cycles of the load spectra.
- Furthermore it appeared that two vehicle types, mostly the artic, 2-axle trailer with a 2 or 3-axle semi-trailer produce together 40 - 50% of the total damage of the population of commercial vehicles. These two types presents 6 - 18% of the total number of commercial vehicles.

Finally it can be concluded that a lot of information is now available about load spectra, stress spectra and their relation to local traffic. It appears that some of the components of the bridge will endure a large number of damaging stress cycles.

However in most cases the stress cycles will be small. Nevertheless it will be important for future bridge codes to include fatigue damage calculations based on the now available data to avoid on one hand unexpected and unwished fatigue failures if someone is thinking only in terms of static loading and on the other hand to avoid unnecessary pessimism if anyone is aware of a possible fatigue damage.



With respect to this the common European research has filled up a large gap in knowledge and has certainly reached the aim of the investigation.

It has been stated already that the determination of a possible fatigue damage is highly depending on the shape of the S-N curve in lower stress regions and on the fatigue limit. Therefore in this final report no definite proposal for a fatigue damage calculation can be made as long as the shapes of the S-N curves in the different countries differ so much (especially at low stress levels). That means that the general problem of fatigue damage at low stress levels and a high number of cycles is one of the most important problems to be solved in near future. A number of fatigue damage calculations in this report prove this statement.



## 6. Reference



- Ref. 6-1 | 1 | Page, J.  
 "Measurement and interpretation of dynamic loads on bridges" - final report - projectnr. 7210-SA/8/809 - Transport and Road Research Laboratory, Crowthorne, Berkshire, 1979.
- | 2 | Zschel, J.M. and Pfeifer, M.R.  
 "Messen und auswerten von Lastkollektiven an brücken" Vertragnr. 7210-KD/1/104 Fraunhofer-Institut für Betriebsfestigkeit, Darmstadt, 1979.
- | 3 | Carracilli, J.  
 "Mesure et interpretation des charges dynamique dans les ponts" - Rapport de synthese l Reserche 7210 KD/3/304 - Laboratoire Central des Ponts et Chaussées, Paris, 1979.
- | 4 | Bruls, A.  
 "Mesure et interpretations des charges dynamique dans les ponts" - Rapport final - Convention 6210-KD/2/204 Université de Liège Institut du Génie Civil, Liège, 1979.
- | 5 | San Paolesi, L.  
 "Misure ed interpretazione dei carichi dinamici sui ponti" - Final report N.7210 SB/401 - Universita di Pisa, Laboratoria Officialle par le experience dei material da Construzione, Pisa, 1979.
- | 6 | Kolstein, M.H. and Back, J. de.  
 "Measurements and interpretation of dynamic loads on bridges - Phase 1 - ECSC contractnr. 7210-KD/6/604 Stevin reports 6-79-5, 6-79-6, 6-79-7. Delft University of Technology, Stevin Laboratory, Steelstructures Delft, 1979.
- Ref. 6-2 | 1 | Kolstein, M.H. and Back, J. de.  
 "Measurements and interpretation of dynamic loads on bridges", Phase 2 - ECSC contractnr. 7210-KD/6/606, Delft University of Technology, Stevin Laboratory Steelstructures.  
 Contract period: 1-7-1980 until 1-7-1982  
 1st technical report : Stevin report 6-81-4  
 2nd technical report : Stevin report 6-81-19  
 3rd technical report : Stevin report 6-82-2  
 4th technical report : Stevin report 6-82-9

- Ref. 6-3 |1| Kolstein, M.H. and Back, J. de  
"Measurements and interpretation of dynamic loads on bridges" - Phase 2 - ECSC contractnr. 7210-KD/6/606, Delft University of Technonoly, Stevin Laboratory, Steelstructures.  
- Final report "Haagsche Schouw Bridge"  
Stevin report 6-79-5  
- Final report "Rheden Bridge"  
Stevin report 6-79-6  
- Final report "Leiderdorp Bridge"  
Stevin report
- Ref. 6-4 |1| Heering, C.A.  
"Een onderzoek naar de mogelijkheid om voertuigen te detecteren m.b.v. signalen van transducers die op een brugconstructie zijn aangebracht"  
Technische Hogeschool Delft, Afd. Elektrotechniek, 1977 (in Dutch).
- Ref. 6-5 |1| Bruls, A.  
"Mesures et interpretation des charges dynamiques dans les ponts" - 2ème phase - Rapport Semestriel nr. 1 - 7210-KD/208 F.4 1/80. Université de Liège.
- Ref. 6-6 |1| Page, J. and Tilly, G.P.  
"Some analysis of traffic data for three steelbridges"  
TRRL Supplementary Report 598.
- Ref. 6-7 |1| Page, J.  
"Measurements and interpretation of dynamic loads on bridges"  
Progress report nr. 1 - 7210-KD/804.
- Ref. 6-8 |1| Bats, J.D. and Kingma, A.  
"Bepaling van de spanningsverdeling in een orthotrope plaatvloer en de invloed van de slijtlaag hierop"  
Stevin rapport 6-64-5 Deel I en II (in Dutch).

## 7. Appendix





APPENDIX A

List of tables Page

Haagsche Schouw Bridge

A.III.4.1. : Analysed hours A-1  
A.III.4.2. : Date of measurements A-2

Rheden Bridge

A.III.4.3. : Analysed hours Group A A-3  
A.III.4.4. : Analysed hours Group B A-4  
A.III.4.5. : Analysed hours Group C A-5  
A.III.4.6. : Date of measurements A-6

Leiderdorp Bridge

A.III.4.7. : Analysed hours A-7  
A.III.4.8. : Date of measurements A-8

APPENDIX B

List of tables	Page
<u>Haagsche Schouw Bridge</u> 82 hours	
B.III.4.1.- : Axle loads histograms	B-1-
B.III.4.8.	B-8
B.III.4.9.- : Axle distance histograms	B-9-
B.III.4.12	B-12
<u>Rheden Bridge</u> 62 hours	
B.III.4.13- : Axle loads histograms	B-13-
B.III.4.20	B-20
B.III.4.21- : Axle distance histograms	B-21-
B.III.4.24	B-24
<u>Leiderdorp Bridge</u> 24 hours	
B.III.4.25- : Axle loads histograms	B-25-
B.III.4.32	B-32
B.III.4.33- : Axle distance histograms	B-33-
B.III.4.36	B-36

APPENDIX C

List of tables	Page
<u>Haagsche Schouw Bridge</u>	
Measuring points 2,3, 13-16, 18-21 (4.25 hours)	
Rainflow counts	C-1
Levelcrossings	C-2
Measuring points 14, 15, 20 (11,45 hours)	
Rainflow counts	C-3
Levelcrossings	C-4
Measuring points 2, 3, 13-18, 20, 21 (66,04 hours)	
Rainflow counts	C-5
Levelcrossings	C-6
<u>Rheden Bridge</u>	
<u>Group A : Traffic in fast and slow lane</u>	
Measuring points 1-10 (44,91 hours)	
Rainflow counts	C-7
Levelcrossings	C-8
Measuring points 1, 2, 11-18 (8,86 hours)	
Rainflow counts	C-9
Levelcrossings	C-10
Measuring points 1-6, 11-14 (7,96 hours)	
Rainflow counts	C-11
Levelcrossings	C-12

